

DIFFERENTIAL REGULATION OF HIF-1 $\alpha$  IN TAY-SACHS NEUROGLIA

DIFFERENTIAL REGULATION OF HIF-1 $\alpha$  IN HUMAN TAY-SACHS NEUROGLIA

By: ROSEMARIE E. VENIER, B.Sc. (Hons)

A Thesis Submitted to the School of Graduate Studies in Partial Fulfillment of the  
Requirements for the Degree Master of Science

McMaster University © Copyright by Rosemarie E. Venier, August 2012

All Rights Reserved

MASTER OF SCIENCE Biology (2012)

McMaster University  
Hamilton, Ontario, Canada

TITLE: Differential Regulation of HIF-1 $\alpha$  in Human Tay-Sachs Neuroglia

AUTHOR: Rosemarie E. Venier, B.Sc. (Hons) (McMaster University)

SUPERVISOR: Suleiman A. Igdoura, PhD

NUMBER OF PAGES: xi, 114

## ABSTRACT

Lysosomal storage diseases (LSDs) are devastating neurological disorders caused by mutations in lysosomal hydrolases that result in accumulations of hydrolase substrates. Tay-Sachs disease (TSD) is an LSD that specifically results in the accumulation of GM2 gangliosides causing the activation of inflammatory signaling pathways, and leading to microglial activation and apoptotic cell death. The detailed mechanisms through which cell death occurs have not been completely elucidated, however, excitotoxicity is thought to play a major role. Here, we investigated the role of hypoxia-inducible factor-1 $\alpha$  (HIF-1 $\alpha$ ) and its effector microRNA, miR-210, and the impact they have on the expression of important molecules involved in excitotoxicity, namely neuronal pentraxin 1 (NPTX1) and potassium channel KCNK2 (KCNK2). We discovered that TSD neuroglia are inefficient at stabilizing HIF-1 $\alpha$  in hypoxic conditions. Furthermore, miR-210 expression is significantly higher in TSD neuroglia compared to normal neuroglia at baseline and during hypoxia. In addition, TSD neuroglia expressed *NPTX1*, *NPTX2* and *KCNK2* at higher levels, and neuronal pentraxin receptor at lower levels than normal neuroglia, implicating excitotoxicity in disease pathogenesis. We also confirmed that miR-210 binds to the 3' UTR of *NPTX1* to repress its expression in TSD neuroglia. The presence of reverse hypoxia response elements in the promoter of *KCNK2* and the repression of *KCNK2* expression by HIF-1 $\alpha$  stabilization suggest that *KCNK2* is directly regulated by HIF-1 $\alpha$ . Moreover, the glucosylceramide synthase inhibitor, NBDNJ, which is used to reduce ganglioside synthesis, caused expression of *NPTX1* to decrease but *KCNK2* expression to increase, indicating this drug can modify multiple parameters of disease.

This study identifies major gene expression changes between normal and TSD neuroglia that affect the excitability and therefore the viability of TSD cells. This information provides new insight into the mechanisms of neurodegeneration experienced by TSD neuroglia.

## ACKNOWLEDGEMENTS

I would like to express my sincerest thanks to my supervisor Dr. S. Igdoura for mentoring me these past three years as an undergraduate and graduate student. Without your guidance and support I would not be the scientist I am today (I probably wouldn't have the nickname "Pumpkin" either). I am happy to be your student and am grateful for your encouragement and advice throughout my degrees and am thankful that you shared your enthusiasm for science with me. I would also like to acknowledge the other students and members of the laboratory who have taught me many scientific techniques but also life lessons, like making sure all my pens are labeled. You have truly been great teachers and friends and I am very thankful for everything you've done for me.

Next, I'd like to thank my family and friends for standing by me and continuing to support me throughout my degree. It was you that I called complaining or crying when I was frustrated and you always set me back on track. Mom and dad, even though you may not be able to explain what I've studied to any of your friends, I know you're proud of me anyways. My drive to succeed is no doubt your doing, but it was my sense of humor and ability to kick back that helped me through the tough times during my degree, which I also owe to you. Danny boy, keep working hard at school. I'm glad we can have scientific conversations and ponder the future of the world together. I hope my experience in graduate school has given you insight into your future and helped you decide what you want to do with your life – although it seems to have made this more complicated for me. Stephanie and Amanda, you've been the greatest support network anyone could ask for: pushing me forward when I needed a kick in the pants but also helping me realize when I

needed to relax to keep my sanity. Thanks for putting up with me living so far away, I'm glad we've always been able to pick up where we've left off with a glass of wine or a cup of coffee. Coop, thank you for motivating me when I wanted to give up and for always making me smile, surely I would've completely lost my mind without you. I love all of you so much, thank you.

Lastly, to the person I miss most: Grandma, I wish you were here to celebrate this accomplishment with me. I would not be the person I am today without you and not a day goes by that I don't think of you. Thank you for being the best grandmother a girl could ask for.

## TABLE OF CONTENTS

ABSTRACT	iii – iv
ACKNOWLEDGEMENTS	v – vi
LIST OF ABBREVIATIONS	x – xi
1. INTRODUCTION	pages 1 – 28
• <i>Lysosomal storage disorders</i>	1 – 11
• <i>Hypoxia inducible factor-1</i>	11 – 16
• <i>Excitotoxicity</i>	16 – 21
• <i>Neuronal pentraxins</i>	21 – 24
• <i>Potassium channel KCNK2</i>	25 – 28
2. MATERIALS AND METHODS	pages 29 – 36
• <i>Cell culture</i>	29
• <i>Genotyping</i>	29
• <i>SDS-PAGE and western blotting</i>	29
• <i>Immunocytochemistry</i>	30
• <i>RNA isolation, reverse transcription and RT-PCR</i>	30
• <i>Taqman and SYBR green quantitative real time PCR</i>	31
• <i>Vector construction</i>	32 – 33
• <i>Transfection</i>	34
• <i>Luciferase assay</i>	34
• <i>Ganglioside Isolation</i>	34 – 35
• <i>Thin Layer Chromatography</i>	35 – 36
• <i>Chemicals and antibodies</i>	36
• <i>Statistics</i>	36
3. RESULTS	pages 37 – 69
• <i>Characterization of disease causing mutations in TSD neuroglia</i>	37 – 38
• <i>HIF-1<math>\alpha</math> stabilization is defective in TSD neuroglia</i>	39 – 41
• <i>Cellular localization of HIF-1<math>\alpha</math></i>	42 – 44
• <i>Gene expression of neuronal molecules is altered in TSD neuroglia</i>	45 – 46
• <i>DMOG and AMPA modify expression of NPTX1, KCNK2 and VEGF</i>	47 – 49
• <i>HIF-1<math>\alpha</math> represses expression of NPTX1 and KCNK2</i>	50 – 52
• <i>miR-210 is expressed at higher levels in TSD neuroglia</i>	53 – 55
• <i>miR-210 is predicted to bind the 3' UTR of NPTX1</i>	56 – 57
• <i>miR-210 represses NPTX1 expression</i>	58 – 60
• <i>Expression of NPTX1 in transfected TSD neuroglia</i>	61 – 62

• <i>Regulation of potassium channel KCNK2 expression</i>	63 – 65
• <i>Treatment of TSD neuroglia with NBDNJ alters gene expression</i>	66 – 69
4. DISCUSSION	pages 70 – 86
• <i>Impact of HIF-1<math>\alpha</math> deficiency on gene expression in TSD neuroglia</i>	70 – 73
• <i>Role of miR-210 in TSD neuroglia</i>	74 – 77
• <i>Regulation of NPTX1 in TSD neuroglia</i>	77 – 79
• <i>Regulation of KCNK2 in TSD neuroglia</i>	79 – 80
• <i>Substrate reduction therapy with NBDNJ</i>	81 – 83
• <i>Conclusions</i>	84 – 86
5. REFERENCES	pages 87 – 114

**LIST OF FIGURES**

• <i>Figure 1 TSD neuroglia are compound heterozygotes</i>	38
• <i>Figure 2 HIF-1<math>\alpha</math> stabilization is deficient during hypoxia in TSD neuroglia</i>	41
• <i>Figure 3 DMOG localizes HIF-1<math>\alpha</math> to the nucleus in normal neuroglia</i>	43
• <i>Figure 4 DMOG localizes HIF-1<math>\alpha</math> to the nucleus in TSD neuroglia</i>	44
• <i>Figure 5 Gene expression of neuronal molecules in TSD neuroglia</i>	46
• <i>Figure 6 DMOG and AMPA modify NPTX1, KCNK2 and VEGF expression in TSD neuroglia</i>	49
• <i>Figure 7 NPTX1 and KCNK2 expression is higher in TSD neuroglia</i>	52
• <i>Figure 8 miR-210 expression is higher in TSD neuroglia</i>	55
• <i>Figure 9 Predicted binding of miR-210 to the 3' UTR of NPTX1</i>	57
• <i>Figure 10 Mutation of NPTX1 3' UTR</i>	59
• <i>Figure 11 Mutant 1 reduces binding of miR-210</i>	60
• <i>Figure 12 NPTX1 associates in multimers and is glycosylated</i>	62
• <i>Figure 13 KCNK2 gene structure</i>	64
• <i>Figure 14 Three major KCNK2 transcript variants in TSD neuroglia</i>	65
• <i>Figure 15 NBDNJ increases GM2 in TSD neuroglia</i>	68
• <i>Figure 16 NBDNJ alters expression of NPTX1 and KCNK2</i>	69
• <i>Figure 17 Working model</i>	84

## LIST OF ABBREVIATIONS

AA	Arachidonic acid
AD	Alzheimer's disease
ALS	Amyotrophic lateral sclerosis
AMPA	2-amino-3-(3-hydroxy-5-methylisoxa-zol-4-yl) proprionate
A $\beta$	Amyloid- $\beta$
BMT	Bone marrow transplant
CaMKII	Calcium/calmodulin-dependent protein kinase II
CGN	Cerebellar granule neurons
CNS	Central nervous system
DAG	Diacylglycerol
EAAT	Excitatory amino acid transporter
ERK1/2	Extracellular-signaling regulated kinase
FIH1	Factor inhibiting HIF-1
GalNAc	N-acetylgalactosamine
GalNAcT	$\beta$ -1,4-N-acetyl-galactosaminyl transferase
GAPDH	Glyceraldehyde-3-phosphate dehydrogenase
GPI	Glycosylphosphatidylinositol
GRIP	Glutamate receptor-interacting protein
GSK3 $\beta$	Glycogen synthase kinase 3 $\beta$
GSLs	Glycosphingolipids
HEXA	$\beta$ -hexosaminidase A
HEXB	$\beta$ -hexosaminidase B
HI	Hypoxic-ischemic
HIF-1 $\alpha$	Hypoxia-inducible factor-1 $\alpha$
HRE	Hypoxia response element
HSP90	Heat-shock protein 90
i-DCs	Immunogenic dendritic cells
IL1- $\beta$	Interleukin 1- $\beta$
IP <sub>3</sub>	Inositol 1,4,5-triphosphate
IPAS	Inhibitory PAS
I $\kappa$ B	Inhibitor of NF- $\kappa$ B
KA	Kainic acid
KCNK2	Potassium channel subfamily K member 2
LSDs	Lysosomal storage diseases
LTD	Long-term depression
LTP	Long-term potentiation
MHC	Major histocompatibility complex
miR-210	microRNA-210
miRISC	microRNA-containing RNA-induced silencing complex
miRNA	microRNA
NBDNJ	N-butyldeoxynojirimycin
NF- $\kappa$ B	Nuclear factor $\kappa$ B

NMDA	N-methyl-d-aspartate
NO	Nitric oxide
NPC	Niemann-Pick type C
NPR	Neuronal pentraxin receptor
NPTX1	Neuronal pentraxin 1
NPTX2	Neuronal pentraxin 2
ODDD	Oxygen dependent death domain
PAS	Per/Arnt/Sim
PCR	Polymerase chain reaction
PHD	Prolyl hydroxylase domain
PICK1	Protein interacting with C-kinase-1
PIP <sub>2</sub>	Phosphatidylinositol 4,5-bisphosphate
PKC	Protein kinase C
PLC	Phospholipase C
pre-miRNA	Precursor microRNA
pri-miRNA	Primary microRNA
PSD	Post-synaptic density
PUFA	Poly-unsaturated fatty acid
pVHL	von Hippel-Lindau protein
RGC	Retinal ganglion cell
rHRE	Reverse hypoxia response element
ROS	Reactive oxygen species
RT-PCR	Reverse transcription polymerase chain reaction
SD	Sandhoff disease
SERCA	Sarco/endoplasmic reticulum calcium ATPase
TACE	Tumor necrosis factor- $\alpha$ converting enzyme
TARPs	Transmembrane AMPA receptor regulatory proteins
TF	Transcription factor
TLR	Toll-like receptor
TNF- $\alpha$	Tumor necrosis factor- $\alpha$
TSD	Tay-Sachs disease
UTR	Untranslated region
VEGF	Vascular endothelial growth factor

## INTRODUCTION

### Lysosomal Storage Disorders

Glycosphingolipids (GSLs) are glycolipids found within the plasma membrane. They are important molecules that are localized in microdomains called lipid rafts, which facilitate cell-cell interactions and effective signaling. Lipid rafts are enriched in sphingolipids, cholesterol, and glycosylphosphatidylinositol (GPI)-anchored proteins positioned to enable efficient localization of signaling proteins.<sup>1</sup> Gangliosides are a subclass of GSL that contain a ceramide backbone and at least one sialic acid residue on the glycan. The ceramide moiety of the GSL functions to anchor the molecule in the plasma membrane and positions its glycan moieties on the cell surface.<sup>2</sup>

GSLs are essential to early development as demonstrated by the embryonic lethality observed in the mouse gene knockout of glucosylceramide synthase – the enzyme that facilitates the first committed step of ganglioside synthesis.<sup>3</sup> Knockout of other enzymes responsible for later steps of synthesis are not embryonic lethal but do result in neurological defects. As such, knockout of  $\beta$ -1,4-N-acetyl-galactosaminyl transferase (GalNAcT) in mice, which is the enzyme responsible for synthesis of GM2 ganglioside from GM3, causes reduced neural conduction velocity due to disrupted nodes of Ranvier,<sup>4,5</sup> axonal degeneration, reduced myelination and dysmyelination.<sup>6,7</sup> Some of these pathologies are attributed to a disruption in the interactions between ganglioside ligands and myelin-associated glycoprotein, which has been shown to maintain myelin stability.<sup>7</sup>

Localization of gangliosides to lipid rafts serves a significant biological function. In fact, both ganglioside deficiency, and addition of exogenous gangliosides leads to the disruption of lipid rafts.<sup>8,9</sup> Small lipid rafts are found throughout the cell at steady state,<sup>10</sup> but certain stimuli cause the rafts to rearrange into large platforms to allow recruitment of downstream signaling molecules.<sup>11-13</sup> Similarly, the post-synaptic density (PSD) is an important component of the post-synaptic neuron composed of scaffold and signaling proteins required for neuronal signal transmission.<sup>14,15</sup> Lipid rafts are known to associate with the PSD,<sup>16</sup> which implicates gangliosides in synaptic signaling. Disruptions in raft composition have been found to reduce the stability of signaling molecules at the cell surface, including ionotropic glutamate receptors (AMPA and NMDARs).<sup>17</sup> Recent evidence suggests increased GM1 and GM2 gangliosides alter lipid rafts in Alzheimer's disease (AD) and contribute to myelin degradation and disease pathogenesis.<sup>18</sup> Gangliosides are thus intricately involved in neuronal signaling and survival, and altered ganglioside levels affect cell viability.

As part of normal turnover, gangliosides are internalized and targeted to the lysosome for degradation. Here, individual sugars are cleaved from the molecule in a step-wise fashion by specific lysosomal hydrolases.<sup>1</sup> Mutations in these hydrolases can cause a deficiency or complete loss of enzyme activity leading to accumulation of enzyme substrate in the lysosome. This occurrence is detrimental to individual cells and physiologically results in developmental retardation, paralysis, dementia, blindness, and death early in life.<sup>2</sup> Collectively, diseases of this nature are termed lysosomal storage disorders (LSDs).

The focus of this report will be two related LSDs that are classified as GM2 gangliosidoses: Tay-Sachs disease (TSD) and Sandhoff disease (SD). These diseases are autosomal recessive disorders, which are caused by a mutation in *HEXA* or *HEXB* genes, respectively. This results in a deficiency or loss of function in lysosomal  $\beta$ -hexosaminidase. The *HEXA* gene encodes for the  $\alpha$  subunit of  $\beta$ -hexosaminidase A and the *HEXB* gene encodes for the  $\beta$  subunit of  $\beta$ -hexosaminidase A ( $\alpha\beta$  subunits) and  $\beta$ -hexosaminidase B ( $\beta\beta$  subunits). These enzymes are responsible for the catabolism of GM2 ganglioside (HEXA), and globoside and GA2 (HEXB), by removing a terminal N-acetylgalactosamine residue. Cells with one or more mutations in either gene lead to substrate accumulation and eventually succumb to death. Diseased neurons are large and swollen, and undergo neurodegeneration characteristic of these diseases.<sup>2</sup>

TSD is much more common in the Ashkenazi Jewish population compared to the general population due to founder mutations. Founder mutations occur when a small, isolated population is first established. Although the population may grow in size subsequently, the gene pool is derived from the genes of the original founders. Therefore, mutations are more likely to be inherited from both parents, which increases the frequency of homozygous recessive offspring.<sup>19</sup> The severity of TSD varies from infantile, to juvenile, to adult onset depending on residual enzyme activity. Less enzyme activity is correlated with earlier onset and more severe disease progression.<sup>20</sup> The most common mutations in the Ashkenazi population are a four basepair insertion (1278insTATC) in exon 11 and a splice site mutation in intro 12 (IVS12+1G $\rightarrow$ C). The insertion mutation

causes a frameshift and premature stop codon, whereas the transversion mutation causes abnormal splicing and both result in deficient *HEXA* mRNA.<sup>21</sup>

Despite what is known about the genetics and biochemistry of the disease, the mechanism through which cell death occurs is still under investigation. In addition to substrate accumulation, there is evidence to show that inflammation,<sup>22-25</sup> microglial activation,<sup>26, 27</sup> and apoptosis<sup>22, 28, 29</sup> contribute to the pathology of TSD and SD.

It is widely accepted that chronic inflammation occurs in TSD and SD, as well as other LSDs. This is due to an inappropriate immune response to lysosomal accumulations. The pathophysiological mechanisms involved are still unknown, but mouse models have been helpful in elucidating these events.<sup>30</sup> *Hexb*<sup>-/-</sup> mice are used for the study of TSD and SD because *Hexa*<sup>-/-</sup> mice are asymptomatic due to a bypass that results in desialylation of GM2 to GA2 and subsequent removal of the terminal GalNAc residue by HEXB. Human sialidase does not effectively facilitate the same catabolic bypass.<sup>31</sup> Studies on *Hexb*<sup>-/-</sup> mice have found altered blood-brain barrier permeability, microglial activation and infiltration, and higher pro-inflammatory cytokine secretion when compared with wild type mice. Inflammatory damage pre-dates clinical symptoms of disease and becomes more extensive as the disease progresses.<sup>22</sup> Bone marrow transplant (BMT) introduces healthy microglia to the brain and thus has been observed to decrease activation and expansion of resident diseased *Hexb*<sup>-/-</sup> microglia, and prevent apoptosis.<sup>26</sup> It has also been shown *in vitro* in human immunogenic dendritic cells (i-DCs) that either HEXA or HEXB is required for immunostimulatory function. Because i-DCs are responsible for tailoring

T-cell responses and activation, this provides a potential explanation for the inappropriate inflammatory response seen in TSD and SD.<sup>25</sup>

Clinically, TSD and SD are incurable diseases, however, there are many treatment options that attempt to ameliorate symptoms of these and other LSDs. Enzyme replacement therapy and substrate reduction, which are largely used in the treatment of Gaucher disease,<sup>32, 33</sup> bone marrow transplant (BMT)<sup>26, 34</sup> and viral gene therapy<sup>29, 35</sup> are the most promising options.

N-butyldeoxynojirimycin (NBDNJ, Miglustat) is an iminosugar that acts as a structural ceramide mimic to inhibit glucosylceramide synthase and functions to reduce glucosylceramide entering the ganglioside synthesis pathway. This method of disease treatment is called substrate reduction therapy.<sup>36, 37</sup> The ability of NBDNJ to block GSL synthesis at such an early step, as well as cross the blood brain barrier,<sup>38</sup> makes it a useful drug for the treatment of multiple lysosomal storage diseases. NBDNJ is marketed under the name Miglustat and has been approved by the United States Food and Drug Administration, the European Union, and over 30 other countries for the treatment of adults with type I Gaucher disease for which enzyme replacement therapy is unsuitable. In addition, it has been approved in the European Union for the treatment of progressive neurological manifestations in adult and pediatric patients with Niemann-Pick type C (NPC).<sup>32</sup>

Overall, NBDNJ appears to be a useful and beneficial drug for substrate reduction therapy, particularly for the treatment of Gaucher disease where the drug target is immediately upstream of the accumulating substrate, and NPC where GSL accumulation

is secondary. Gaucher disease results from a deficiency in acid  $\beta$ -glucosidase characterized by lysosomal storage of glucosylceramide, the substrate of acid  $\beta$ -glucosidase.<sup>39</sup> In contrast, GSL accumulation is secondary to a cholesterol transport defect in NPC. This leads to the accumulation of cholesterol, sphingomyelin, phospholipids and glycolipids in the liver and spleen.<sup>40</sup> However, the exact degree to which GSLs can be decreased in mammals safely, is unknown. Gangliosides play a pivotal role in development and in neuronal function; it is therefore imperative to determine the possible molecular consequences of this therapy before implementing it as a standard treatment for all glycosphingolipidoses.

Proof of principle for substrate reduction therapy has been established using mouse models that lack functional ganglioside synthases. Embryogenesis was arrested in glucosylceramide synthase knockout mice during gastrulation, indicating the necessity for glycosphingolipids in early development.<sup>3</sup> As previously mentioned, mice with a disruption in the  $\beta$ -1,4-N-acetyl-galactosaminyl transferase (*GalNAcT*) gene, the enzyme responsible for synthesis of GM2 and GD2, are not embryonic lethal. The absence of complex gangliosides caused GM3 and GD3 gangliosides, and lactosylceramide levels to increase, however, other than seminiferous tubule degeneration causing infertility in males, *GalNAcT*<sup>-/-</sup> mice were phenotypically normal.<sup>41</sup> When *GalNAcT*<sup>-/-</sup> mice were crossed with *Hexb*<sup>-/-</sup> mice, the double knockouts showed GSL profiles identical to *GalNAcT*<sup>-/-</sup> single knockouts. Double knockouts lived throughout the experimental period and did not initially experience the behavioural deficiencies that *Hexb*<sup>-/-</sup> mice did. Eventually, double knockouts developed progressively worsening ataxic gait at seven

months and muscle wasting and hunched posture at nine. Severe ataxia in these mice corresponded with the widespread loss of cerebellar Purkinje cells, which was not observed in *GalNAcT*<sup>-/-</sup> single knockouts. Nonetheless, double knockout of *HexB* and *GalNAcT* prolonged the life of the animals compared to single knockout of *HexB*,<sup>41</sup> suggesting that substrate reduction therapy would be beneficial for the treatment of TSD and SD.

As mentioned earlier, studies of *GalNAcT*<sup>-/-</sup> mice reinforce the idea that complex gangliosides play an important role in neuronal signal transduction. In addition to reduced neural conduction velocity,<sup>4</sup> and axonal degeneration,<sup>6, 7</sup> depolarizing K<sup>+</sup> levels or glutamate caused apoptosis in cerebellar granule neurons of *GalNAcT*<sup>-/-</sup> mice due to persistent intracellular Ca<sup>2+</sup> elevation.<sup>42</sup> These studies suggest that complex gangliosides are important in Ca<sup>2+</sup> homeostasis, axonal maintenance and neuronal transmission; therefore, the administration of substrate reduction therapy may harbor negative consequences especially in children and adolescents where myelination may still be occurring as treatment begins.

*In vitro* studies in the promyelocytic cell line, HL-60 showed decreased levels of neutral glycolipids and gangliosides when cells were treated with NBDNJ. More specifically, GM1 was reduced by 90% in HL-60 cells and three other cell lines upon NBDNJ treatment, indicating inhibition of glycolipid biosynthesis. Further investigation by this group showed that lipid accumulation was prevented in the presence of NBDNJ in a murine macrophage cell line (WEHI-3B) treated with conduritol β-epoxide to mimic the

lysosomal storage phenotype of Gaucher disease,<sup>43</sup> which led to the administration of NBDNJ *in vivo*.

Healthy C57Bl/6 mice treated with NBDNJ presented with smaller spleens and thymuses and grew slower than untreated controls.<sup>44</sup> These findings were encouraging since splenomegaly is a common symptom of lysosomal storage diseases,<sup>45</sup> however, the concentration used to decrease lymphoid organ size was greater than the equivalent clinical dose in humans. Nonetheless, NBDNJ was found to alter lymphocyte populations in these mice. Treated mice had more T cells but fewer B cells in the spleen. As well, thymuses had increased levels of CD4<sup>+</sup> or CD8<sup>+</sup> cells at the expense of CD4<sup>+</sup>/CD8<sup>+</sup> cells.<sup>44</sup> Studies have shown the importance of lipids, specifically gangliosides in lymphocyte development and maturation<sup>46-48</sup> indicating that NBDNJ has the ability to affect immune cell function, which may directly counteract the extensive inflammation present in some LSDs.

Overall, in C57Bl/6 mice, cell surface gangliosides decreased upon NBDNJ treatment but sphingomyelin levels increased.<sup>44</sup> This occurrence may be due to a compensatory mechanism in place to prevent ceramide accumulation by shunting it to other pathways, which is known to initiate apoptosis at high levels.<sup>49</sup> Additionally, while lipid levels recovered two weeks after the drug was removed from the diet, GM2 was the slowest to return to normal.<sup>44</sup> This difference may suggest a more specific, long-term effect of NBDNJ on GM2 synthesis, which may be useful for treatment of the GM2 gangliosidoses. These findings led to the administration of NBDNJ to mouse models of lysosomal storage diseases including TSD and SD.

Tay Sachs disease mice (*Hexa*<sup>-/-</sup>) treated with NBDNJ showed improved neuropathology and significantly less GM2 accumulation than age matched, untreated controls.<sup>38</sup> Similar results were seen in *Hexb*<sup>-/-</sup> mice.<sup>50</sup> In addition to reducing ganglioside levels, NBDNJ significantly reduced the rate of decline of *Hexb*<sup>-/-</sup> mice compared to untreated controls by increasing life expectancy from 125 to 170 days. NBDNJ treated animals performed well in behavioural testing when age matched *Hexb*<sup>-/-</sup> controls were at an advanced stage of disease. Additionally, apoptosis assays done on these mice stained positive in untreated but not NBDNJ treated mice, in most of the brain. However, characteristic tremor at 12 weeks was unavoidable even with treatment.<sup>50</sup> Other studies have observed apoptosis in *Hexb*<sup>-/-</sup> mice as well as human TSD and SD brain, indicating a prevalent role in pathogenesis.<sup>28</sup> Therefore, the ability of NBDNJ to reduce these parameters indicates its relevance to treating LSDs as well as the importance of early intervention.

Further, NBDNJ can act in conjunction with other modes of treatment and has been found to result in synergy. *Hexb*<sup>-/-</sup> mice administered NBDNJ after they had undergone BMT had significantly delayed symptom onset, performed better in behavioural tests, and had the slowest rate of decline compared to untreated mice or those treated with either NBDNJ or BMT alone. Moreover, GA2 levels in treated mice were comparable to untreated SD controls although they lived longer, which suggests that GA2 is not affected by NBDNJ and levels of GA2 may not be a major life expectancy determinant. While brain GM2 levels were similar in untreated, NBDNJ and BMT mice, the NBDNJ/BMT combination resulted in 30% higher GM2. However, the combination

therapy still enhanced survival for *Hexb*<sup>-/-</sup> mice.<sup>34</sup> Based on these data, the authors suggest that pathology is not solely due to a GM2 storage level threshold. This evidence suggests lysosomal accumulations may initiate neuropathology but not propagate it.

Moreover, further studies on the properties of NBDNJ indicate it is proficient at altering other disease symptoms. Elevated levels of pro-inflammatory cytokines TNF- $\alpha$  and IL1- $\beta$  normally observed in *Hexb*<sup>-/-</sup> mice were reduced to near normal levels in those treated with NBDNJ. Additionally, MHC class II and CD68 expression – markers of inflammation – were reduced to normal levels upon NBDNJ treatment as well.<sup>22</sup> This provides further evidence of NBDNJ's wide-reaching impact on disease.

Clinical trials of NBDNJ for use in Gaucher disease treatment have generally been successful, with all reporting a significant reduction in liver and spleen volumes and reduction of disease biomarkers.<sup>33, 51</sup> The major side effect noted by the majority of patients was diarrhea, which responded well to loperamide or a lactose free diet. This symptom is due to  $\alpha$ -glucosidase inhibition.<sup>37</sup> Success in these trials led to the administration of NBDNJ to patients with other LSDs. Jacobs et al. administered NBDNJ to a child with TSD after BMT,<sup>52</sup> and similarly, Bembi et al. studied two young girls with TSD who were also given the drug.<sup>53</sup> Neither study found that NBDNJ was able to arrest neurological deterioration, however, Bembi et al. found it prevented macrocephaly.<sup>53</sup> It is hard to draw any concrete conclusions from these studies; yet, it is likely that due to the severe nature of infantile TSD, NBDNJ must be administered at a very young age before substantial accumulation has taken place for it to have a largely observable affect.

Studies performed on areas other than the brain indicate the wide range of therapeutic effects of NBDNJ. Misago et al. found that NBDNJ stimulated proliferation of human granuloid progenitors from bone marrow blood, yet suppressed the maturation from myelocytes to segmented neutrophils. In addition, NBDNJ slightly induced apoptosis in these cells as measured by flow cytometry.<sup>54</sup> Since neutrophils are strong producers of reactive oxygen species (ROS), and neutrophils isolated from Parkinson's and Alzheimer's patients show higher levels of ROS, this evidence may indicate a role for neutrophils in neurodegeneration.<sup>55</sup> There has also been evidence to suggest NBDNJ can be atheroprotective by altering plasma lipid, lipoprotein and C reactive protein levels in Gaucher patients.<sup>56</sup> These data further suggest a role for NBDNJ in regulation of inflammation as well as GSL reduction, contributing further to its neuroprotective effects.

It is obvious from the aforementioned studies that the complex molecular events in TSD are important modulators of disease pathogenesis. Therefore, gene expression changes specific to TSD can help identify the pathways involved in cellular dysfunction and death. Moreover, treatment with NBDNJ may help elucidate which changes are beneficial and which are detrimental. With this knowledge, it is possible to design new and more effective therapies for the treatment of the disease. The goal of this study is to specifically investigate the role of hypoxia-inducible factor-1 $\alpha$  (HIF-1 $\alpha$ ) and its effectors in TSD.

### Hypoxia Inducible Factor-1

HIF-1 is a protein that consists of an  $\alpha$  and  $\beta$  subunit which are members of the Per/Arnt/Sim (PAS) protein family. This protein family consists of basic helix-loop-helix

proteins that are able to dimerize due to their PAS domain.<sup>57</sup> HIF-1 $\alpha$  is constitutively synthesized and degraded during normoxia,<sup>58</sup> however, under hypoxic conditions, it undergoes modifications that prevent its degradation and subsequently lead to accumulation,<sup>59, 60</sup> dimerization with the constitutively expressed HIF-1 $\beta$ <sup>61, 62</sup> and upregulation of target genes.

HIF- $\alpha$  has three paralogs: HIF-1 $\alpha$ , -2 $\alpha$  and -3 $\alpha$ .<sup>63</sup> Once HIF-1 moves to the nucleus, it recognizes and binds the hypoxia response element (HRE) with the consensus sequence (A/G)CGTG.<sup>64</sup> HIF-1 $\alpha$  is more widely expressed than HIF-2 $\alpha$ , and expression patterns are complementary rather than redundant.<sup>65, 66</sup> HIF-3 $\alpha$  is believed to act as a negative regulator of HIF-mediated transcription.<sup>67</sup> An alternatively spliced product of HIF-3 $\alpha$  called IPAS (inhibitory PAS) dimerizes with HIF-1 $\beta$  to inhibit transcription. This splicing event can be induced by hypoxia and thus provides a regulatory feedback mechanism.<sup>68, 69</sup> The pro-inflammatory cytokine TNF- $\alpha$  increases expression of IPAS and decreases HIF-1 target gene expression in rat PC12 cells but not human Hep3B cells, indicating that its action may be cell type specific, yet could be involved in regulating inflammatory responses.<sup>70</sup>

To function as an oxygen sensor, degradation of constitutively expressed HIF-1 $\alpha$  is mediated through ubiquitylation and proteosomal degradation. It occurs through modification of an oxygen-dependent degradation domain (ODDD), which is flanked by the N-terminal activation domain and the C-terminal activation domain.<sup>59</sup> In the presence of oxygen, iron and 2-oxoglutarate, HIF-1 $\alpha$  is hydroxylated by prolyl hydroxylase domain (PHD) proteins which specifically hydroxylate proline residues 402 and 564 in the

ODDD at a conserved Leu-X-X-Leu-Ala-Pro motif.<sup>60</sup> Hydroxylation allows the von Hippel-Lindau protein (pVHL) to bind HIF-1 $\alpha$ , initiating poly-ubiquitylation and proteosomal degradation.<sup>71-73</sup> As an additional control, hydroxylation of asparagine residue 803 prevents HIF-1 $\alpha$  from interacting with its coactivator p300/CBP.<sup>74-76</sup> This modification is facilitated through factor inhibiting HIF1 (FIH1), which, similarly to PHDs, needs iron, 2-oxoglutarate and O<sub>2</sub> for proper function.<sup>74</sup> Consequently, under hypoxic conditions, both PHDs and FIH1 are inhibited, allowing HIF-1 $\alpha$  stabilization and activation.

Post-translational modification and protein-protein interactions of HIF-1 $\alpha$  are essential for fine-tuning its actions. For example, phosphorylation by ERK1/2 promotes nuclear translocation, interaction with HIF-1 $\beta$  and transactivation of HIF-1.<sup>77, 78</sup> On the other hand, phosphorylation by GSK3 $\beta$  causes destabilization of HIF-1 $\alpha$  independent of pVHL.<sup>79</sup> Another VHL-independent interaction occurs between HIF-1 $\alpha$  and HSP90 via the PAS domain.<sup>80-83</sup> Since this domain is needed for dimerization with HIF-1 $\beta$ , it competes with HSP90 for binding to HIF-1 $\alpha$ . HSP90 thus keeps HIF-1 $\alpha$  accessible and prevents nonspecific degradation.<sup>82</sup> Modifications like these allow refinement of HIF-1 $\alpha$  responses so the appropriate actions may be carried out based on the activation of different signaling pathways.

HIF-1 is classically known to activate genes involved in cellular processes including angiogenesis, glycolysis and vasodilation, which help the cell adapt to hypoxic conditions.<sup>84</sup> Nonetheless, HIF-1 $\alpha$  can be activated under normoxic conditions via transition metals, nitric oxide (NO), ROS and growth factors,<sup>85</sup> indicating that it is

capable of responding in oxygen-independent ways as well. Therefore, HIF-1 $\alpha$  can be thought of as a general stress-response protein rather than a solely hypoxic response protein.

One well studied target of HIF-1 $\alpha$  is microRNA-210 (miR-210).<sup>86, 87</sup> microRNAs (miRNAs) are small endogenous RNA molecules, 19-22 nucleotides long. They are responsible for regulating gene expression by targeting mRNAs for cleavage or repressing their translation.<sup>88</sup> Most miRNAs are found in intronic regions of known genes.<sup>89, 90</sup> miRNAs are transcribed by RNA polymerase II as long, hairpin containing primary transcripts (pri-miRNA) with a 5' cap and poly A tail.<sup>91-93</sup> The miRNA hairpin is cropped from the primary transcript by an enzyme called Drosha into precursor (pre-)miRNA.<sup>94</sup> The hairpin is then exported through exportin-5-RanGTP,<sup>95-97</sup> into the cytoplasm where Dicer cleaves off the hairpin loop leaving a miRNA duplex.<sup>98-101</sup> The mature miRNA is loaded into miRISC (miRNA-containing RNA-induced silencing complex), ready to bind and repress its target.<sup>102</sup>

The first 2-8 nucleotides of a mature miRNA make up the “seed” sequence. It is these nucleotides that bind within the 3' untranslated region (UTR) of their target(s) to repress gene expression.<sup>103</sup> The discovery of miRNAs is rather recent, yet they have been implicated in many molecular processes including CNS development.<sup>104-106</sup> Conditional knockdown of Dicer, leads to neurodegeneration in many different brain cells including cerebellar Purkinje cells,<sup>107</sup> cortical neurons,<sup>108</sup> and astrocytes.<sup>109</sup>

With such an important role in development, it is not surprising that dysregulated miRNA expression has been shown to contribute to neurodegeneration. For instance, an

increase in proinflammatory cytokines has been linked to the accumulation of amyloid- $\beta$  (A $\beta$ ) in Alzheimer's disease (AD).<sup>110</sup> More specifically, these cytokines increase NF- $\kappa$ B, which in turn increases expression of miR-146. miR-146 represses complement factor H, which helps to control the immune and inflammatory response of the brain, thus miR-146 propagates the pro-inflammatory response.<sup>111, 112</sup> In addition, another miRNA, let-7, activates the RNA-sensing Toll-like receptor 7 which results in neuronal cell death. This miRNA is upregulated in the CSF of AD patients,<sup>113</sup> indicating its role in neurodegeneration in AD. Studies like these illustrate miRNAs are a major influence on gene expression regulation and suggest dysregulated miRNA levels may contribute to many pathologies.

The diversity of HIF-1 $\alpha$  regulation and responses indicate it is important for many cellular events. Relevant to LSDs, there is evidence to suggest that HIF-1 $\alpha$  is protective in neurodegenerative diseases. For example, HIF-1 $\alpha$  protein levels are decreased in the brains of AD patients, which results in reduced expression of glucose transporters 1 and 3 – gene targets of HIF-1 $\alpha$ . Impaired glucose uptake leads to the hyperphosphorylation of tau protein contributing to AD pathogenesis.<sup>114</sup> Furthermore, astrocyte activation induced by A $\beta$  was reduced by HIF-1 $\alpha$  stabilization.<sup>115</sup> This is encouraging since astrocyte activation is believed to play a role in many neurodegenerative diseases, including TSD.<sup>8, 26, 27, 116</sup>

Lastly, deletion of the HRE in the promoter of vascular endothelial growth factor (VEGF, another HIF-1 $\alpha$  target gene) results in mice with a progressive motor neuron disease similar to amyotrophic lateral sclerosis (ALS) in humans.<sup>117</sup> Furthermore,

overexpression of VEGF<sup>118</sup> and its receptor (VEGFR2)<sup>119</sup> improved the phenotype of SOD1 mice, a true model of ALS. HIF-1 $\alpha$  and HIF-2 $\alpha$  knockout mice are embryonic lethal and neuron specific deletion of HIF-1 $\alpha$  results in hydrocephalus and reduction in neural stem cells.<sup>120, 121</sup> These examples indicate that HIF-1 $\alpha$  plays a significant role in neuroprotection by counteracting pathways involved in disease and is required for proper neural development.

### Excitotoxicity

Another process that has been investigated in neurodegenerative disease pathology is glutamate excitotoxicity. Excitotoxicity is defined as neuronal death caused by excessive glutamate excitation.<sup>122</sup> It occurs via the excitatory neurotransmitter glutamate, which activates metabotropic or ionotropic glutamate receptors; this facilitates synaptic transmission through release of intracellular calcium stores or opening of ion channels.<sup>123</sup> Ionotropic glutamate receptors include the *N*-methyl-d-aspartate receptor (NMDAR), kainite receptor and the 2-amino-3-(3-hydroxy-5-methylisoxazol-4-yl) propionate receptor (AMPA). AMPAR activation mediates fast excitatory postsynaptic potentials, which increase cell permeability to sodium, potassium and calcium ions. The receptors themselves are tetramers – dimer of dimers – composed of GluR1-4 subunits.<sup>124</sup> Activation of AMPARs and subsequent cell depolarization removes the NMDAR Mg<sup>2+</sup> block, which further increases cation influx, particularly Ca<sup>2+</sup> and leads to cell depolarization and signal transduction.<sup>125</sup>

AMPARs are found throughout the central nervous system in both neurons and glia,<sup>126, 127</sup> and are not confined to the synapse, but are rather found throughout the

membrane where they laterally diffuse to the PSD.<sup>128-131</sup> The position and number of AMPARs present at the synapse is under tight control. Modulation of these parameters contributes to long-term depression (LTD) or potentiation (LTP), that is, the decrease or increase of synaptic efficacy, respectively.<sup>132, 133</sup> Evidence has shown that AMPARs directly across from the site of neurotransmitter release open with ~60% probability, however, receptors positioned even 50 nm from this site are less likely to open.<sup>134-136</sup> This suggests that clustering of AMPARs within a particular location also determines the efficiency of neuronal transmission.

Each GluR subunit has a large extracellular N-terminal domain, four membrane spanning domains (three transmembrane, one re-entrant loop), and a C-terminal intracellular domain.<sup>137, 138</sup> While the N-terminal domains of the four subunits are highly similar, C-terminal domains are not, and thus permit interactions with different proteins allowing receptors to respond differently based on their subunit composition.<sup>139</sup> GluR1, GluR2L (a splice variant of GluR2) and GluR4 have long C-terminal tails whereas GluR2, GluR3 and GluR4c (a splice variant of GluR4) have short C-terminal tails.<sup>140</sup> Differential regulation of GluR subunits is exemplified by the interaction of GluR2 and GluR3 with PDZ domain interacting proteins such as glutamate receptor-interacting protein (GRIP) and protein interacting with C-kinase-1 (PICK1), which do not interact with other GluR subunits.<sup>141, 142</sup> GRIP and PICK1 both bind the same region of GluR2 and GluR3, however, phosphorylation of Ser880 on GluR2/3 by PKC favours association with PICK1.<sup>143</sup> Studies on GRIP and PICK1 knockouts determined that they are not necessary for AMPAR trafficking to the synapse,<sup>144, 145</sup> but instead may regulate its localization to

intracellular pools or stabilization at the membrane.<sup>146, 147</sup> On the other hand, the synaptic protein SAP97 associates exclusively with GluR1 to localize it to the synapse.<sup>148</sup>

AMPARs also interact with transmembrane AMPA receptor regulatory proteins (TARPs). Stargazin and other TARPs function to regulate many aspects of AMPARs by forming very stable interactions.<sup>137, 149-153</sup> TARPs increase AMPAR localization to the membrane as well as their activity,<sup>154-157</sup> and regulate channel gating by slowing desensitization and controlling channel opening rates.<sup>158-163</sup> In addition to GluR1-4, stargazin also associates with PSD-95; phosphorylation of stargazin by PKA and MAPKs prevent this interaction and decrease its localization to the PSD, altering AMPAR localization as well.<sup>164, 165</sup> Phosphorylation of stargazin by Ca<sup>2+</sup>/calmodulin-dependent protein kinase II (CaMKII) prevents diffusion of AMPARs from the synapse. This impedes the normal diffusional exchange of desensitized receptors from the synapse, reducing AMPAR activation.<sup>166</sup> Regulation of AMPAR localization by TARPs may be cell-type specific since cerebellar LTD in Purkinje neurons requires dephosphorylation of stargazin rather than phosphorylation.<sup>167</sup> AMPAR subunit composition and cell type are therefore important in modulating cellular response.

Some synapses only contain NMDARs and are called “silent synapses” since there are no AMPARs to release the NMDAR Mg<sup>2+</sup> block.<sup>168-173</sup> Activity-dependent insertion of AMPARs at the membrane “un-silences” the synapse and facilitates LTP.<sup>174-176</sup> In addition, while membrane expression of AMPARs is maintained at a relatively constant level by dynamically matching endo- and exocytosis, constitutive endocytosis of AMPARs to provide rapid turnover has been documented.<sup>177-180</sup> This process is Ca<sup>2+</sup>

independent,<sup>180, 181</sup> in contrast to NMDAR-dependent internalization which requires the  $\text{Ca}^{2+}$ /calmodulin-dependent phosphatase calcineurin.<sup>182-185</sup> In other cell types however, LTD depends on protein kinase C activation.<sup>186-188</sup> Again, it is likely that due to different AMPAR subunit combinations, different effector molecules are required for cell specific plasticity.

Fundamentally, AMPARs allow the influx of ions including  $\text{Ca}^{2+}$ , which cause a cellular response. Calcium functions as a signaling molecule and effects cell growth and differentiation, membrane excitation and synaptic activity. Intracellular levels are kept low (100 nM) in neurons at rest. This allows for small elevations to efficiently activate cellular events. Normally, neurons are able to control  $\text{Ca}^{2+}$  levels by managing influx and efflux through buffering and compartmentalization. However, excessive influx, for example by over activation of glutamate receptors, or release from intracellular stores, can over-saturate regulatory mechanisms and cause inappropriate activation of  $\text{Ca}^{2+}$ -dependent processes.<sup>189</sup> This can be detrimental in multiple ways by activating proteases, lipases, phosphatases, endonucleases and calpains, increasing levels of oxidative and nitrosative stress, and decoupling electron transfer from ATP synthesis, ultimately leading to cell death.<sup>190</sup> Molecules that block ER calcium release, or that chelate intracellular calcium, have been shown to prevent glutamate induced death<sup>191</sup>, which implicates calcium directly in excitotoxicity.

GluR2 subunits are unique in that they determine  $\text{Ca}^{2+}$  permeability of the AMPAR. mRNA editing of GluR2 results in an arginine to glutamine switch and introduces a positive charge in the re-entrant loop.<sup>192</sup> This charge prevents the passage of

divalent cations through the channel.<sup>193, 194</sup> The majority of AMPARs in the CNS contain GluR2, and are thus  $\text{Ca}^{2+}$  impermeable.<sup>127, 195</sup> During early postnatal development, however, GluR2's expression is low compared to GluR1.<sup>196</sup> This suggests that  $\text{Ca}^{2+}$  permeable AMPARs play a role in shaping early synapse development. Inclusion of GluR2 into AMPARs alters channel properties and hence alters cellular response to glutamate and  $\text{Ca}^{2+}$ .

Dysregulated  $\text{Ca}^{2+}$  homeostasis has been evidenced to play a role in LSDs. GM2 accumulation in *Hexb*<sup>-/-</sup> mice inhibits the sarco/endoplasmic reticulum  $\text{Ca}^{2+}$  ATPase (SERCA), decreasing cytosolic  $\text{Ca}^{2+}$  uptake, and rendering neurons more sensitive to cell death. Reduction of GM2 storage by the glycolipid synthesis inhibitor NBDNJ, reversed these events.<sup>197</sup> Cerebellar granule neurons from *GalNAcT*<sup>-/-</sup> mice undergo apoptosis in response to depolarizing  $\text{K}^+$  levels or exposure to glutamate due to persistent intracellular  $\text{Ca}^{2+}$  elevation.<sup>42, 198</sup> Therefore, these studies show that gangliosides are likely important in the  $\text{Ca}^{2+}$  buffering process since both excess and lack of gangliosides alters homeostasis. In addition, inflammation has been observed to alter AMPAR function. In particular,  $\text{TNF-}\alpha$  increases neuronal excitotoxic susceptibility by increasing  $\text{Ca}^{2+}$  permeable AMPARs at the cell surface which may have implications for LSDs.<sup>199-201</sup>

Since excitotoxicity is so detrimental, there are cellular mechanisms in place to prevent it. The concentration of glutamate in the synapse determines the level of receptor activation and hence must be controlled. Glutamate is removed from the extracellular fluid via excitatory amino acid transporters (EAATs) which are present on neurons and the surrounding glia.<sup>202</sup> These transporters exchange three sodium ions, one proton, and

glutamate for one potassium ion.<sup>203</sup> Glutamate transport therefore results in a net positive charge into the cell and is thus stimulated by a negative membrane potential.<sup>202</sup> The glutamate transport cycle can operate in both directions and is reversible.<sup>203</sup>

Inactivity of EAATs allows glutamate accumulation within the synapse providing a mechanism for excitotoxicity, although cells are capable of protecting themselves to a certain extent. Inactivity of neuronal EAAT3 reduces membrane AMPAR expression and inhibition of EAAT3 reduces total and membrane AMPARs. Internalized receptors are then degraded in a proteasome-dependent fashion thought to be controlled by activation of parasynaptic NMDARs.<sup>204</sup> Regulation of glutamate signaling is hence very complex involving multiple receptors, signaling effectors and re-uptake transporters. Changes in any of these mechanisms have the potential to be detrimental to cellular viability and therefore warrant investigation in excitotoxic diseases.

### Pentraxins

Neuronal pentraxin 1 (NPTX1) and the related proteins neuronal pentraxin 2 (NPTX2) and neuronal pentraxin receptor (NPR) are important neuronal molecules involved in AMPAR localization, apoptosis and synaptic scaling. NPTX1, one of the major focuses of this report, was first discovered as a binding protein for the snake venom toxin taipoxin. It is most highly expressed in neurons of the cerebellum, hippocampus and cerebral cortex.<sup>205</sup> All three of the neuronal pentraxins contain an N-terminal coiled coil domain that facilitates heteromultimerization. Based on X-ray crystallography, NPTX1 and NPTX2 are believed to form hexameric structures, held together by cysteine bonds.<sup>206</sup> This is in contrast to the classical pentraxins which form pentameric structures.<sup>207, 208</sup>

Molecular studies of NPTX2 suggest cysteine (C)14 and C26 interact with the cysteine residues on neighbouring pentraxins to form a radially symmetrical hexamer, while C79 facilitates hexamer-hexamer interactions. NPTX1 can form heteromers with NPTX2 in a similar manner.<sup>206</sup>

The C-terminal pentraxin domain facilitates AMPAR clustering by interacting with the extracellular N-terminal domain of subunits GluR1-4.<sup>206, 209-211</sup> These interactions cluster AMPARs at the synapse, a process characteristic of excitatory synapse formation.<sup>209</sup> Interactions between NPTX1 and NPTX2 affect each others functions. For example, NPTX2 is more effective at clustering AMPARs and increases the efficiency of NPTX1 to do so. In addition, NPTX2 is an activity regulated gene, whereas NPTX1 is constitutively expressed. Therefore, their interactions affects AMPAR signaling in response to different stimuli, and at different times during development.<sup>206</sup> The ability of neuronal pentraxins to modulate AMPAR clustering suggests they may play a role in neuronal excitation since clustering enhances the chance of activation by a stimulus.<sup>134-136</sup>

Both NPTX1 and NPTX2 are secreted, glycosylated proteins,<sup>205, 212</sup> whereas NPR is a transmembrane protein that tethers the secreted pentraxins to the membrane.<sup>212</sup> Cleavage of NPR by the matrix metalloprotease, TACE (tumor necrosis factor- $\alpha$  converting enzyme), releases it from the membrane. Activation of mGluR1/5 is sufficient for TACE activation via PKC. Since NPTX1 and NPTX2 interact with AMPAR subunits and NPR, it is believed that after NPR cleavage, all four components accumulate in

endosomes. This process facilitates mGluR1/5-mediated LTD, and requires neuronal pentraxins.<sup>211</sup>

In addition to its AMPAR clustering capabilities, NPTX1 has been associated with neurodegenerative processes. Levels of NPTX1 mRNA and protein were increased in cerebellar granule neurons (CGNs) cultured under low  $K^+$  or hypoxic-ischemic (HI) conditions. NPTX1 anti-sense oligonucleotides reduced apoptosis and cytotoxicity, and increased cell viability in these experiments.<sup>213,214</sup> Under low  $K^+$  conditions, NPTX1 is mainly localized to mitochondria where it acts upstream of the apoptotic protein, Bax.  $K^+$  reduction decreased mitochondrial length and increased mitochondrial fragmentation, release of cytochrome c, cleavage of caspase-3 and cell death. Although mitochondrial shortening was not prevented with shRNA for NPTX1, fragmentation was, indicating NPTX1 is required for this event. Furthermore, NPTX1 significantly increased levels of Bax in CGNs, however low  $K^+$ -induced NPTX1 overexpression in CGNs from *Bax*<sup>-/-</sup> mice did not undergo apoptosis, demonstrating that NPTX1 acts upstream of Bax.<sup>215</sup> The NPTX1-mediated apoptotic effects of HI have also been linked to GSK3 $\alpha/\beta$ . HI inhibits Akt, leading to activation of GSK3 $\alpha/\beta$  and a corresponding increase in NPTX1. Neurons from *Nptx1*<sup>-/-</sup> mice were protected from the effects of HI,<sup>216</sup> indicating NPTX1 is required for HI-induced apoptosis.

NPTX1 has also been implicated in Alzheimer's disease. Cells cultured with A $\beta$ , showed increased NPTX1 protein levels and cleaved caspase-3 corresponding to increased apoptosis. Again, anti-sense NPTX1 reversed the changes A $\beta$  caused within the cell, including reduced neurite outgrowth, reduced dendrite length and synapse loss.

Overexpression of NPTX1 mimicked the effects of A $\beta$ ,<sup>217</sup> emphasizing a major role for NPTX1 in neurodegeneration.

In addition to the aforementioned functions of NPTX1, it has also been found to be involved in synaptic scaling. Mice lacking NPTX1, NPTX2 and NPR, are viable, fertile, and possess no gross cerebral, cerebellar or hippocampal changes.<sup>212, 218</sup> Nevertheless, NPR knockout reduces the amount of NPTX1 and NPTX2 that can be purified by 50%, indicating it is important for the stabilization of the secreted NPTXs at the membrane.<sup>218</sup> Despite the absence of gross morphological changes, NPTX1 and NPTX2 knockouts have a defect in dorsal lateral geniculate nucleus formation due to a failure in retinal ganglion cell (RGC) axon refinement. RGCs cultured from knockout mice had few synaptic currents with small amplitudes, indicating that glutamatergic synaptic function was delayed without NPTX1 and NPTX2.<sup>218</sup> Other members of the pentraxin family including serum amyloid P component, C-reactive protein and pentraxin-3, interact with the complement protein C1q to activate the complement cascade. Complement proteins function to mark targeted cells for destruction and are an important component of immunity.<sup>219-221</sup> Although it has not been proven, based on the aforementioned evidence, it is likely NPTX1 and NPTX2 are capable of this interaction as well and are therefore fundamental to synaptic maintenance.

Studies on NPTX1 undoubtedly indicate its involvement in AMPAR regulation, and provide it with a role in excitotoxic cell death and neurodegeneration that deserves further study. Here, we attempt to determine its involvement in LSDs, particularly TSD.

### Potassium Channel KCNK2

The potassium channel KCNK2 (also called TREK1) is a dimeric, outwardly rectifying, background potassium channel. In humans, KCNK2 is primarily found in the CNS, particularly in the striatal tissues of the caudate and putamen, spinal cord, amygdala, thalamus and fetal brain.<sup>222</sup> Studies in rat brain have localized it particularly to GABAergic interneurons, where it can be observed on the cell body and cell processes.<sup>223</sup> It is also found at lower levels in the stomach and intestinal tract.<sup>222</sup>

Three mRNA variants of human KCNK2 have been documented. They differ in their 5' ends and therefore two potential promoters have been identified,<sup>224</sup> which provides another degree of control over channel properties. Most published studies on human KCNK2 investigate variant 2 or 3.<sup>225-227</sup> More specifically, variant 3 contains an alternative translation initiation site that results in a  $\Delta 1-56$  truncated protein. This causes shortening of the N-terminal intracellular domain and reduced outward  $K^+$  currents. The deletion also causes a depolarizing shift in resting membrane potential due to the channel's increased permeability to  $Na^+$ .<sup>228</sup> Furthermore, a splice variant missing exon 4 has been described. This variant has no channel activity and is in fact retained in the cytosol. It acts as a dominant negative KCNK2 by dimerizing with full length KCNK2 and preventing it from travelling to the cell surface. This dominant negative form involves interactions with the N-terminus of full-length KCNK2.<sup>229</sup>

Each KCNK2 channel is composed of two subunits and each subunit has four transmembrane and two pore (P) domains.<sup>230</sup> Both P domains of KCNK2 contain a Gly-Phe-Gly motif which makes up the selectivity filter. As a background or "leak"  $K^+$

channel, the activity of KCNK2 drives neuronal membrane potential closer to the  $K^+$  equilibrium potential (-90 mV) by allowing ions to leak out of the cell and therefore tends to reduce cell excitability.<sup>231</sup>

Neurotransmitters like glutamate are known to inhibit background potassium channels to induce membrane depolarization and firing of an action potential.<sup>232-234</sup> This occurs via the postsynaptic group 1 mGluRs (mGluR1/5): glutamate-induced activation of  $G_q$ -coupled mGluRs activates phospholipase C (PLC) and leads to cleavage of  $PIP_2$  into DAG and  $IP_3$ . DAG activates PKC and  $IP_3$  induces intracellular  $Ca^{2+}$  release.<sup>235-238</sup> Evidence suggests DAG directly interacts with KCNK2, whereas PKC phosphorylates it to cause its inhibition. Conversely, related channels KCNK3 and KCNK9 are thought to be regulated by the other side of the pathway via  $IP_3$  instead.<sup>235, 239-243</sup> KCNK2 is not a “pure” open rectifier in that it is blocked by  $Mg^{2+}$  at negative membrane potentials,<sup>244</sup> and phosphorylation by PKA can render it voltage-dependent.<sup>245</sup> These modifications cause KCNK2 activation at depolarized potentials. Together, these events illustrate an important role for KCNK2 in maintenance of cell potential in which glutamate stimulus causes KCNK2 inhibition and subsequent membrane depolarization which thereafter activates KCNK2 to return the cell to resting potential. Moreover, inflammatory molecules can cause activation of mGluR1/5 as well, causing KCNK2 inhibition.<sup>238, 245, 246</sup> This may have implications in TSD where inflammatory cytokines are high.

Because KCNK2 must be able to maintain cellular membrane potential under many conditions, other molecules and environmental changes can cause its activation. Poly unsaturated fatty acids like arachidonic acid (AA),<sup>247</sup> membrane stretch,<sup>248</sup> heat,<sup>249,</sup>

<sup>250</sup> volatile anaesthetics,<sup>251, 252</sup> intracellular acidosis,<sup>248, 253</sup> activation of mGluR2 and mGluR4,<sup>243, 254</sup> and stimulation of p38 and ERK pathways all increase activity.<sup>255</sup> AA and membrane stretch change cell membrane curvature to activate KCNK2. This is reinforced by the observation that lysophospholipids stimulate KCNK2 when present in the outer leaflet of the lipid bilayer, but inhibit KCNK2 when they are present in the inner leaflet because of the convex and concave membrane deformations they create.<sup>231, 256</sup> Residues in the C-terminus of KCNK2 are responsible for facilitating most of these responses.<sup>231</sup>

KCNK2 knockout mice have been useful in determining the physiological function of KCNK2. *Kcnk2*<sup>-/-</sup> mice are more sensitive to epileptic seizures induced by kainic acid (KA), and ischemia. PUFAs, which activate the channel and hyperpolarize the cell, protected wild type mice from KA-induced excitotoxic neuronal death but not *Kcnk2*<sup>-/-</sup> mice, indicating a role for KCNK2 in neuroprotection.<sup>257</sup>

Knockouts are also more sensitive to painful heat stimulation,<sup>258</sup> require higher concentrations of, and longer exposure to volatile anesthetics,<sup>251, 257</sup> and display an antidepressant phenotype due to inhibition of serotonin reuptake.<sup>259</sup> KCNK2 is present pre- and postsynaptically,<sup>249, 260</sup> and extrapolations from work with the yeast homolog, S-type K<sup>+</sup> channel suggest that presynaptic KCNK2 is thus capable of affecting neurotransmitter release.<sup>246</sup> Stimulation of the serotonin receptor lowers cAMP. Since cAMP inhibits KCNK2, serotonin receptor activation would increase KCNK2 activation to hyperpolarize the cell, reduce the action potential firing rate and decrease serotonin release. Therefore, loss of KCNK2 prevents hyperpolarization and increases serotonin release, which has implications for the development of antidepressants.<sup>231</sup>

Consequently, KCNK2 is an important molecule involved in neural signal transduction, with a key role in neuroprotection. Modifications to its activity or expression levels could cause major cellular changes that may affect cell viability.

### Conclusion

Understanding the process through which neurons die in TSD and SD will lead to the development of new therapies and increased quality of life for patients. In addition, TSD and SD share common disease pathways with other neurodegenerative diseases like Alzheimer and Parkinson's diseases. Regardless, there are still many details of the neurodegenerative process that must be worked out. It is the hope that the experiments hereafter help to further our knowledge of these devastating diseases. Inherent regulation of molecules like HIF-1 $\alpha$ , miR-210, NPTX1 and KCNK2 is important to neuronal viability, and alterations in their expression levels may contribute to disease pathology together with ganglioside accumulation, inflammation and microglial activation.

## METHODS

*Cell Culture* - Normal and TSD cerebellar neuroglia were obtained from Dr. Brooks at the Kingsbrook Jewish Medical Centre in New York. Cells were cultured in a 37°C humidified incubator with 21% O<sub>2</sub> and 5% CO<sub>2</sub> and cultured in Dulbecco's modified eagle medium (Invitrogen, 12800017) supplemented with 15% fetal calf serum (12483020), 1% penicillin/streptomycin (15140122) and 0.1% fungizone (15290018) from Invitrogen.

*Genotyping* - DNA from TSD and normal neuroglia was isolated using standard phenol extraction ethanol precipitation. Cells were incubated in lysis buffer (100 mM Tris-HCl pH 8.0, 5 mM EDTA pH 8.0, 0.2% SDS, 200 mM NaCl) with proteinase K (0.1 mg/ml) for 30 minutes. Phenol was added, vortexed, and spun down for 10 min at 16,400 RPM. The top aqueous layer was mixed with ice-cold ethanol and the precipitated DNA was removed and dissolved in water. Primers for exon 11 insertion genotyping were as follows: forward 5'-GCCAGACACAATCATAACAGG-3' and reverse 5'-AGGG GTTCCACTACGTTAGAA-3'. Splice site mutation primers were: forward 5'-CCCCTGAGCAGAAGGCTCTGGTG-3' and reverse 5'-TCCTGCTCTCAGGCCCAACCCTC-3'. The PCR program denatured DNA at 95° for 5 min, then cycled 95°, 55°, 72°, 30 seconds each for 30 cycles. A final extension was done at 72° for 7 minutes.

*SDS-PAGE and Western Blotting* - Cell lysates were harvested in RIPA buffer with protease inhibitors (Complete Mini, Roche, 04693124001) and protein concentrations were estimated using the DC protein assay (Bio-Rad, 500-0111). Samples were added to 6x Laemmli sample buffer and boiled for 10 min before SDS-PAGE. Proteins were

transferred to nitrocellulose membranes and subsequently blocked with 5% non-fat milk in TBS-Tween for 1 hour. Primary antibodies were incubated on the membrane in blocking solution O/N at 4°C with rocking. The following day, blots were washed with TBS-Tween and incubated with secondary antibody for 1 hour. Proteins were detected using Amersham ECL detection reagents and hyperfilm (GE Healthcare, RPN2106 and 28906839). Protein levels were quantified using integrated band density estimated by ImageJ software.

*Immunocytochemistry* - Cells were grown on cover slides overnight and then treated. At harvest, media was removed and cells were washed with cold PBS. Cells were then fixed with 3.8% formaldehyde in PBS for 30 min at RT, washed with PBS and permeabilized with 0.5% Triton-X 100 for 30 min at RT with rocking. After washing, cells were blocked with 20% goat serum for 1 hour at RT and then incubated with primary antibodies in 1% goat serum O/N at 4° C. The following day, cells were washed with PBS-Tween (0.05%), secondary antibodies were diluted in 1% goat serum and incubated with rocking on cells for 1 hour at RT. Cells were washed with PBS-Tween and stained with Hoechst, to visualize nuclei. Once washed, cover slips were lifted from the culture dish, dipped in ddH<sub>2</sub>O and mounted on glass slides with ProLong gold antifade (Invitrogen, P36930).

*RNA Isolation, Reverse Transcription and Reverse Transcription-PCR* - Total RNA from confluent cells was isolated by scraping cells in lysis buffer containing 1% β-mercaptoethanol and passing lysate through an 18½ gauge needle (Norgen Total RNA Purification Kit, 17200 or Ambion Purelink RNA Isolation Kit, 12183018A). RNA was reverse transcribed with oligodT or random primers according to the Superscript III

protocol (Invitrogen Superscript III, 18080-093). RNA, dNTPs, and primers were incubated at 65°C for 5 min, then on ice for 1 min. First strand buffer, DTT, RNase OUT and Superscript III were added to the mixture and incubated at 25°C for 5 min if random primers were used. Then, the mixture was incubated at 50°C for 1 hour and inactivated at 70°C for 15 min.

RT-PCR was performed for KCNK2 variants from cDNA with the following primers: variant 1 forward 5'-CAAACCTTGTGAGAATAAGTGAC-3' and reverse 5'-TCCGTAATTTCCAAAACAGA-3'; variants 2 and 3 forward 5'-CGCTCTCCCCACC TTGTAAA-3' and reverse 5'-GGTTTGGAGTTCTGAGCGGC-3'. cDNA was amplified with the following cycle: 95° for 4 min, then 35 cycles of 95° for 30 s, 44° for 30 s (variant 1) or 53° for 30 s (variants 2 and 3), 72° for 45 s; then 72° for 7 min.

*Taqman Gene Expression Assays* - Taqman assays were performed with Taqman gene expression master mix (Applied Biosystems, 4370048) using cDNA obtained as described above. cDNA was mixed with master mix, and gene specific probes and added to a MicroAmp Optical 96-well Reaction Plate (Applied Biosystems, 4316813). The plate was spun down quickly to remove bubbles and placed in the 7900HT Sequence Detection System (Applied Biosystems). Thermal cycling conditions were as follows: 50°C for 2 min, 95°C for 10 min, then 40 cycles of 95°C for 15 sec, 60°C for 1 min. A standard curve was used and final values are expressed as relative gene of interest divided by the endogenous control (GAPDH). Primers and probes used were as follows: NPTX1 Hs00159652\_m1, KCNK2 Hs00247951\_m1, GriA1 Hs00181348\_m1, NPTX2

Hs00383983\_m1, NPR Hs00204729\_m1, GAPDH Hs99999905\_m1 (Applied Biosystems).

Reverse transcription of miRNA was done separately from total RNA, the SuperScriptIII system was used as above, however, miR-210 and U18 have specific RT primers, (Applied Biosystems, 4427975, miR210 Assay ID: Hs04231470\_s1, U18 Assay ID: 001204) and use a different thermocycler program (16° 30 min, 42° 30 min, 85° 5 min).

*SYBR Green gene expression assays* – SYBR Green assays were performed with SYBR Green PCR Master Mix (Applied Biosystems, 4309155) using cDNA obtained as described above. Primers were as follows: NPTX1 forward 5'-AGCAAGATCGATGAGCTG-3', reverse 5'-TGTCTTTCTGACCTTTCTCG-3' KCNK2 forward 5'-AGCCTCATGAGATTCACAG-3' and reverse 5'-CCTATGGTTATAACAGTGC-3' VEGF forward 5'-AGGGCAGAATCATCACGAAGT-3' and reverse 5'-GGTCTCGATTGGATGGCAGTA-3' and GAPDH forward 5'-CATGAGAAGTATGACAACAGCCT-3' and reverse 5'-AGTCCTTCCACGATACCAAAGT-3'. Samples, master mix and primers were added to a MicroAmp Optical 96-well Reaction Plate (Applied Biosystems, 4316813). The plate was spun down quickly to remove bubbles and placed in the 7900HT Sequence Detection System (Applied Biosystems). Thermo cycling conditions were as follows: 50°C, 2 min, 95°C, 10 min, 40 cycles of 95° C, 15s; 60°C, 1min. SDS (v.2.3) (SABiosciences) was used to analyze all gene expression data.

*Construction of vectors* – For the construction of pGL3-CMV NPTX1 3' UTR: Human brain total RNA (Clontech, 636530) was reverse transcribed using random primers; 732

bp of the 3' end of *NPTX1* was amplified using a forward primer 5'-CTGGGACCGCAAGCTGACCC-3' and a reverse primer 5'-CCCCCGG CCTTTGACAAACC-3'. The amplification program was 4 min at 95°C, 35 cycles of 95°C for 30 sec, 57°C for 30 sec and 72°C for 1 min, and a final extension of 72°C for 7 min. The band was cut, extracted from the gel (GeneClean MP Biomedicals), and cloned into pCR2.1 (TA cloning kit Invitrogen, K2020). pGL3-CMV (as described previously,<sup>261</sup>) was digested with *XbaI* (NEB, R0145) and dephosphorylated with calf alkaline phosphatase (Boehringer Mannheim, 1243284). The 3' UTR sequence was cut from pCR2.1 using *SpeI* (NEB, R0133) and *XbaI* and ligated into pGL3-CMV following agarose gel extraction. Site-directed mutagenesis primers were as follows: mutant 1 forward 5'-ACCGAGGCCGTCGCCCCTGCACCTAAGTCCGCACACAGCCTGGTT TTGTCC-3', mutant 1 reverse 5'-GGACAAAACCAGGCTGTGTGCGGACTTAGGTG CAGGGGCGACGGCCTCGGT-3', mutant 2 forward 5'-GGCCGTCGCCCCTGCACACGCACCTAAGTCCAGCCTGGTTTTGTCCTCA TGCA-3' and mutant 2 reverse 5'-TGCATGAGGACAAAACCAGGCTGGACTTAGGTGCGTGTGCAGGGGCGAC GGCC-3'. Amplification was performed as recommended by manufacturer (Agilent QuikChange II, 200523).

For the construction of pCDNA3-premir210: Human genomic DNA was used as a template for premir-210 amplification using a forward primer 5'-TCGG ACGCCCAAGTTGGAGGGG-3' and a reverse primer 5'-CAGGAACTCCGC ACACTGGT-3'; the program was the same as above except the annealing temperature was 58.6°C for 30 sec and elongation was 72°C for 45 sec. The insert was cloned into

pCR2.1 as described above, then removed with *Bam*HI (Fermentas, ER0051) and *Not*I (NEB, R0189) and ligated into pcDNA3 (Invitrogen). All clones were confirmed by direct sequencing.

*Transfection* - Cells were transfected with the indicated amounts of DNA as recommended by the manufacturer for three days (Qiagen Effectene Transfection Reagent, 301425). Briefly, DNA, DNA-condensation buffer and Enhancer were incubated at room temperature for 5 min, then Effectene was added to the mixture and incubated for an additional 10 min. Media containing serum and antibiotics was added to the complexes and added drop-wise to the cells. Dishes were gently swirled to ensure even distribution of the complexes. pCMV6-NPTX1 was obtained from Origene (RC212316) and contains Myc and DDK tags. As a control, pCMV6-NPTX1 was digested with *Sa*II (NEB, R0138) and *Xho*I (NEB, R0146), gel purified and re-ligated. The clone was named pCMV6-Empty and confirmed with sequencing.

*Luciferase Assays* - Dual luciferase assays were carried out as recommended by the manufacturer (Promega, E1910). Briefly, cells were transfected as described and harvested in 100 µl passive lysis buffer. Lysates were cleared for 30 sec at top speed; 20 µl was plated per well and 50 µl of LARII and Stop & Glo were injected per well automatically by a Luminoscan Ascent luminometer with a 10 second measurement period and a 2 second delay between readings. Values are represented as firefly luciferase activity normalized to *Renilla* luciferase activity.

*Ganglioside Isolation* – Normal and TSD neuroglia were scraped in water and sonicated. Then, a 1:1 mixture of chloroform:methanol was added to the sample to result in a final

concentration of 10:10:1 C:M:H<sub>2</sub>O. Samples were sonicated in a cold water bath for a total of 15 min: 20 sec on, 20 sec off. Next, they were spun down for 15 min at 4°C, 3000 RPM. The supernatant (S1) was removed, 10:10:1 C:M:H<sub>2</sub>O was added to the pellet and sonicated again. The supernatant (S2) was combined with S1. Sonication was repeated again, this time with 30:60:8 C:M:NaAcetate (0.8M); supernatant was combined with S1 and S2. Combined supernatants were evaporated O/N. The next day, 30:60:8 C:M:H<sub>2</sub>O was added to samples and heated to 50°C for 4 hours. The pH was kept at 11 with 4M KOH. Once cooled, glacial acetic acid was used to neutralize samples to pH 7 and samples were spun for 10 min at 4°C, 3000 RPM. Supernatant was transferred to a new tube and evaporated O/N. The following day, samples were resuspended in 700 µl 10:10:1 C:M:H<sub>2</sub>O, loaded onto Sephadex G-50 fine columns (Roche 11273965001) and spun for 2 min at 700 RPM. Then, sample was loaded into prepared columns of DEAE Sepharose Fast Flow (GE Healthcare, 17070901) and washed with 30:60:8 C:M:H<sub>2</sub>O and finally with 30:60:8 C:M:NaAcetate (0.8M) before O/N evaporation. The next day, samples were resuspended in 3:48:47 C:MKCl (0.1M) and loaded onto equilibrated Sep-Pak C-18 columns (Waters, WAT051910). Gangliosides were eluted with 2:1 C:M and evaporated O/N.

*Thin layer chromatography* - Ganglioside samples were resuspended in 10:10:1 C:M:H<sub>2</sub>O and spotted drop-wise with a Hamilton pipette. All sample concentrations were estimated with DC protein assay (BioRad) performed on the original lysate. Acetone phase was run until the front was ~ 1cm from the top of the plate. Then, the plate was removed and allowed to dry before the second 60:35:8 C:M:CaCl<sub>2</sub> (0.2%) phase was run. Plate was

sprayed with 0.2%(w/v) resorcinol (Sigma 2835052 398047) in 10% H<sub>2</sub>SO<sub>4</sub> and then cooked for ~ 1 hour at 120°C.

*Chemicals and Antibodies* - Alexa Fluor 594 goat anti-mouse IgG (Invitrogen, A11005), Alexa Fluor 488 goat anti-rabbit IgG (Invitrogen, A11008), rabbit polyclonal anti-HIF-1 $\alpha$  (H-206) (Santa-Cruz, SC10790), mouse monoclonal anti- $\beta$ -Actin (8H10D10) (Cell Signaling, 3800), mouse monoclonal anti-neuronal pentraxin 1 (BD Transduction Laboratories, 610369), dimethylallyl glycine (DMOG) (Cayman Chemical, 71210), 2-amino-3-(3-hydroxy-5-methylisoxazol-4-yl) propionic acid (AMPA) (Toronto Research Chemicals, A611500), N-butyldeoxynojirimycin (Sigma-Aldrich, B8299), rabbit polyclonal anti-DYKDDDDK tag (Cell Signaling, 2368), N-glycosidase F (Roche, 11365185001), goat anti-rabbit IgG-HRP (Santa Cruz, sc-2004), and goat anti-mouse IgG-HRP (Santa Cruz, sc-2005).

*Statistical analyses* – All statistics were done using a student's unpaired t-test unless indicated differently. All values are reported as the mean  $\pm$  standard error.

## RESULTS

### *Characterization of disease causing mutations in TSD Neuroglia*

In this study, we utilized human normal and Tay Sachs neuroglia cell lines obtained from Dr. Brooks (Kingsbrook Jewish Medical Center, New York, NY) as an *in vitro* model of TSD. Since the cells originated from the offspring of a Jewish couple, we sought to screen for the most common TSD mutations in Ashkenazi Jews. A four base pair insertion, TATC, in exon 11 of *HEXA* causes a frameshift.<sup>21</sup> To detect this mutation, part of exon 11 was amplified from genomic DNA isolated from TSD and normal neuroglia. The PCR product was cleaved with HaeIII. The wild type product resulted in four fragments of 78, 43, 36 and 12 bp. The heterozygous mutant, however, resulted in a 43/47 bp doublet that was detectable on a 12% polyacrylamide gel. In addition, uncleaved mutant product ran as a heteroduplex. Furthermore, the heterozygotic mutation forms a “bubble” of DNA called a heteroduplex that migrates slower than the homozygously paired DNA (Figure 1A).

The second mutation these cells were screened for was the G→C transversion in intron 12. This mutation creates a splicing defect in *HEXA* and creates a DdeI site.<sup>262-264</sup> A section of genomic TSD and normal neuroglia DNA was amplified containing the intron 12 splice junction. The mutant product was cleaved into four fragments: 85, 35, 19 and 12 bp while the wild type product was cleaved into three: 120, 19 and 12 bp (Figure 1B). This confirmed that the neuroglia cells are from a TSD patient compound heterozygotic for the two most common mutations in the Ashkenazi Jewish population.

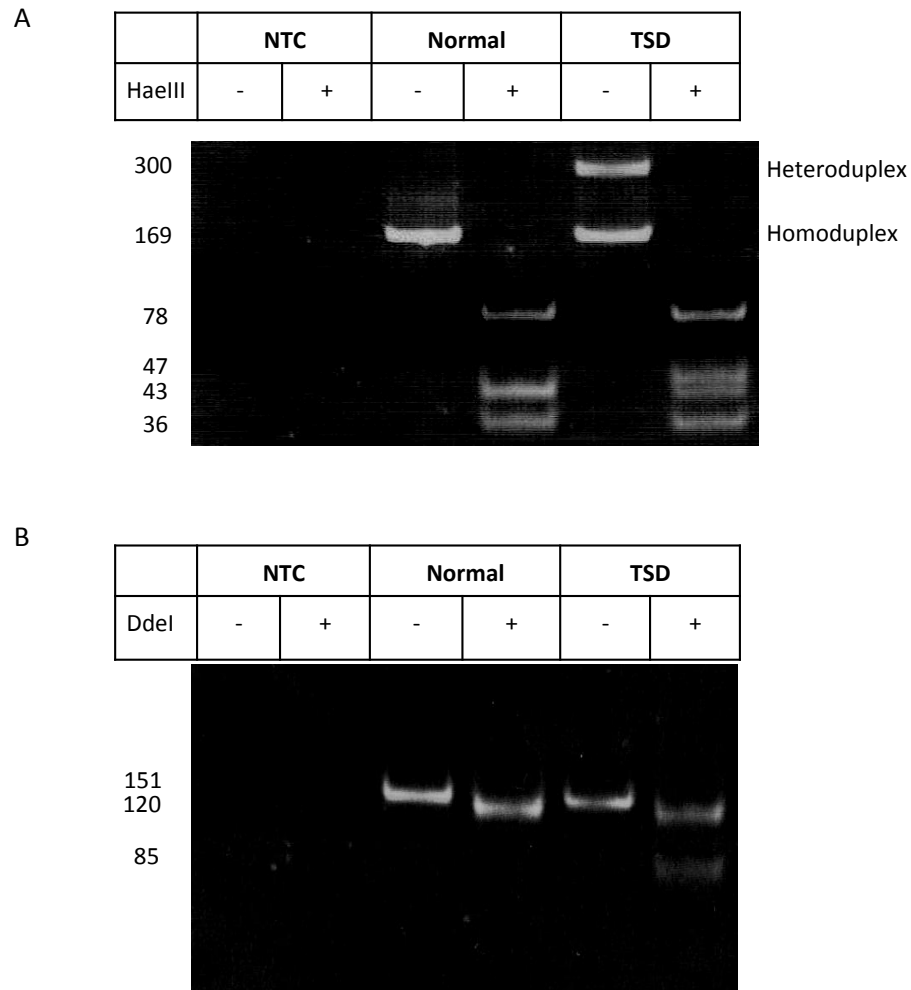


**Figure 1. TSD neuroglia are compound heterozygotes.** DNA from human TSD neuroglia was amplified and cleaved with either HaeIII or DdeI, then visualized on a 12% polyacrylamide gel. A) The four basepair insertion (TATC) in exon 11 of *HexA* is detectable by cleavage of the PCR product with HaeIII. HaeIII cuts normal DNA into four pieces: 78, 43, 36 and 12 bp, three of which are observed above. The mutant product gives a band of 47 instead of 43 bp. This patient has both a 43 and 47 bp band indicating it is heterozygous for the exon 11 insertion. During PCR of the TSD template, heteroduplexes form, which migrate slower than the wild type homoduplex. B) The G→C substitution in the first nucleotide of intron 12 creates a DdeI site; thus, in normal cells, cleavage of the PCR product results in fragments of 120, 19 and 12 bp, whereas cleavage of TSD PCR product results in 85, 35, 19 and 12 bp fragments. These data indicate that the TSD neuroglia have one allele with the insertion and one with the splicing defect.

***HIF-1 $\alpha$  stabilization is defective in TSD neuroglia***

Lysosomal storage diseases like TSD create a very stressful molecular environment. In addition to substrate accumulations, other changes occur, altering signaling pathways which exacerbate disease progression by increasing cytokine expression and activating pro-inflammatory pathways.<sup>23</sup> HIF-1 $\alpha$  was initially studied as an oxygen sensing transcription factor.<sup>265</sup> More recently however, it has also been regarded as a general responder to stress.<sup>85</sup> We performed western blot analyses to investigate the expression of HIF-1 $\alpha$  in normal and TSD neuroglia. Cells were incubated for 48 hours under normoxic or hypoxic conditions, or with the hypoxic mimetic DMOG under normoxic conditions. The experiment was performed in biological triplicate and samples were run on three polyacrylamide gels that were then blotted for HIF-1 $\alpha$  (and GAPDH) in parallel. All cells were approximately 90% confluent at the time of harvest. Protein quantification was performed using ImageJ and levels of HIF-1 $\alpha$  were normalized to GAPDH and averaged. We demonstrated that both cell lines have very little steady state HIF-1 $\alpha$  expression under normoxic conditions. When PHDs were inhibited by DMOG, HIF-1 $\alpha$  accumulated within both cell types, as expected, indicated by a doublet in western blots; however, levels of HIF-1 $\alpha$  expression in TSD neuroglia treated with 2 mM DMOG were lower than that in normal neuroglia ( $2.791 \pm 0.2196$  vs.  $1.354 \pm 0.1385$ , normal vs. TSD respectively,  $n = 3$ ,  $p < 0.005$ ). In addition, under hypoxic conditions, HIF-1 $\alpha$  accumulated in normal neuroglia but not in TSD neuroglia indicating a downregulation of HIF-1 $\alpha$  expression in TSD cells ( $1.309 \pm 0.4407$  vs.  $0.2776 \pm 0.1267$ , normal vs TSD respectively,  $n = 3$ ,  $p < 0.05$ ; Figure 2A,B). Since TSD neuroglia do not

respond to hypoxia by stabilizing HIF-1 $\alpha$ , it is anticipated that gene expression and signaling are altered in these cells as a result of HEXA deficiency. Moreover, cerebellar lysates from C57Bl/6 and *HexB*<sup>-/-</sup> mice indicated that the diseased mice also express lower levels of HIF-1 $\alpha$  (Figure 2C). This supports the idea that hexosaminidase deficiency alters HIF-1 $\alpha$  expression *in vivo*.

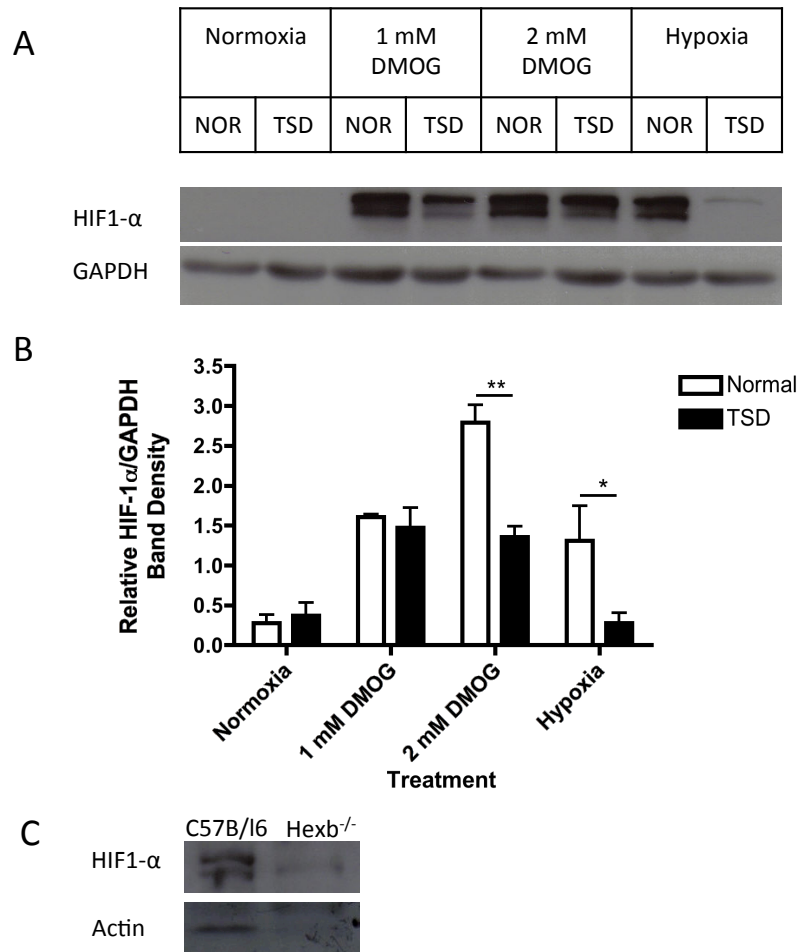


**Figure 2. HIF-1 $\alpha$  stabilization is deficient during hypoxia in TSD neuroglia.** To determine how TSD affects HIF-1 $\alpha$  expression, western blot analysis was performed on normal and TSD neuroglial lysates during normoxia, hypoxia and in the presence of the hypoxia mimetic DMOG for 48 hours. TSD neuroglia were insufficiently able to stabilize HIF-1 $\alpha$  under 2 mM DMOG and hypoxic conditions. A) A representative blot of lysates probed for HIF-1 $\alpha$  and the internal control GAPDH. HIF-1 $\alpha$  appears as a doublet. B) Quantification of relative HIF-1 $\alpha$  expression normalized for GAPDH show a significant difference between TSD and normal cells with 2 mM DMOG treatment and hypoxic conditions. Bars represent average band density of biological triplicates  $\pm$  SEM, n = 3, one-tailed t test, \* p < 0.05, \*\* p < 0.005. C) Western blot of mouse cerebellum from C57Bl/6 and *Hexb*<sup>-/-</sup> mice probed for HIF-1 $\alpha$  and actin showed reduced HIF-1 $\alpha$  levels in *Hexb*<sup>-/-</sup> mice at baseline.

***Cellular localization of HIF-1 $\alpha$*** 

DMOG is a PHD inhibitor that prevents HIF-1 $\alpha$  hydroxylation, resulting in its accumulation within the cell. We used immunocytochemistry to observe the localization of HIF-1 $\alpha$  in response to DMOG in both normal and TSD neuroglia. Cells were plated on glass coverslips overnight, media was replaced the next day with or without DMOG and cells were incubated for 24 hours before they were permeabilized and fixed. We detected HIF-1 $\alpha$  staining in cells without treatment, staining was diffuse in the cytosol of both TSD and normal neuroglia. However, in the presence of DMOG, HIF-1 $\alpha$  staining was brighter and prominently nuclear. This indicates that DMOG stabilizes HIF-1 $\alpha$  and promotes its localization to the nucleus (Figures 3, 4).

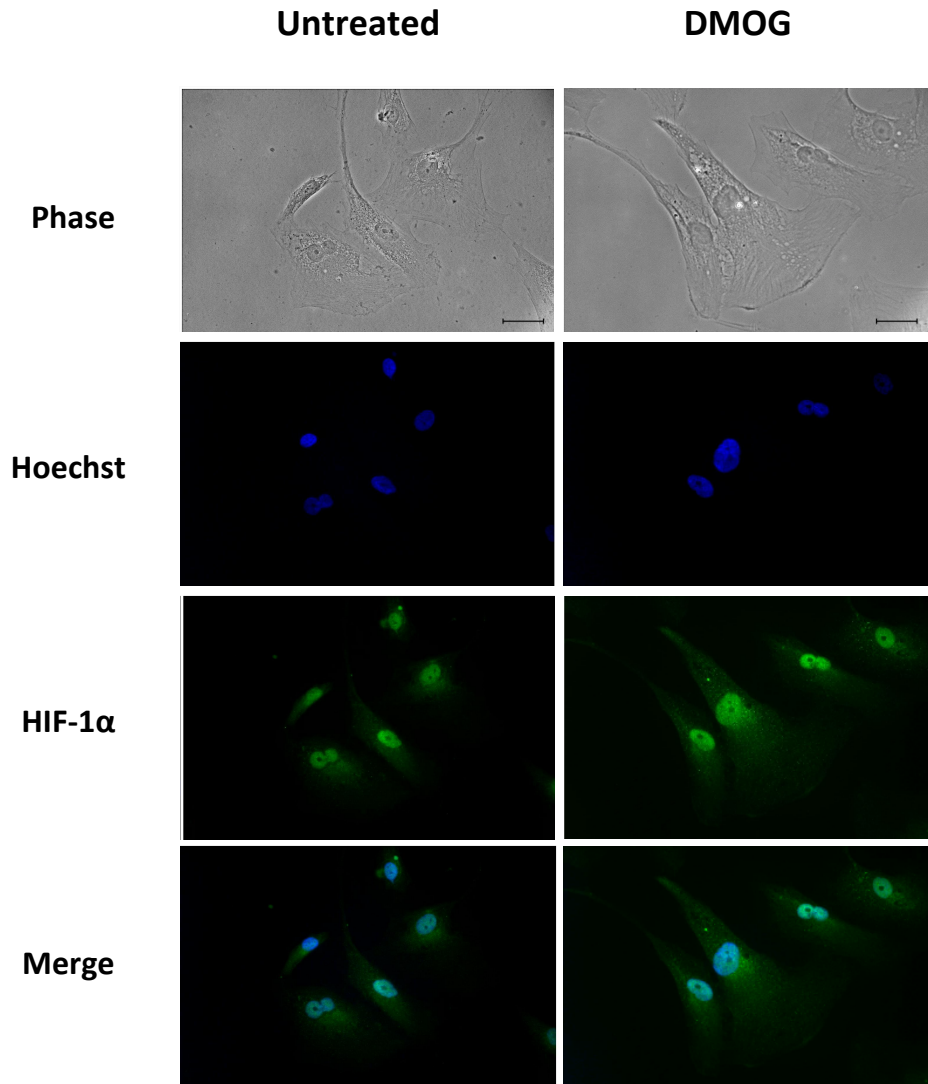


**Figure 3. DMOG localizes HIF-1 $\alpha$  to the nucleus.** Normal neuroglia were plated on coverslides and cultured in media with or without 1 mM DMOG. Cells were fixed, permeabilized and stained for HIF-1 $\alpha$ . DMOG increased the stabilization of HIF-1 $\alpha$  and its localization to the nucleus compared with untreated samples. Scale bars represent 20  $\mu$ m.

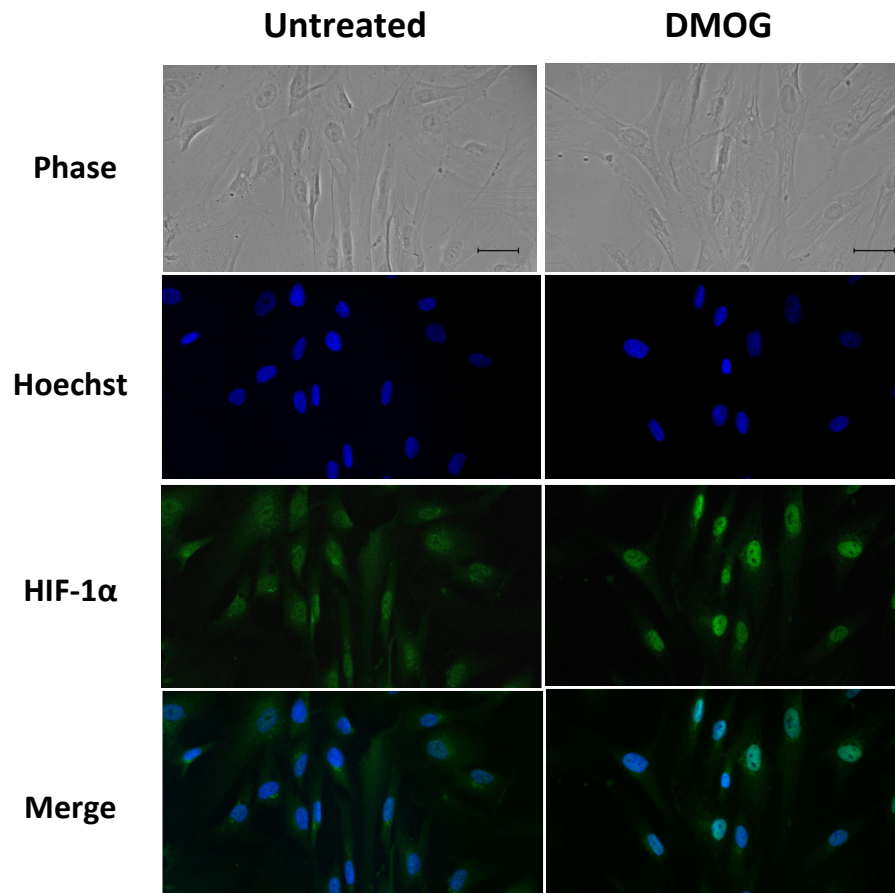


**Figure 4. DMOG localizes HIF-1 $\alpha$  to the nucleus.** TSD neuroglia were plated on coverslides and cultured in media with or without 1 mM DMOG. Cells were fixed, permeablized and stained for HIF-1 $\alpha$ . DMOG increased the stabilization of HIF-1 $\alpha$  and its localization to the nucleus compared with untreated samples. Scale bars represent 20  $\mu$ m.

***Gene expression of neuronal molecules is altered in TSD neuroglia***

In a previous study, we demonstrated that TSD neuroglia are more sensitive to glutamate treatment and as a consequence, to neurotoxicity.<sup>266</sup> In order to examine the roles of molecules involved in glutamate cell response, we measured the expression level of *NPTX1*, *NPTX2*, *NPR*, *GluR1* and *KCNK2* in normal and TSD neuroglia. At baseline, *NPTX1*, *NPTX2* and *KCNK2* expression was significantly higher, whereas *NPR* was significantly lower in TSD compared to normal neuroglia (*NPTX1*  $0.004751 \pm 0.001178$  vs.  $1.649 \pm 0.1456$ ,  $p < 0.0005$ ; *NPTX2*  $0.7894 \pm 0.3334$  vs.  $6.728 \pm 2.158$ ,  $p < 0.005$ ; *KCNK2*  $0.1330 \pm 0.07006$  vs.  $1.001 \pm 0.2121$ ,  $p < 0.01$ ; *NPR*  $0.2551 \pm 0.06079$  vs.  $0.08645 \pm 0.02368$ ,  $p < 0.05$ , normal vs. TSD respectively,  $n = 3$ ; Figure 5). The large increases in *NPTX1*, *NPTX2* and *KCNK2* expression suggest that these molecules are involved in TSD pathology. To investigate the role of these molecules further, and to determine whether this dysregulation was related to the defect in HIF-1 $\alpha$  stabilization, we examined the effect of DMOG and AMPA, the AMPA receptor agonist, on TSD neuroglia.

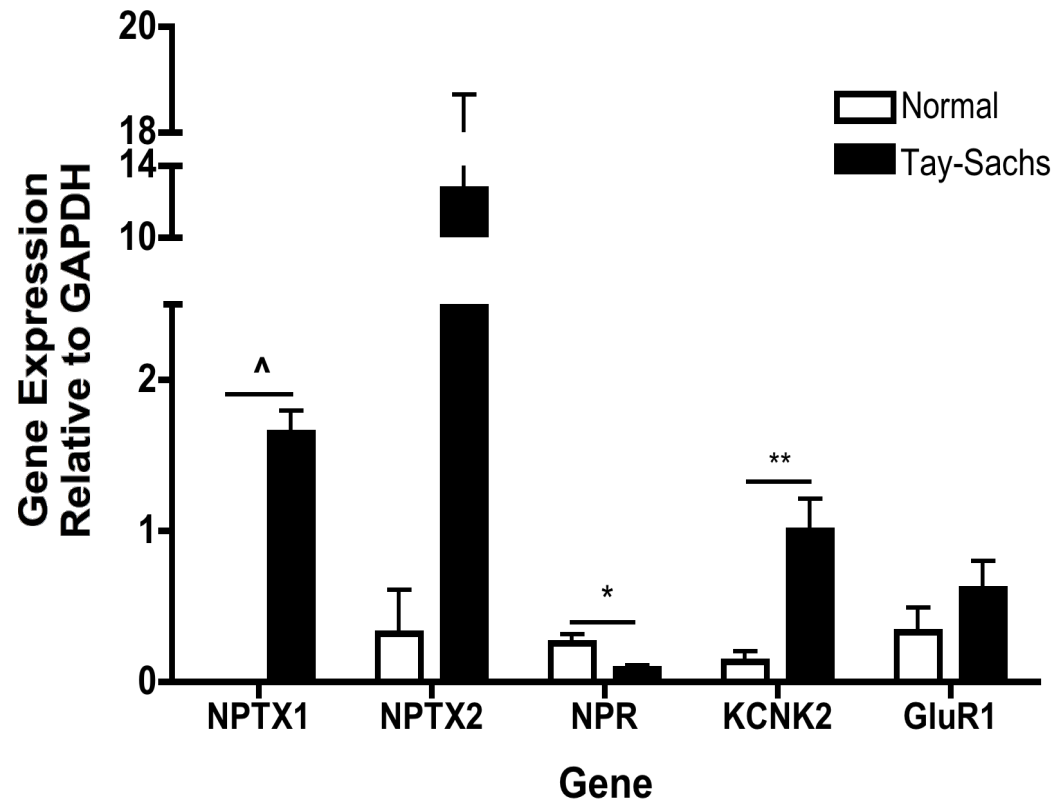


**Figure 5. Gene expression of neuronal molecules in TSD neuroglia.** Neuroglial gene expression of specific neuronal molecules was measured to determine if they were altered by disease. Total RNA was isolated from both genotypes and quantified using Taqman gene expression assays. *NPTX1* and *KCNK2* expression were significantly higher, whereas *NPR* expression was lower in diseased cells versus the control. Bars denote mean  $\pm$  SE,  $n=3$ ; one tailed t-test, \* $p < 0.05$ , \*\* $p < 0.01$ , <sup>^</sup> $p < 0.001$ .

***DMOG and AMPA modify expression of NPTX1, KCNK2 and VEGF***

HIF-1 $\alpha$  regulates many genes in response to hypoxia and cell stress to facilitate cell survival. AMPAR activation can cause neuronal depolarization, and excessive activation may lead to cell death. Low levels of HIF-1 $\alpha$  expression during hypoxia and an increased susceptibility of TSD neuroglia to glutamate suggest that these treatments may contribute to the expression of important neuronal molecules. TSD cells were treated with DMOG (1mM) or AMPA (200  $\mu$ M) for 24 hours. SYBR green q-RT PCR was performed to measure relative RNA levels. We found that *NPTX1* showed a trend to be decreased by HIF-1 $\alpha$  stabilization ( $1.950 \pm 0.3004$ ,  $n = 3$  vs.  $1.014 \pm 0.2138$ ,  $n = 2$ , no treatment vs. DMOG respectively) and was significantly decreased by AMPAR activation ( $1.950 \pm 0.3004$  vs.  $1.149 \pm 0.2204$ ,  $p < 0.05$ , no treatment vs. AMPA respectively,  $n = 3$ ). DMOG/AMPA together further reduced *NPTX1* expression ( $1.950 \pm 0.3004$  vs.  $0.4288 \pm 0.1944$ ,  $p < 0.01$ , no treatment vs. DMOG/AMPA,  $n = 3$ , Figure 6A). *KCNK2* was also repressed by AMPA ( $5.617 \pm 0.5260$  vs.  $3.195 \pm 0.9800$ ,  $p < 0.05$ , no treatment vs. AMPA respectively,  $n = 3$ ) and DMOG ( $5.617 \pm 0.5260$   $n = 3$  vs.  $0.4135 \pm 0.01909$   $n = 2$ , no treatment vs. DMOG respectively). Simultaneous treatment with DMOG and AMPA significantly reduced *KCNK2* expression ( $5.617 \pm 0.5260$  vs.  $0.3160 \pm 0.1834$ ,  $p < 0.0005$ , no treatment vs. DMOG/AMPA respectively,  $n = 3$ , Figure 6B). Reduction of *NPTX1* and *KCNK2* expression by HIF-1 $\alpha$  stabilization and AMPAR activation may therefore control neuronal excitation.

*VEGF* is a target gene of HIF-1 $\alpha$ .<sup>267</sup> Its promoter contains an HRE, where HIF-1 is known to bind to induce gene expression.<sup>64</sup> In addition, loss of VEGF has been shown to

be involved in neurodegenerative diseases like ALS<sup>118</sup> and its expression has been found to increase axon growth and promote neuronal survival.<sup>268</sup> We measured expression of VEGF in TSD neuroglia to determine its involvement in the disease. DMOG, AMPA and the combination treatment altered VEGF expression. DMOG induced expression of VEGF on its own ( $1.671 \pm 0.3585$ ,  $n = 3$  vs.  $3.252 \pm 0.2163$   $n = 2$ , no treatment vs. DMOG respectively) and in the presence of AMPA ( $1.671 \pm 0.3585$   $n = 3$  vs.  $7.727 \pm 3.058$ ,  $n = 2$ , no treatment vs. DMOG/AMPA respectively). Conversely, AMPA by itself significantly reduced VEGF expression ( $1.671 \pm 0.3585$  vs.  $0.6066 \pm 0.07225$ ,  $p < 0.05$ , no treatment vs. AMPA respectively,  $n = 3$ , Figure 6C). These data support the evidence that suggests a neuroprotective role for VEGF. Since VEGF contributes to the stimulation of growth and survival of neurons and glia, its repression by AMPAR activation may contribute to neurodegeneration.

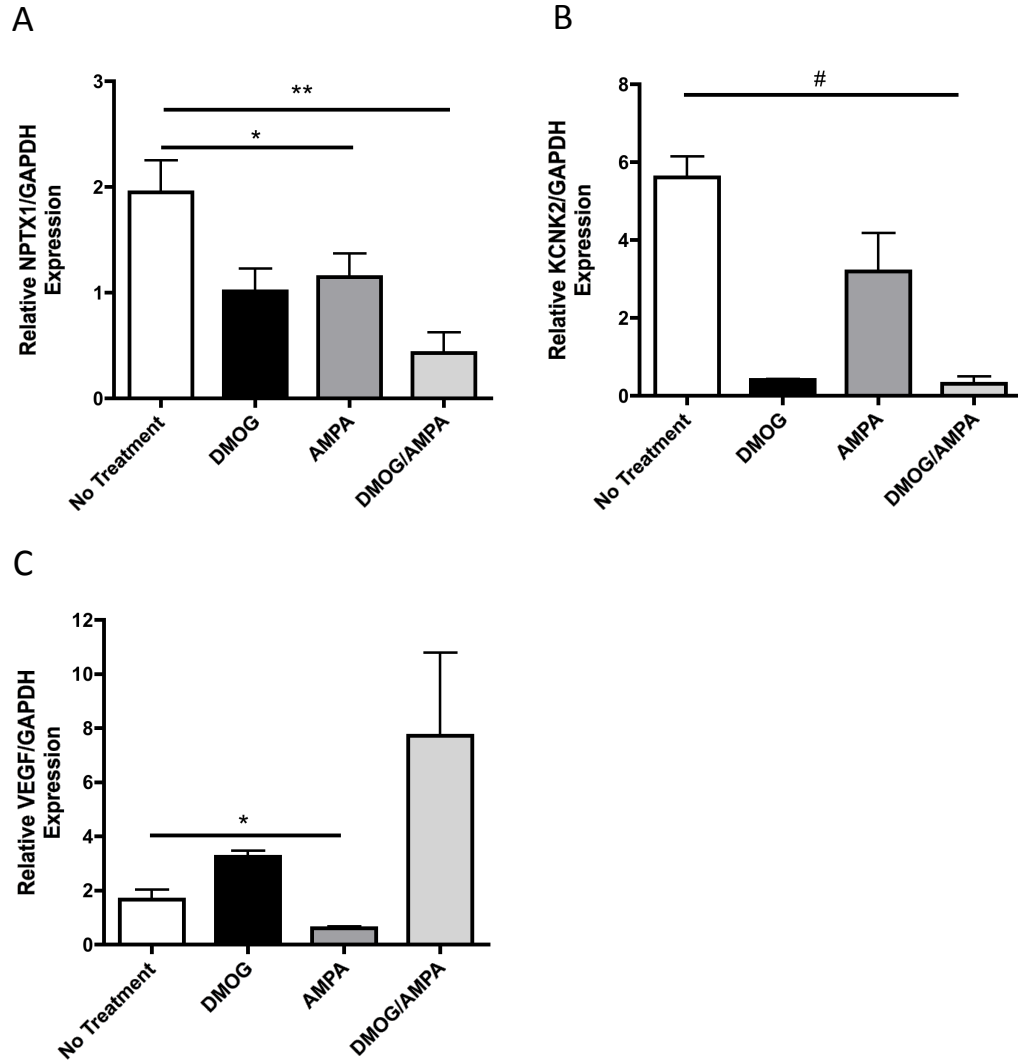


**Figure 6. DMOG and AMPA modify NPTX1, KCNK2 and VEGF expression.** Neuroglial gene expression was measured after 24 hours of treatment with 1 mM DMOG or 200 μM AMPA to determine how HIF-1α stabilization and AMPAR activation affected NPTX1, KCNK2 and VEGF. A and B) DMOG and AMPA reduced NPTX1 and KCNK2 expression alone and together. C) VEGF is a known target of HIF-1α. DMOG caused a significant increase in VEGF expression, however, AMPA caused a reduction compared to baseline and DMOG alone. DMOG is capable of upregulating VEGF despite the presence of AMPA. Bars denote mean ± SE, n=3; one tailed t-test, \*p < 0.05, \*\*p < 0.01, #p < 0.0005.

***HIF-1 $\alpha$  represses expression of *NPTX1* and *KCNK2****

Since HIF-1 $\alpha$  is a major regulator of cellular response to stress, we hypothesized that the difference in HIF-1 $\alpha$  expression in TSD cells would contribute to the changes seen in the genes mentioned above. To investigate the effect of stabilized HIF-1 $\alpha$ , Taqman qRT-PCR was performed on samples from cells treated with DMOG or cultured under hypoxic conditions for 48 hours (Figure 7). *NPTX1* expression was significantly higher in TSD neuroglia compared to normal neuroglia under normoxic conditions ( $0.4965 \pm 0.004653$  vs.  $12.08 \pm 0.9210$ ,  $p < 0.0005$ , normal vs. TSD neuroglia,  $n = 3$ ), this trend was maintained after DMOG-mediated HIF-1 $\alpha$  stabilization, although two samples did not amplify during the qRT-PCR reaction and therefore statistical tests could not be performed ( $0.05650 \pm 0.0009337$ , normal neuroglia 1 mM DMOG,  $n = 3$ ;  $0.9543 \pm 0.1512$ , TSD neuroglia 1 mM DMOG,  $n = 2$ ;  $0.1713 \pm 0.03725$ , normal neuroglia 2 mM DMOG,  $n = 3$ ;  $0.4768 \pm 0.1263$ , TSD neuroglia 2 mM DMOG,  $n = 2$ ). During hypoxic conditions, the level of *NPTX1* expression decreased compared to normoxic levels ( $0.4965 \pm 0.004653$  vs.  $0.2080 \pm 0.009281$ ,  $p < 0.0001$ , normal normoxia vs. normal hypoxia,  $n = 3$ ;  $12.08 \pm 0.9210$  vs.  $1.509 \pm 0.1967$ ,  $p < 0.0005$ , TSD normoxia vs. TSD hypoxia,  $n = 3$ ), however, TSD neuroglia still expressed higher *NPTX1* compared to normal neuroglia ( $0.2080 \pm 0.009281$  vs.  $1.509 \pm 0.1967$ ,  $p < 0.005$ , normal vs. TSD,  $n = 3$ , Figure 7A).

As seen previously, *KCNK2* expression was significantly higher in TSD neuroglia compared to normal neuroglia under normoxic conditions ( $2.195 \pm 0.1250$  vs.  $12.46 \pm 0.9093$ ,  $p < 0.0005$ , normal vs. TSD,  $n = 3$ ). This difference between genotypes was

maintained with 1 mM DMOG treatment ( $0.04552 \pm 0.002893$  vs.  $0.1494 \pm 0.00947$ ,  $p < 0.0005$ , normal vs. TSD,  $n = 3$ ), 2 mM DMOG treatment ( $0.02122 \pm 0.001508$  vs.  $0.07232 \pm 0.008656$ ,  $p < 0.005$ , normal vs. TSD,  $n = 3$ ) and hypoxia ( $0.6941 \pm 0.02679$  vs.  $2.622 \pm 0.2421$ ,  $p < 0.001$ , normal vs. TSD,  $n = 3$ ). HIF-1 $\alpha$  stabilization by DMOG or hypoxia in normal neuroglia significantly decreased *KCNK2* expression compared to normoxic levels (one-way ANOVA,  $p < 0.001$  for all), as it does in TSD neuroglia as well (one-way ANOVA, normoxia vs. hypoxia  $p < 0.001$ ; DMOG vs hypoxia  $p < 0.05$ ). However, although *KCNK2* expression during hypoxia is still repressed, the larger difference between normal and TSD neuroglia suggests *KCNK2* expression is under the control of HIF-1 $\alpha$  (Figure 7B). Nevertheless, the decrease in expression of *NPTX1* and *KCNK2* during hypoxia suggests that while HIF-1 $\alpha$  regulation may be impaired in TSD neuroglia, it is not completely absent.

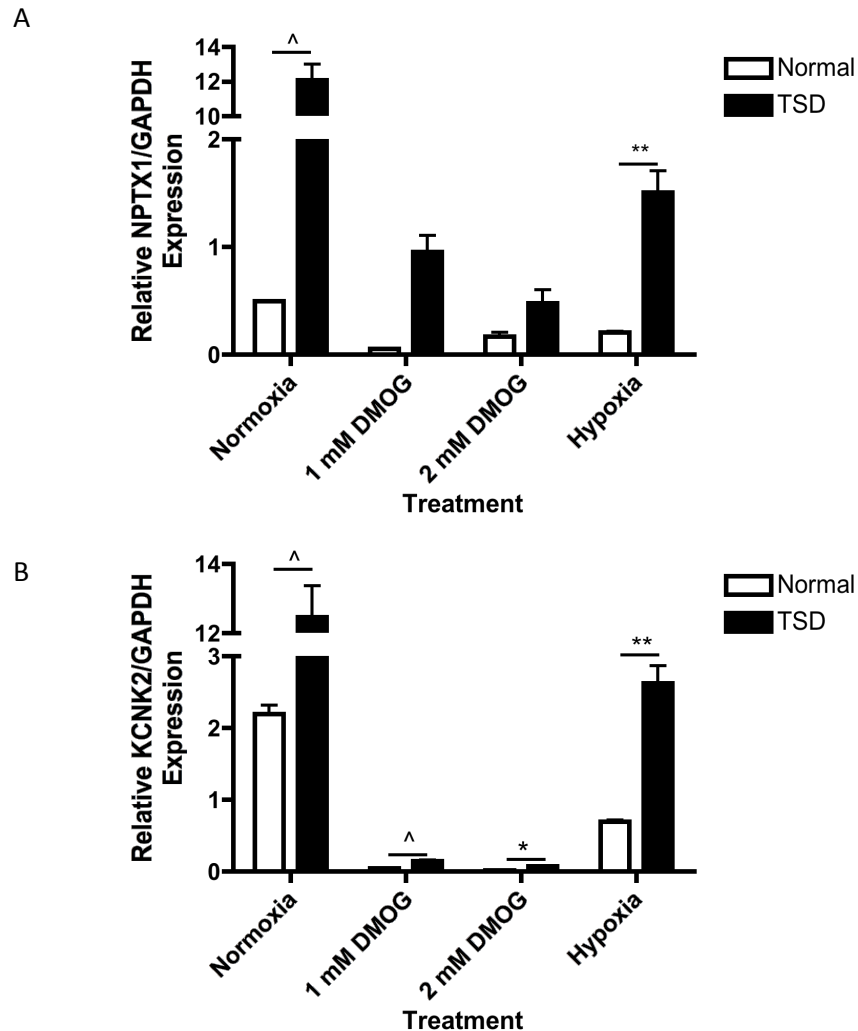


**Figure 7. *NPTX1* and *KCNK2* expression is higher in TSD cells; hypoxia and hypoxia mimetic DMOG decrease their expression.** A) Prediction algorithms suggest miR-210 binds the 3' UTR of *NPTX1* resulting in reduced expression. *NPTX1* expression was measured to determine if levels of miR-210 expression were inversely correlated in the presence of hypoxia or its mimetic. Gene expression was measured after cells were treated for 2 days. TSD cells showed significantly higher levels of *NPTX1* compared to normal cells. Significance was maintained when HIF-1 $\alpha$  was stabilized chemically or physiologically, although total expression levels decreased compared to baseline. B) To determine if *KCNK2* expression was also altered during hypoxic conditions, its expression was measured under the same conditions. Hypoxia and DMOG significantly reduced *KCNK2* expression compared to baseline, however, TSD neuroglia consistently expressed higher levels when compared to normal neuroglia. Bars denote mean  $\pm$  SE, n=3, n=2 for two TSD samples (one each from *NPTX1*, 1 mM DMOG and 2 mM DMOG); one tailed t-test \* p < 0.005, \*\*p < 0.001, ^ p < 0.0005.

***miR-210 is expressed at higher levels in TSD neuroglia.***

HIF-1 $\alpha$  is a transcription factor responsible for the regulation of many different cellular processes. One of the molecules it is known to regulate is miR-210.<sup>86, 269</sup> The promoter of miR-210 contains a hypoxia response element (HRE) that is not only present in humans but is conserved in mice, rats, and dogs (Figure 8A).<sup>269</sup> We hypothesized that differences in HIF-1 $\alpha$  stabilization in TSD cells would also alter miR-210 expression. This was investigated using Taqman qRT-PCR for miR-210, which is normalized to the control miRNA, U18. Our results demonstrated a slight but significant increase in miR-210 expression in TSD cells at baseline ( $0.1520 \pm 0.02809$  vs.  $0.2507 \pm 0.03253$ , normal vs. TSD respectively,  $n = 3$ ,  $p < 0.05$ ; Figure 8B), indicating that regulation of miR-210 at baseline in TSD neuroglia is independent of HIF-1 $\alpha$  regulation.

Furthermore, to investigate how miR-210 responds to HIF-1 $\alpha$  stabilization, miR-210 expression levels were measured in the presence of DMOG (1 mM or 2 mM) at normoxic conditions (21% O<sub>2</sub>) and under hypoxic conditions (1% O<sub>2</sub>) for 48 hours. The difference in miR-210 expression between normal and TSD cells under these conditions was intensified, with TSD neuroglia showing higher levels of expression in all treatments ( $0.5956 \pm 0.04452$  vs.  $1.484 \pm 0.08680$ ,  $p < 0.0005$ , 1 mM DMOG;  $0.6994 \pm 0.03729$  vs.  $1.138 \pm 0.04147$ ,  $p < 0.001$ , 2 mM DMOG;  $0.7515 \pm 0.02807$  vs.  $1.587 \pm 0.1552$ ,  $p < 0.005$ , hypoxia; normal vs. TSD respectively,  $n = 3$ ; Figure 8B). These data indicate that although miR-210 is higher in TSD cells at baseline, it is still, at least partly, under the transcriptional control of HIF-1 $\alpha$ . miR-210 expression is significantly increased in TSD neuroglia when HIF-1 $\alpha$  is stabilized pharmacologically and physiologically, in

comparison to normal cells. This may indicate that miR-210 is regulated differently in TSD neuroglia, or that these cells are missing a level of control that normal neuroglia possess.

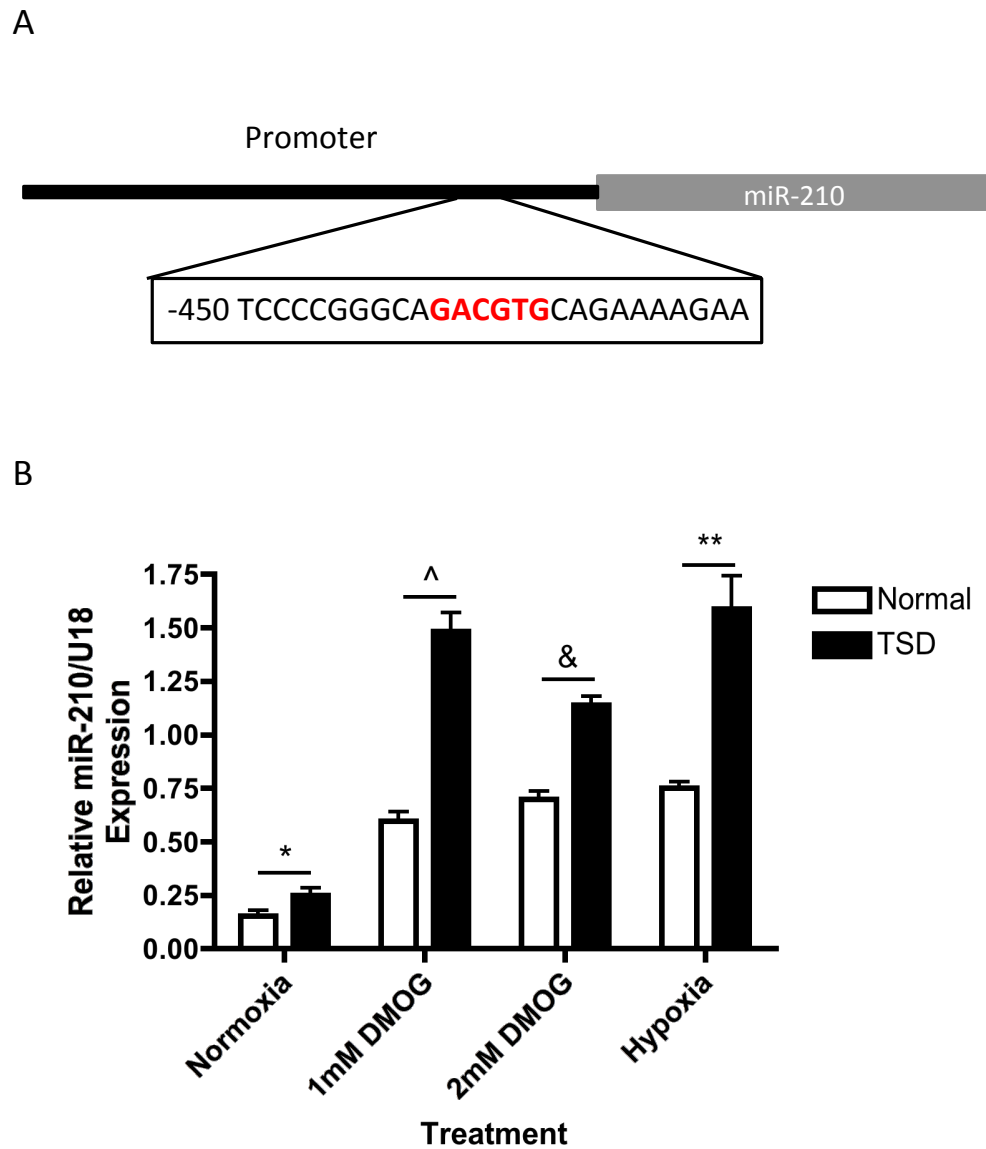


**Figure 8. miR-210 expression is higher in TSD cells; hypoxia and hypoxia mimetic DMOG, increase miR-210 expression.** A) miR-210 is under the control of HIF-1 $\alpha$ . Its promoter contains an HRE (indicated in red). B) To determine the effect deficient HIF-1 $\alpha$  had on miR-210 expression, miR-210 was measured after cells were treated for 2 days with or without DMOG under normoxic conditions, or without treatment under hypoxic conditions. TSD cells showed significantly higher levels of miR-210 compared to normal cells at baseline. Significance increased when HIF-1 $\alpha$  was stabilized chemically or physiologically. Bars denote mean  $\pm$  SE, n=3; one tailed t-test \* p < 0.05, \*\*p < 0.005, & p < 0.001, ^ p < 0.0005.

***miR-210 is predicted to bind the 3' UTR of NPTX1***

miRNAs are gene regulators.<sup>88</sup> The differential expression of miR-210 in normal and TSD neuroglia suggests that its targets are potentially dysregulated in TSD. To investigate potential targets of miR-210, we used the online miRNA target predictor PicTar.<sup>270</sup> miR-210 was predicted to bind to the 3' UTR of *NPTX1* (Figure 9). We therefore examined the expression levels of *NPTX1* in TSD neuroglia to investigate whether a connection exists between *NPTX1* expression and aberrant miR-210 levels.

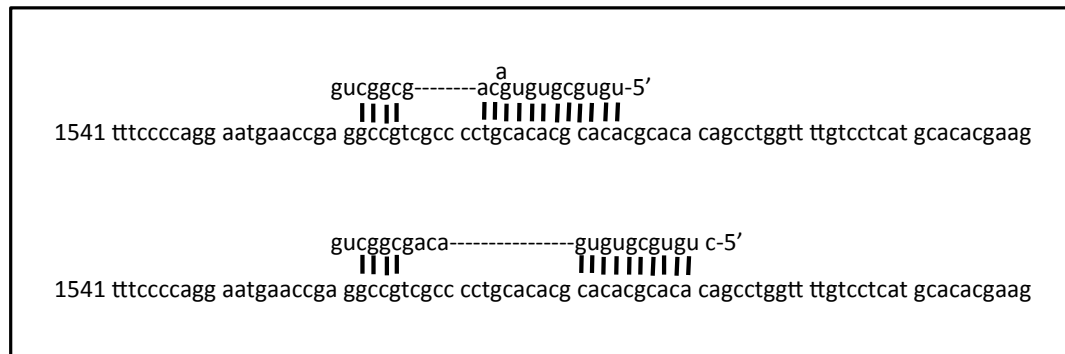


**Figure 9. Predicted binding of miR-210 to the 3' UTR of *NPTXI*.** The online miRNA target predictor PicTar suggested miR-210 may bind to the 3' UTR of *NPTXI*. Pictured above are two possible binding orientations. The sequence shown is 1541-1620 bp of *NPTXI* 3'UTR, miR-210 is above the mRNA sequence in the opposite orientation.

***The effect of miR-210 on NPTX1 expression***

To determine if miR-210 directly represses *NPTX1* expression, we used the dual luciferase reporter assay (Promega). Expression vectors containing the 3' UTR of *NPTX1* were created using cDNA from TSD neuroglia. The sequence was cloned into pGL3-CMV and site directed mutagenesis was performed to mutate seven nucleotides that form putative seed sequences (Figure 10). TSD cells were co-transfected with pGL3-CMV *NPTX1* 3' UTR, pGL3-CMV *NPTX1* 3' UTR Mutant 1 or pGL3-CMV *NPTX1* 3' UTR Mutant 2 (0.2 µg) and pRL-CMV control (0.02 µg). Half were also transfected with pCDNA3-premir210 (0.2 µg). After 72 hours, cells were harvested and luciferase activity was measured. Both mutant vectors were expressed at significantly higher levels compared to pGL3-CMV at baseline ( $36.62 \pm 1.919$  vs.  $47.34 \pm 1.937$  mutant 1,  $p < 0.01$ ,  $n = 3$ ; vs.  $46.30 \pm 1.278$  mutant 2,  $p < 0.01$ ,  $n = 3$ ; 2-way ANOVA). Co-expression of pCDNA3-premir210 caused expression from pGL3-CMV 3' UTR *NPTX1* and mutant 2 to decrease compared to pGL3-CMV, whereas mutant 1 did not ( $34.04 \pm 3.253$  pGL3-CMV 3' UTR *NPTX1*,  $33.61 \pm 1.520$  mutant 2 vs.  $41.49 \pm 1.615$ ,  $p = 0.0547$  mutant 1;  $n = 3$   $p < 0.01$ , 2-way ANOVA, Figure 11). This indicates that miR-210 represses expression of *NPTX1*, the binding site of which is maintained when the nucleotides in mutant 2, but not mutant 1, are changed.



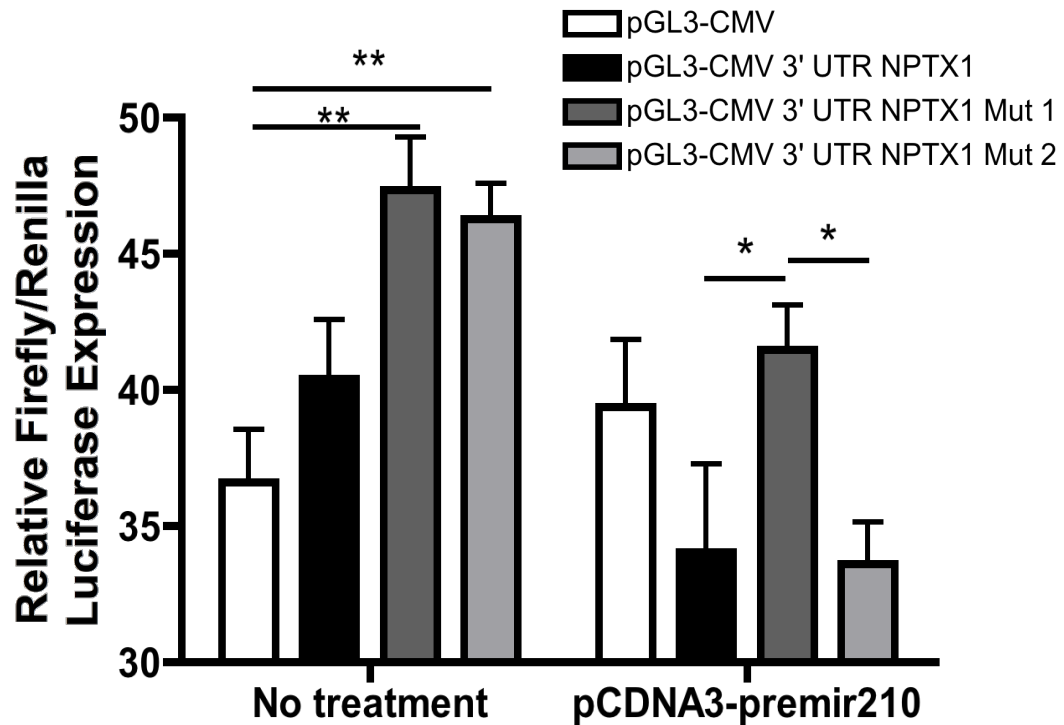


**Figure 11. Mutant 1 reduces binding of miR-210.** Predicted binding sites for miR-210 were mutated to determine the exact site of miR-210 binding in the 3' UTR of NPTX1. Luciferase expression increased in both mutant vectors compared to pGL3-CMV and pGL3-CMV 3' UTR NPTX1 without treatment. When miR-210 was co-transfected (as pCDNA3-premir210), expression from pGL3-CMV 3' UTR and mutant 2 decreased compared to pGL3-CMV. On the other hand, luciferase expression from mutant 2 was significantly different from that of mutant 1. Expression from mutant 1 showed a trend toward an increase in expression compared to pGL3-CMV 3' UTR NPTX1 ( $p=0.0547$ ). Together, this suggests that the nucleotides mutated in mutant 1 participate in binding of miR-210. Bars denote mean  $\pm$  SE,  $n=3$ ; 2-way ANOVA \*  $p < 0.05$ , \*\* $p < 0.01$ .

### ***Expression of Neuronal Pentraxin 1***

Despite high mRNA levels in TSD neuroglia, endogenous protein levels are hard to detect. Similar results are described in the literature, suggesting high protein turnover or low translational efficiency.<sup>205</sup> To study modifications of the protein, we used a vector overexpressing NPTX1. TSD neuroglia were transfected with 2 µg pCMV6-NPTX1 or a control empty vector. Lysates and media were collected 72 hours after transfection. Western blotting with the tag antibody DDK revealed 51 and 120 kDa bands in lysates and a smaller 49 kDa band in media (Figure 12A). These findings confirm that NPTX1 forms multimers in TSD neuroglia. Also, a truncated form of the protein was secreted in the media, which is most likely missing the signal peptide found at the N-terminus.

Further, lysates were treated with 1 unit N-glycosidase F per µl of sample (15 µg total protein) overnight and then subjected to western blotting. Blots probed with anti-DDK indicate both the multimeric and monomeric forms of NPTX1 are glycosylated (Figure 12B).

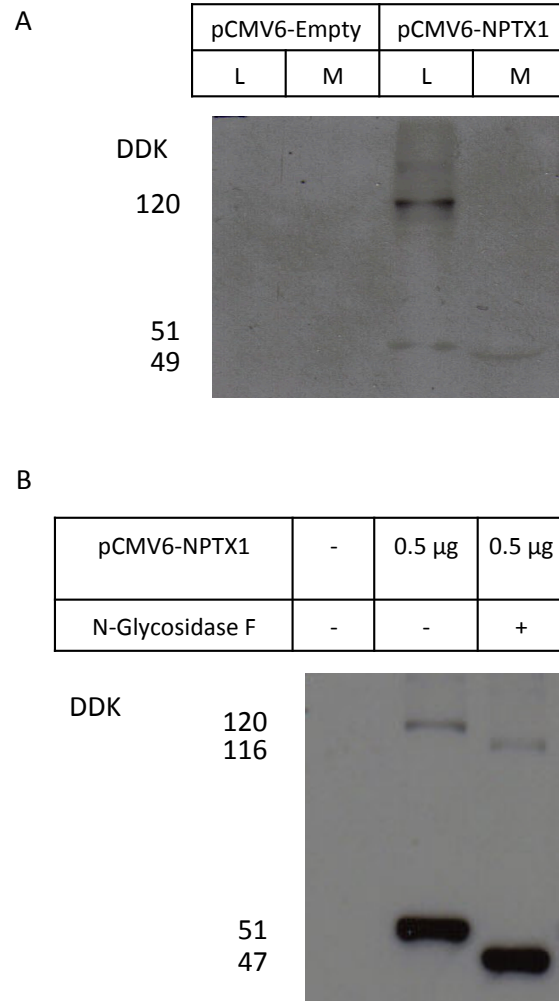


**Figure 12. NPTX1 associates in multimers and is glycosylated.** A) Endogenous levels of NPTX1 are low in both normal and TSD cells, however, TSD neuroglia express higher levels compared to normal neuroglia. B) TSD neuroglia were transfected with 2 µg of pCMV6-Empty or pCMV6-NPTX1. Media was collected and cells were harvested 72 hours after transfection. Probing with anti-DDK revealed bands with molecular weights of 51 and 120 kDa in lysates and a slightly smaller 49 kDa band in media, indicating that NPTX1 associates in  $\beta$ -mercaptoethanol-resistant multimers and is secreted into the media. C) Samples of TSD neuroglia transfected with pCMV6-NPTX1 were deglycosylated with N-glycosidase-F to investigate post-translational modification. The membrane was probed with anti-DDK, therefore only transfected NPTX1 is visualized. Monomeric and multimeric complexes are detected on the blot. The shift indicates glycosylation of NPTX1 in both forms. L, lysate M, media.

### ***Regulation of Potassium Channel KCNK2 Expression***

*KCNK2 promoter analysis reveals rHREs.* There are multiple transcript variants for *KCNK2*. NCBI Aceview indicates that the variants differ in their first exons and 5' UTR, but share exons 2-7 (Figure 13). In order to investigate the observed down regulation of *KCNK2* expression via HIF-1 $\alpha$ , we analyzed both putative promoters 2 kb upstream of the transcription start sites. Knowing that DMOG and hypoxia are capable of repressing expression of *KCNK2* (Figures 6,7), we examined the putative promoter sequences specifically for reverse HRE (rHRE) elements (consensus sequence TGCAC). We discovered three putative rHREs in promoter 1 and two rHREs in promoter 2 (Figure 13). This suggests that *KCNK2* may be negatively regulated by HIF-1 $\alpha$  via a rHRE site.

*Three major variants of KCNK2 are expressed in TSD neuroglia.* Exon skipping in *KCNK2* variants results in three putative proteins of varying lengths. All three have validated 5' caps, but only the longest isoform, which we refer to as variant 1, contains a validated polyA signal.<sup>224</sup> Variant 1 uses a different first exon than the other variants. Variants 2 and 3 share the 5' end of their first exons but variant 3 contains an additional 125 bp at its 3' end before the next common exon. To determine which variants were present in TSD cells, we designed primers that were specific for the 5' end of each variant. RNA was isolated from TSD cultures, reversed transcribed with oligodT primers and amplified using PCR. All three variants were detected. Since variants 2 and 3 share a common 5' end, the reaction amplified two different sized fragments (Figure 14). These results indicate that any or all variants may contribute to the increased *KCNK2* expression observed in these cells and may alter *KCNK2* function and cell excitability.

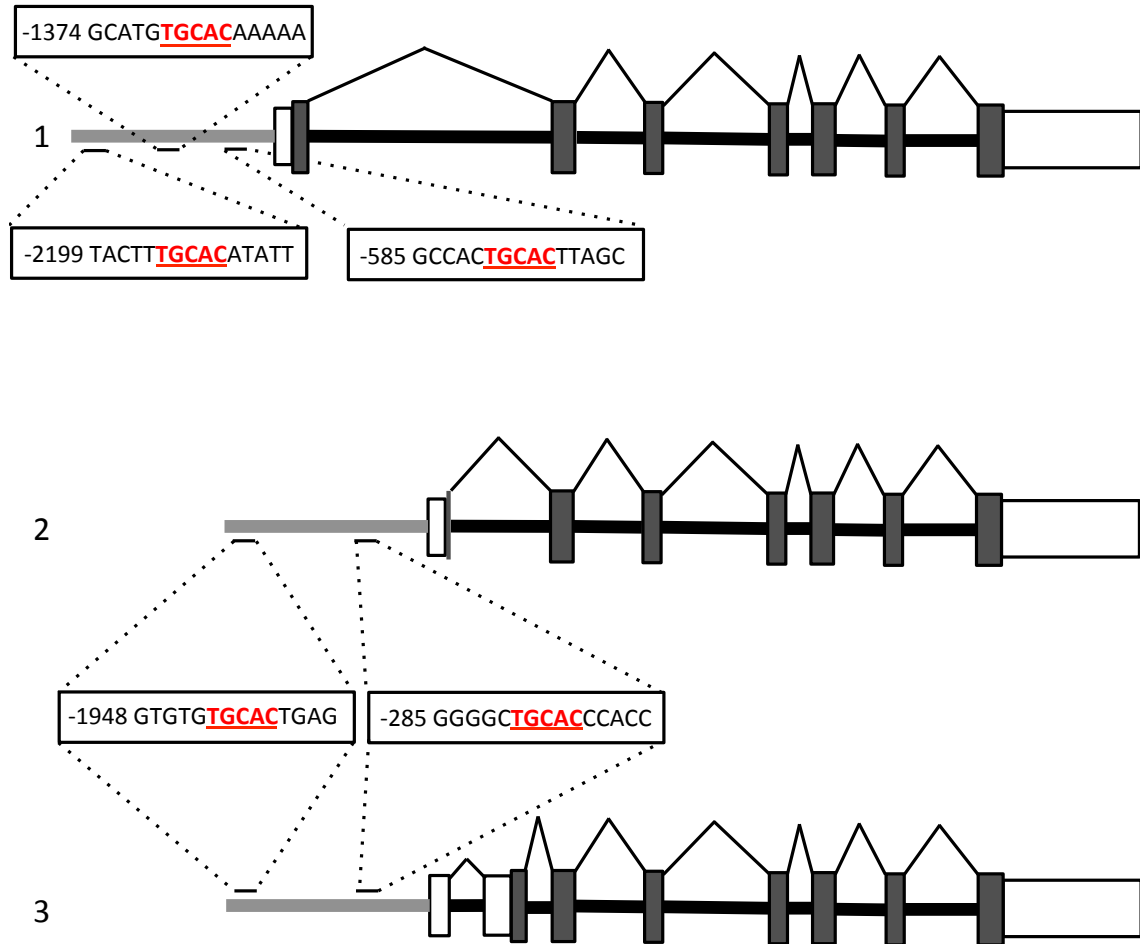


**Figure 13. *KCNK2* gene structure.** There are three transcript variants of *KCNK2*. Exons 2-7 are common to all variants, however, exon 1 differs. Variant 1's first exon is furthest upstream on chromosome 1. Variants 2 and 3 share similar first exons, both start with the same UTR but variant 3 contains 124 bp at the 3' end of the UTR. In this diagram, filled rectangles are the ORF, empty rectangles represent UTRs, lines above exons represent introns, the grey line represents putative promoters, small black lines above the promoter indicate predicted rhREs which are bolded and underlined in the sequence. Numbers before the sequences indicate basepairs upstream of the transcription start site.

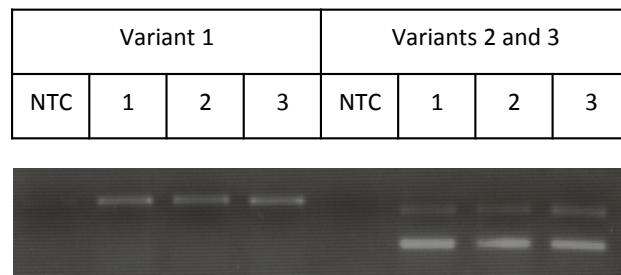


**Figure 14. The three major *KCNK2* transcript variants are present in TSD neuroglia.** Expression of *KCNK2* mRNA is high in TSD cells. To determine if one or all variants are expressed, TSD RNA was reverse transcribed using oligodT primers and amplified by PCR using primers specific for exon one of each variant. Variant 1 uses an upstream exon 1 whereas variants 2 and 3 use the same exon 1 but variant 3 contains an additional 125 basepairs. All three variants are present in TSD neuroglia.

***Treatment with NBDNJ***

*NBDNJ increases ganglioside levels in TSD neuroglia.* The glucosylceramide synthase inhibitor, NBDNJ has been approved for clinical use to treat Gaucher disease and NPC.<sup>32</sup> It has been useful in reducing ganglioside accumulations in these diseases and in mouse models of TSD and SD and therefore, we chose to investigate its effects at the cellular level in TSD neuroglia.

TSD neuroglia were treated with 100  $\mu$ M NBDNJ for 1, 3 or 6 days. Cells were then lysed and gangliosides were isolated using chloroform-methanol extraction. Purified samples were spotted on a TLC plate based on estimates from total protein present at the beginning of the isolation. Samples were separated based on size and gangliosides were visualized with resorcinol. We observed a marked increase in GM2 and GM3 ganglioside in TSD neuroglia the longer NBDNJ was present.

To determine whether the increase we saw was due to time in culture, we observed cells that were grown in parallel, half not treated and half treated with NBDNJ. The increase in GM2 ganglioside was apparent over time in both sets of samples; however, NBDNJ seemed to increase these levels further compared to cells that were not treated (Figure 15). These results suggest that NBDNJ is capable of directly increasing GM2 and GM3 gangliosides.

*NBDNJ alters expression of NPTX1 and KCNK2.* To investigate the effects of NBDNJ at a molecular level, expression of *NPTX1* and *KCNK2* was measured (Figure 16). We found that expression of *NPTX1* increased in TSD neuroglia after the first three days of culturing without treatment ( $1.293 \pm 0.3082$  vs.  $2.454 \pm 0.1147$  no treatment 3

days vs. no treatment 6 days respectively,  $p < 0.05$ ,  $n = 3$ ). Similarly, NBDNJ treated samples showed increased *NPTX1* expression as time passed ( $0.6981 \pm 0.08857$  NBDNJ 1 day vs.  $1.134 \pm 0.02372$  NBDNJ 3 days, and vs.  $1.567 \pm 0.1691$  NBDNJ 6 days,  $p < 0.01$ ; NBDNJ 3 days vs. NBDNJ 6 days,  $p < 0.05$ ,  $n = 3$ ); however, NBDNJ prevented *NPTX1* expression from increasing to levels of untreated neuroglia after 6 days ( $2.454 \pm 0.1147$  vs.  $1.567 \pm 0.1691$ ,  $p < 0.01$ , no treatment 6 days vs. NBDNJ 6 days respectively,  $n = 3$ ).

*KCNK2* expression showed a similar pattern in that it was significantly increased in TSD neuroglia in culture without treatment ( $0.7231 \pm 0.4550$  no treatment 1 day vs.  $0.9486 \pm 0.07786$  no treatment 3 days, and  $0.8657 \pm 0.01469$  no treatment 6 days,  $p < 0.05$ ,  $n = 3$ ), and treatment with NBDNJ also increased expression of *KCNK2* over time ( $0.5811 \pm 0.08017$  no treatment 1 day vs.  $0.9995 \pm 0.03936$  no treatment 3 days; and vs.  $1.042 \pm 0.03605$  no treatment 6 days,  $p < 0.01$ ,  $n = 3$ ). However, NBDNJ significantly increased *KCNK2* expression when compared to no treatment control after 6 days ( $0.8657 \pm 0.01469$  vs.  $1.042 \pm 0.03605$ ,  $p < 0.01$ , no treatment 6 days vs. NBDNJ 6 days respectively,  $n = 3$ ).

These results indicate that NBDNJ is capable of altering gene expression as well as ganglioside accumulation. Furthermore, the contrasting effects of NBDNJ on *NPTX1* and *KCNK2* expression suggest that these genes may have opposing functions in TSD.

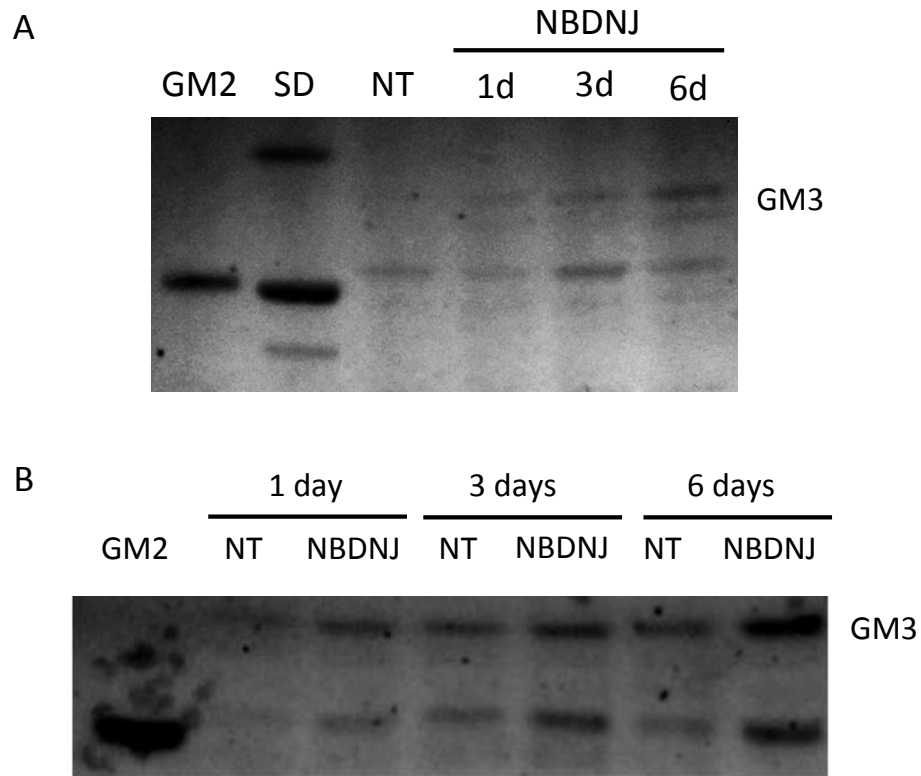


**Figure 15. NBDNJ increases GM2 in TSD neuroglia.** To investigate the effect of NBDNJ on TSD neuroglia, cells were treated for the indicated times with 100  $\mu$ M NBDNJ. Upon experiment termination, gangliosides were isolated via chloroform-methanol extraction and resolved on silica plates. We discovered that NBDNJ increased the level of GM2 ganglioside in TSD neuroglia over time. A) Lane 1, purified GM2 standard, lane 2, SD mouse brain, lane 3, no treatment TSD neuroglia, lanes 4, 5, 6, NBDNJ treatment. B) To compare GM2 ganglioside accumulations over time in untreated and NBDNJ treated TSD neuroglia, cells were cultured in parallel.

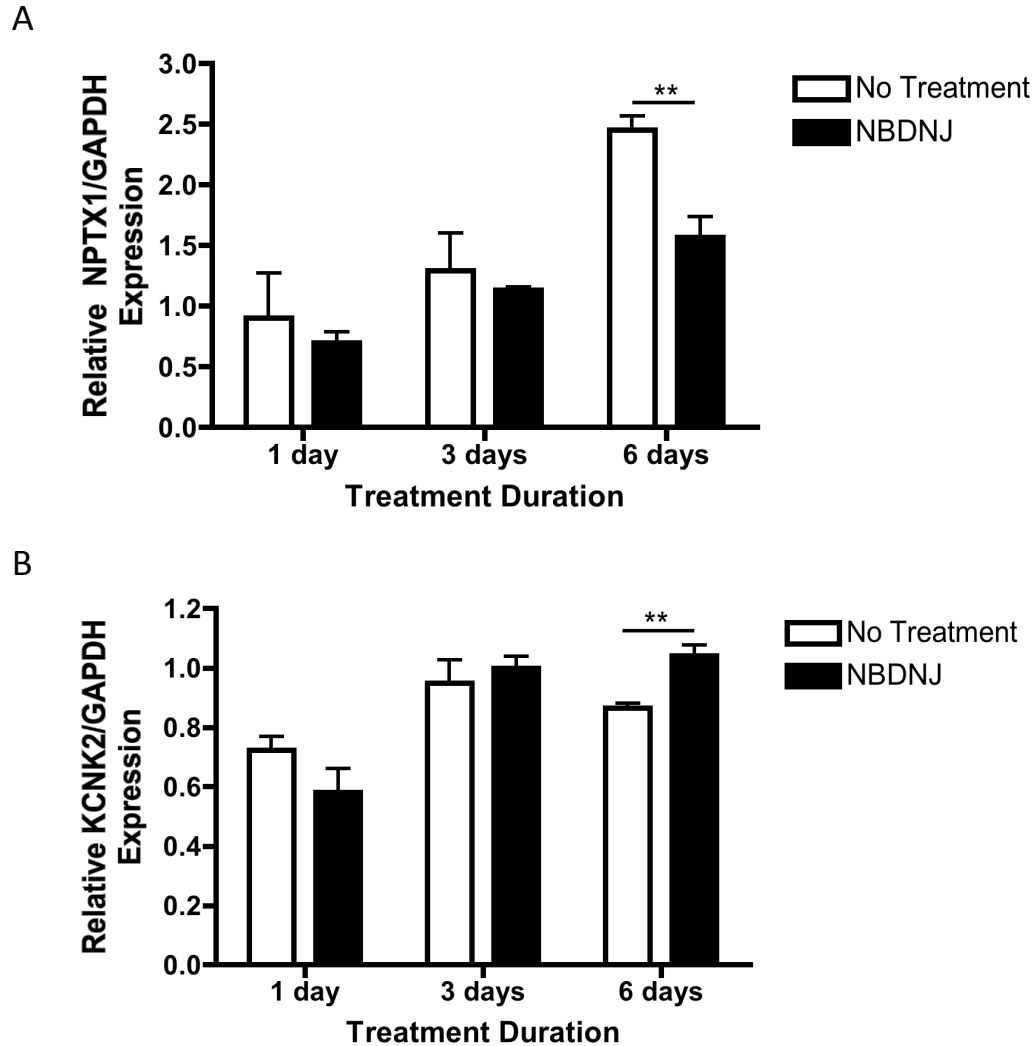


**Figure 16. NBDNJ alters expression of NPTX1 and KCNK2.** TSD cells were treated with 100  $\mu$ M NBDNJ for the indicated times. After 3 days, media was replaced to ensure cells were not starved. The treated cells received fresh media with 100  $\mu$ M NBDNJ. Total RNA was collected and reverse transcribed with oligodT primers. cDNA was used as a template for Taqman qRT-PCR. A) NPTX1 gene expression increased as cells grew in culture. NBDNJ reduced NPTX1 expression after 6 days. B) KCNK2 expression also increased in cells as they grew in culture, however, NBDNJ had the opposite effect compared to NPTX1. NBDNJ increased expression of KCNK2 after 6 days. The contrasting responses to NBDNJ may suggest that NPTX1 and KCNK2 serve opposite purposes. Bars denote mean  $\pm$  SE, n=3; one tailed t-test \*\*p < 0.01.

## DISCUSSION

### *HIF-1 $\alpha$*

In this study, we set out to determine the role of HIF-1 $\alpha$  in TSD neuroglia. HIF-1 is an important transcription factor that is involved in many processes including angiogenesis, glucose metabolism, cell survival and brain development. In fact, complete deficiency of HIF-1 $\alpha$  in mouse embryos is lethal by E10 and embryos possess neural tube defects, cardiovascular malformations and marked cell death especially within the cephalic mesenchyme.<sup>120</sup> As such, although HIF-1 gets its name from its ability to respond to hypoxia, it can be considered a master regulator of many genes and cellular processes. It is for this reason that we chose to investigate its role in TSD, as lysosomal storage of GM2 ganglioside exerts major stress at the cellular level, including increased pro-inflammatory cytokine release and microglial activation.<sup>22-27</sup>

We found that stabilization of HIF-1 $\alpha$  during hypoxia is impaired in TSD neuroglia (Figure 2). These cells, being of Ashkenazi Jewish ancestry, possessed two of the most common mutations in this population. The exon 11 TATC insertion and the splice junction mutation in intron 12 effectively eliminate HEXA activity in these neuroglia. Since treatment of TSD neuroglia with the PHD inhibitor, DMOG, was still capable of stabilizing HIF-1 $\alpha$  under normoxia, the ODDD is likely in tact and does not account for the HIF-1 $\alpha$  deficiency. Furthermore, DMOG-mediated stabilization resulted in localization of HIF-1 $\alpha$  to the nucleus (figures 3, 4) and increased expression of confirmed targets VEGF and miR-210 (figures 6, 8). The staining of HIF-1 $\alpha$  in untreated cells is likely due to the presence of a truncated form of the protein that we have observed

previously (data not shown). TSD neuroglia may lack another level of HIF-1 $\alpha$  control upstream of ODDD hydroxylation. As mentioned previously, HIF-1 $\alpha$  is regulated in many ways including ubiquitination,<sup>71, 72</sup> and phosphorylation.<sup>77-79</sup> In this case, the more relevant aspects of regulation may be those that involve HIF-1 $\alpha$  stabilization during normoxia, or degradation during hypoxia. Alteration of these mechanisms may explain the reduction in stabilized HIF-1 $\alpha$  in TSD neuroglia. A similar pattern of expression was observed in the cerebellum of a *Hexb*<sup>-/-</sup> mouse when compared to a wild type cerebellum, indicating that HIF-1 $\alpha$  deficiency is involved in TSD and SD (Figure 2).

HIF-1 $\alpha$  plays a role in neuroprotection by increasing VEGF expression,<sup>118, 271</sup> and reducing astrocyte activation,<sup>115</sup> and has been shown to be directly involved in the neurodegenerative diseases Alzheimer's and Parkinson's.<sup>114, 272</sup> The deficiency we observed may therefore affect the ability of TSD neuroglia to respond to stress caused by ganglioside accumulation, inflammation and excitotoxicity. For example, cells may be bombarded with signaling molecules that normally elicit a protective response to protect the cell, but chronically cause damage. Therefore, lower levels of HIF-1 $\alpha$  decrease the pre-emptive protection that molecules like VEGF afford.

To study the impact of reduced HIF-1 $\alpha$  in TSD cells, we looked at the levels of expression of neuronal molecules involved in excitotoxicity because we had previously found TSD neuroglia to be more susceptible to AMPA-induced excitotoxic death.<sup>266</sup> Significantly higher expression of both secreted neuronal pentraxins, and KCNK2 was found in TSD neuroglia, whereas the neuronal pentraxin receptor was downregulated in these cells (Figure 5). The neuronal pentraxins have been found to increase AMPAR

clustering at synapses.<sup>206, 209, 210</sup> Therefore, increased *NPTX1* and *NPTX2* expression should increase AMPAR clustering at the membrane. Since expression of *NPR* is decreased in TSD compared to normal neuroglia, and *NPR* can facilitate mGluR1/5-mediated LTD,<sup>211</sup> internalization of the secreted pentraxins may not be as efficient in diseased cells. Indeed, half the amount of *NPTX1* and *NPTX2* from *NPR* knockout mice brains could be purified versus the amount from wild type mice, indicating *NPR* tethers *NPTX1* and *NPTX2* to the membrane.<sup>218</sup> Together, our results suggest that due to such high levels of the secreted pentraxin, AMPAR internalization is deficient in TSD cells, despite higher levels of *NPR* to compensate, resulting in increased vulnerability to excitotoxicity.

To investigate how AMPAR activation affects *NPTX1*, we measured *NPTX1* expression in TSD neuroglia after treatment with the AMPAR agonist, AMPA. In addition, gene expression was measured after DMOG treatment to determine if HIF-1 $\alpha$  directly modulated *NPTX1* expression. We found that AMPA significantly reduced *NPTX1* expression, and when cells were treated with AMPA and DMOG together, there was further repression (Figure 6). Cells internalize AMPARs after stimulation to attenuate glutamate-induced signaling,<sup>273-275</sup> in which neuronal pentraxins play a role.<sup>206, 209-211</sup> Activation of mGluR1/5, induces cleavage of *NPR* surprisingly fast, reaching 60.7% of its original levels after 90 minutes. Subsequent internalization of GluR1-containing receptors occurs rapidly, reducing membrane receptors by 74.1% of the vehicle control after 45 minutes.<sup>211</sup> Since our experiments measured gene expression 24 hours after AMPAR activation, it is possible that *NPTX1* expression is shut down by AMPA in a

negative feedback mechanism after internalization takes place. Further, because AMPAR clustering has been found to increase excitation, lower levels of *NPTXI* would decrease AMPAR clustering at the membrane and hence decrease excitability, which may be desired after receptor activation and cell depolarization. We also observed that stabilization of HIF-1 $\alpha$  by DMOG enhances the AMPA-mediated repression of *NPTXI*. In fact, evidence indicates that hypoxic preconditioning and therefore induction of HIF-1 $\alpha$  stabilization, reduces intracellular [Ca<sup>2+</sup>] increases induced by AMPA.<sup>276</sup> Therefore, AMPA-mediated excitation reduces expression of *NPTXI* in an attempt to decrease excitability and facilitate recovery, which is aided by HIF-1 $\alpha$  directly and indirectly, as described below.

In addition to *NPTXI*, we also measured levels of *VEGF*. *VEGF* is a target of HIF-1 $\alpha$ ,<sup>64</sup> therefore, increased expression of *VEGF* in the presence of DMOG, confirmed stabilization of HIF-1 $\alpha$  and transactivation. Second, VEGF protects from AMPAR-mediated excitotoxicity through the upregulation of GluR2, which, once included in AMPARs renders receptors impermeable to Ca<sup>2+</sup>.<sup>271</sup> Reduced levels of VEGF in the presence of AMPA, and the deficient levels of HIF-1 $\alpha$  in TSD neuroglia during hypoxia, along with the fact that TSD neuroglia are more susceptible to AMPA-induced cell death compared to normal neuroglia,<sup>266</sup> suggests that the intrinsic shortage of HIF-1 $\alpha$  prevents the upregulation of VEGF needed to afford protection from AMPA-induced excitotoxicity. Therefore, when HIF-1 $\alpha$  was stabilized by DMOG, AMPA could not reduce VEGF expression like it could on its own. Consequently, low levels of HIF-1 $\alpha$  in TSD neuroglia may be responsible for their vulnerability to AMPA-induced death.

***miR-210***

We measured expression of miR-210 because it is a HIF-1 $\alpha$  target gene and effector,<sup>86, 269</sup> and a potential regulator of *NPTX1*.<sup>87, 270</sup> First, to determine if miR-210 expression was altered by HIF-1 $\alpha$  expression in TSD neuroglia, we measured miR-210 in the presence of DMOG and under hypoxia (Figure 8). In normal neuroglia, the pattern of miR-210 expression is complementary to HIF-1 $\alpha$  expression and reciprocal to the expression of *NPTX1*, lending merit to our hypothesis that miR-210 represses *NPTX1*. In contrast, in TSD neuroglia, miR-210 levels do not mirror HIF-1 $\alpha$  expression patterns. miR-210 expression is consistently significantly higher in TSD cells than in normal controls. However, in hypoxic conditions, TSD neuroglia are unable to stabilize HIF-1 $\alpha$  efficiently. This was not reflected in the miR-210 expression data. Therefore, miR-210 must be under the control of another molecule, in addition to HIF-1 $\alpha$ . Another study has shown that miR-210 expression can be induced by Akt activation, independent of HIF-1 $\alpha$ .<sup>277</sup> These data suggest that although HIF-1 $\alpha$  does induce miR-210 expression in both TSD and normal neuroglia, evidenced by its increased expression in the presence of DMOG, there are other molecules that can do so as well. miR-210 exerts protective effects by decreasing expression of its target proteins (subsequently described in detail). Moreover, most evidence demonstrates a neurotoxic role for *NPTX1*.<sup>213-217, 278</sup> Taken together, this suggests that TSD neuroglia compensate for low HIF-1 $\alpha$  expression by increasing miR-210 to keep *NPTX1* expression as low as possible. Despite this attempt, *NPTX1* is so highly expressed in TSD neuroglia at baseline that the increase in miR-210 expression is not enough to completely suppress *NPTX1*. It seems that the reduced ability

of TSD neuroglia to stabilize HIF-1 $\alpha$  under hypoxia may affect their ability to respond to other stressful stimuli, i.e. lysosomal storage. TSD neuroglia are therefore intrinsically predisposed to cell death due to increased expression of neuronal molecules involved in excitotoxicity, in addition to ganglioside accumulations.

Direct targets of miR-210 that have been discovered include SHIP-1, a negative regulator of hematopoiesis,<sup>279</sup> EphrinA3, involved in angiogenesis and synapse formation,<sup>280</sup> iron-sulphur cluster assembly proteins 1/2, involved in mitochondrial respiration,<sup>281</sup> NF- $\kappa$ B1 (p105),<sup>282</sup> apoptosis-inducing factor, mitochondrion-associated 3 and HIF-3 $\alpha$ .<sup>277</sup> Generally, targeted degradation of these proteins is neuroprotective.

More specifically, the NF- $\kappa$ B family of transcription factors (TFs), of which NF- $\kappa$ B1 is a part, dimerize with each other to activate gene transcription. NF- $\kappa$ B1 does not contain a transactivation domain and therefore must rely on its dimerization partner to do so.<sup>283, 284</sup> NF- $\kappa$ B1 is constitutively processed into its truncated form, p50, in non-stimulated cells;<sup>285, 286</sup> it dimerizes with RelA and c-Rel, other members of the NF- $\kappa$ B family. NF- $\kappa$ B dimers are sequestered in the cytoplasm by inhibitors of NF- $\kappa$ B (I $\kappa$ B). However, when cells are stimulated by TNF- $\alpha$  or IL-1, I $\kappa$ Bs are phosphorylated, ubiquitinated and degraded, freeing the NF- $\kappa$ B dimer, allowing movement to the nucleus and activation of target genes.<sup>283</sup> Unprocessed NF- $\kappa$ B1 can also function as an I $\kappa$ B.<sup>287-289</sup>

NF- $\kappa$ B signaling can be induced by the binding of lipopolysaccharide (LPS) to the Toll-like receptor 4 (TLR-4).<sup>290</sup> LPS is a molecule found in the membrane of Gram-negative bacteria, which activates TLR-4 to produce an immune response.<sup>291</sup> Murine macrophages treated with LPS induced HIF-1 $\alpha$  and miR-210 expression and miR-210

directly targeted and inhibited NF- $\kappa$ B1, which significantly reduced pro-inflammatory cytokine secretion.<sup>282</sup> In fact, the promoter for HIF-1 $\alpha$  contains a RelA binding site and is thus transcriptionally regulated by NF- $\kappa$ B.<sup>292</sup> Reduction of NF- $\kappa$ B1 thus inhibits the inflammatory signaling cascade and reduces pro-inflammatory cytokines. Therefore, high levels of miR-210 may be anti-inflammatory and neuroprotective in TSD.

While NF- $\kappa$ B-induced gene expression is transiently protective, chronic activation of these pathways can cause damage through highly upregulated inflammatory responses.<sup>283</sup> Furthermore, TLR-4 is also activated by gangliosides, which also increases NF- $\kappa$ B and pro-inflammatory cytokine secretion.<sup>293</sup> Lysosomal exocytosis has been documented as a way for cells to replenish or repair the plasma membrane or remove pathogenic bacteria from infected cells.<sup>294-298</sup> Moreover, there is evidence that illustrates this process occurs in LSDs including SD and sialidosis.<sup>299,300</sup> From this evidence, high levels of pro-inflammatory cytokines characteristic of TSD and SD, and extracellular gangliosides may increase NF- $\kappa$ B signaling, and since HIF-1 $\alpha$  stabilization is deficient during stress, the negative feedback mechanism involving miR-210 is ineffective. miR-210 may be overexpressed in TSD neuroglia by a HIF-1 $\alpha$ -independent mechanism to compensate for the pro-inflammatory response seen within the brain,<sup>22-25</sup> in an attempt to prolong cell viability.

While the targeting of NF- $\kappa$ B1 by miR-210 illustrates a protective role for miR-210 in TSD, we decided to look for other putative miR-210 targets that may be more directly involved in the neurodegeneration of TSD neuroglia. Prediction algorithms including PicTar<sup>270,301</sup> suggested miR-210 may bind to the 3' UTR of NPTX1 (Figure 9).

Based on the excitotoxic nature of NPTX1,<sup>213-215</sup> the overexpression of NPTX1 that we observed in TSD neuroglia is likely detrimental. Furthermore, the inversely correlated levels of miR-210 and *NPTX1* expression during hypoxia or DMOG treatment (Figures 7, 8) add merit to the idea that miR-210 directly binds the 3' UTR of *NPTX1*.

### ***NPTX1***

*NPTX1* expression was significantly higher in TSD neuroglia compared to normal neuroglia (Figure 5). Since HIF-1 $\alpha$  stabilization by DMOG tended to decrease *NPTX1* expression in initial experiments (Figure 6), we used Taqman gene expression assays to better understand how HIF-1 $\alpha$  affects *NPTX1* in TSD neuroglia directly. We measured the expression of *NPTX1* in cells cultured under hypoxic conditions and found that HIF-1 $\alpha$  stabilization reduced *NPTX1* expression in both normal and TSD cell types, although it was more effective at doing so in normal neuroglia. HIF-1 $\alpha$  deficiency in hypoxic TSD neuroglia resulted in significantly higher levels of *NPTX1* in TSD neuroglia compared to normal neuroglia (Figure 7).

To directly test the ability of miR-210 to reduce *NPTX1* expression, we used a luciferase reporter containing the 3' UTR of NPTX1. We also used site-directed mutagenesis to generate two 3' UTR mutants, each with a mutated putative seed sequence (Figure 10). Luciferase expression from the mutant vectors at baseline were significantly different from pGL3-CMV. Long 3' UTRs have been observed to increase mRNA stability,<sup>302</sup> which explains the increase of expression in the mutants compared to pGL3-CMV, which contains the luciferase reporter but does not contain a 3' UTR like the vectors we constructed. Luciferase expression from pGL3-CMV 3' UTR NPTX1 and

from mutant 2 was not significantly different from pGL3-CMV control when co-transfected with pCDNA3-premir210, most likely due to large variation levels. However, expression from pGL3-CMV 3' UTR NPTX1 and mutant 2 is significantly reduced by miR-210 compared to the expression from mutant 1 (Figure 11). This suggests that the nucleotides mutated in mutant 1 facilitate miR-210 binding, since miR-210 is not capable of decreasing its expression like it is of pGL3-CMV 3' UTR NPTX1 and mutant 2. This indicates that higher levels of miR-210 observed in TSD neuroglia may serve to control the excessive *NPTX1* expression in these cells. If NPTX1 is neurotoxic as most evidence indicates, then miR-210 and HIF-1 $\alpha$  are neuroprotective in TSD neuroglia and the intrinsic deficiency in HIF- $\alpha$  is a major cause of pathology.

Since we were unable to detect endogenous levels of NPTX1 protein in TSD cells, we chose to overexpress it to determine its properties in TSD neuroglia. Initial studies of NPTX1 found protein levels were particularly hard to detect in rat brains despite high mRNA levels.<sup>205</sup> We found the same in TSD neuroglia, which is most likely due to the fact that NPTX1 is a secreted protein and that our studies used cell culture and not whole brain lysates. In our studies, we found that NPTX1 forms glycosylated multimers in TSD neuroglia (Figure 12), as predicted by studies on NPTX1 isolated from rat brain.<sup>205</sup> We were also able to detect NPTX1 secreted in the media of transfected cells. It is interesting to note, however, that NPTX1 found in the media was slightly smaller than that in lysates. This suggests that the molecule was cleaved when it was secreted, which fits with the model that describes TACE-mediated NPR cleavage and release of NPTX1/2 from the

membrane.<sup>211</sup> These data confirm that NPTX1 produced in TSD neuroglia is consistent with NPTX1 described elsewhere.

### ***KCNK2***

Previous data from our lab suggested that *KCNK2* expression was increased in TSD neuroglia compared to normal neuroglia. We confirmed this observation with qRT-PCR (Figure 5). *KCNK2* is a background potassium channel that hyperpolarizes neurons and thus decreases their excitability.<sup>231</sup> Nevertheless, glutamate inhibits activation of potassium channels similar to *KCNK2*.<sup>232-234</sup> Therefore, overexpression of *KCNK2* in TSD neuroglia could be a way for these cells to compensate for the increased susceptibility to AMPA-induced cell death.

Perhaps the most interesting observation we found was that hypoxia and DMOG-mediated HIF-1 $\alpha$  stabilization suppressed *KCNK2* expression (Figure 6, 7). There has been some controversy in the literature about the oxygen sensing capabilities of *KCNK2*. Miller et al. illustrated that in stably transfected HEK293 cells, hypoxia (20 mmHg) reduced whole-cell K<sup>+</sup> currents by ~40%. Furthermore, hypoxia was able to prevent the activation of *KCNK2* by AA or membrane stretch.<sup>303</sup> However, the method used to equilibrate the hypoxic solutions in these experiments was shown by Buckler et al. to actually eliminate AA from solution. Moreover, subsequent experiments by Buckler et al. found no change in K<sup>+</sup> current during hypoxia.<sup>225</sup> Nevertheless, our data clearly indicate that HIF-1 $\alpha$  stabilization significantly reduces *KCNK2* expression in TSD neuroglia, and that the deficiency in HIF-1 $\alpha$  in these cells during hypoxia de-represses *KCNK2* expression as expected (Figure 7). Unlike *NPTX1*, we did not find a miR-210 binding site

in the 3' UTR of *KCNK2*. Instead, promoter analysis revealed multiple putative reverse hypoxia response elements (rHREs)(Figure 13). These consensus sequences are HREs on the reverse DNA strand that recruit HIF-1 $\alpha$  binding and repression of gene transcription.<sup>304-306</sup> Our goal in identifying these sites is to clone and test them for their ability to repress reporter gene expression.

As mentioned previously, there are three variants of human *KCNK2* described in GenBank. They are produced by exon skipping and result in three putative proteins of 422, 411 and 426 amino acids. The AceView database suggests that variant 1 uses a different promoter than variants 2 and 3.<sup>224</sup> The probes used to measure *KCNK2* gene expression in our experiments span exons 5 and 6, which would therefore detect all three variants. To determine whether TSD neuroglia express all variants, we performed RT-PCR. We found that all variants are expressed, variant 2 the most so (Figure 14). The predicted alternative promoters of *KCNK2* probably allow regulation of the variants by different transcription factors, however, there have been no previous studies on *KCNK2* promoters. Most studies on human *KCNK2* have involved physiological properties of variants 2 and 3. The differences between variants are present in the N-termini intracellular domain of the protein. There is evidence to suggest that the N-terminus of *KCNK2* may be used as a localization marker.<sup>229</sup> Furthermore, a truncated form of *KCNK2* that is missing 56 N-terminal amino acids increases the channel's Na<sup>+</sup> permeability, which increases cell depolarization.<sup>228</sup> Therefore, it is important to determine the properties of the *KCNK2* channels expressed in TSD neuroglia to better understand their role in excitotoxicity and how they may contribute to neuronal cell death.

***NBDNJ***

The glucosylceramide synthase inhibitor NBDNJ is used for the treatment of Gaucher disease and NPC,<sup>32</sup> and has been investigated for the use in other glycosphingolipidoses as well. In order to determine how ganglioside reduction would affect gene expression levels, we measured the expression of *NPTX1* and *KCNK2* in the presence of NBDNJ. First, we determined what extent NBDNJ reduced gangliosides in TSD neuroglia. However, contrary to what we expected, we found NBDNJ increased GM2 and GM3 gangliosides in TSD neuroglia compared to untreated controls (Figure 15A). Logically speaking, the longer time spent in culture, the more gangliosides TSD neuroglia are expected to accumulate. Nevertheless, when compared in parallel to an untreated control, NBDNJ-treated neuroglia contained more GM2 and GM3 ganglioside (Figure 15B). This indicates that NBDNJ directly causes GM2 and GM3 gangliosides to increase in TSD neuroglia.

NBDNJ acts to inhibit the first committed step in ganglioside synthesis,<sup>37</sup> therefore, it acts to reduce the level of *all* gangliosides present in the cell. In glycosphingolipidoses that are the result of null mutations, this does little to correct the problem. However, in cells with residual hydrolase activity, NBDNJ may reduce the workload for active enzymes and reduce accumulations. It is consequently imperative that NBDNJ be administered early on in disease progression and would be most effective in treatment of less severe forms, i.e. juvenile or adult onset. All this being considered, due to the nature of the mutations in our TSD neuroglia, it is not surprising to see GM2 ganglioside continue to increase as the cells spend time in culture. Most studies on

NBDNJ have been done *in vivo*, using mice with LSDs. In particular, NBDNJ treated SD mice had reduced GM2 accumulations in brain and liver, reduced neuronal apoptosis, improved behaviour indicative of delayed disease symptoms, and increased life span after NBDNJ treatment.<sup>50</sup> Even so, although SD mice treated with NBDNJ lived longer, when they reached endpoint, brain GM2 and GA2 levels had increased versus endpoint untreated controls.<sup>34</sup> This suggests that other effects of NBDNJ may enhance cell survival instead. In fact, NBDNJ is capable of decreasing inflammatory cytokine secretion in SD mice.<sup>22</sup> It is possible that since gangliosides are very important for nervous system development, explained at length in the introduction of this report, TSD neuroglia treated with NBDNJ increase ganglioside production to compensate for the blockage the drug causes. TSD cells are deficient in HEXA, however, and thus are still unable to degrade the now even larger amount of GM2, resulting in its accumulation.

Despite the use of NBDNJ in the clinic, little has been done to determine the consequences it may have at the molecular level on a long-term basis. As mentioned, NBDNJ treated SD mice produced lower pro-inflammatory cytokines than untreated controls. In addition, mice treated with NBDNJ also expressed MHC class II and CD68 at levels closer to normal versus untreated SD mice.<sup>22</sup> Furthermore, NBDNJ altered T cell populations in healthy C57Bl/6 mice, indicating that substrate reduction also affects aspects of cell growth and differentiation.<sup>44</sup> We have found evidence that NBDNJ is capable of altering the gene expression of *NPTX1* and *KCNK2* in TSD neuroglia, two important molecules involved in excitotoxicity.

Furthermore, time-course experiments indicated that *NPTX1* expression increased overtime as TSD neuroglia were cultured. Although NBDNJ did not completely prevent this increase, it did suppress *NPTX1* expression compared to untreated controls, after 6 days (Figure 16A). These data, considered with evidence of the neurotoxic role of NPTX1, indicate that in addition to the mechanisms noted above, NBDNJ may be neuroprotective by reducing expression of excitatory molecules.

In contrast, *KCNK2* expression was fairly steady over time in culture; however, after 6 days, NBDNJ treated TSD neuroglia expressed higher levels compared to untreated controls (Figure 16B). This effect of NBDNJ treatment may also be neuroprotective, since higher expression of *KCNK2* could hyperpolarize neurons and protect them from excitotoxicity. Our data therefore demonstrate that NBDNJ is capable of altering gene expression as well as ganglioside synthesis. Moreover, it also suggests that while ganglioside accumulations may initiate disease mechanisms, other factors including cytokine secretion, inflammation and microglial activation may propagate disease pathogenesis despite ganglioside levels.

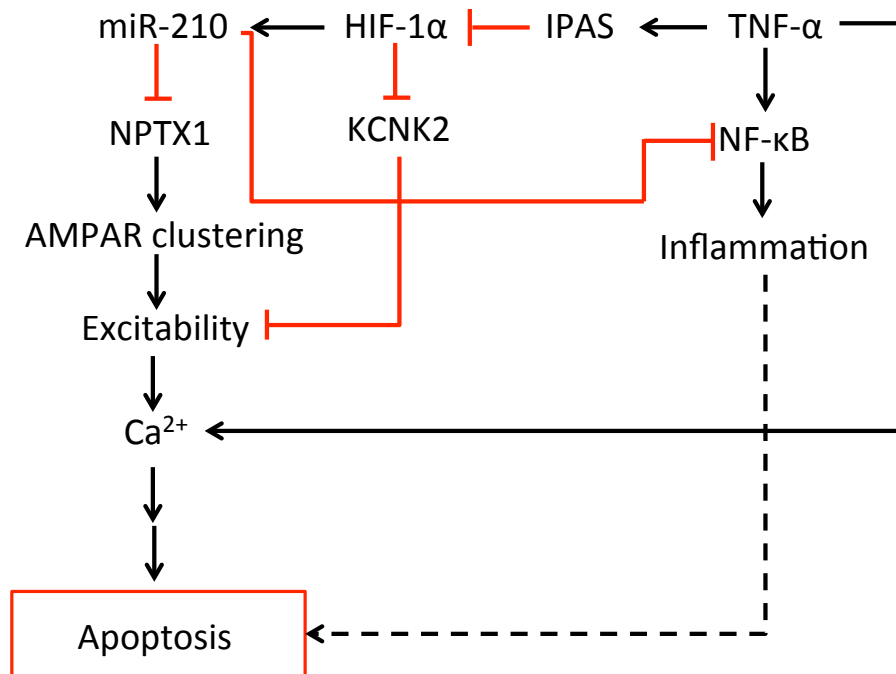


**Figure 17. Working model.** HIF-1 $\alpha$  induces expression of miR-210, which binds to and suppresses NPTX1 expression in TSD neuroglia. The AMPAR clustering capabilities of NPTX1 increase cellular excitability. Increased cell excitability enhances the chances of excitotoxicity and therefore high intracellular Ca<sup>2+</sup>, which causes mitochondrial dysfunction, protease activation, formation of reactive oxygen species, etc, resulting in apoptosis. TNF- $\alpha$  activated inflammatory responses lead to the inflammation characteristic of TSD and SD to propagate disease and activate microglia, but also increase Ca<sup>2+</sup> permeable AMPARs at the cell surface. KCNKK2 is inhibited by HIF-1 $\alpha$ , which decreases cell excitability by hyperpolarizing the cell. TSD neuroglia stabilize low levels of HIF-1 $\alpha$  during hypoxia de-repressing KCNKK2 but not affecting miR-210 levels. miR-210 is therefore regulated differently under these conditions.

Taken together, we propose that due to ganglioside accumulations intrinsic to TSD neuroglia, there are multiple cellular molecules affected. The altered levels of HIF-1 $\alpha$ , miR-210, NPTX1 and KCNK2 that we have characterized here, probably affect cellular interactions in the whole brain, and thus should next be investigated *in vivo*. We have demonstrated that TSD neuroglia are unable to respond to hypoxia as efficiently as normal neuroglia by stabilizing HIF-1 $\alpha$ . This may be due to high levels of TNF- $\alpha$  that inhibit HIF-1 $\alpha$  and increase the number of Ca<sup>2+</sup> permeable AMPARs at the cell surface, as well as activate NF- $\kappa$ B to induce higher pro-inflammatory cytokine secretion.<sup>199</sup> These occurrences, in addition to NPTX1-mediated AMPAR clustering, could increase susceptibility of TSD neuroglia to excitotoxicity. High *KCNK2* and miR-210 expression may be a mechanism in TSD neuroglia, that attempts to compensate for neurotoxic events by hyperpolarizing TSD cells and directly inhibiting *NPTX1* expression, respectively, in an attempt at neuroprotection. Furthermore, low levels of HIF-1 $\alpha$  during hypoxia de-repress *KCNK2* expression to facilitate neuroprotection (Figure 17). TSD neuroglia are beneficial to study the course of disease because they have not differentiated and therefore illustrate the inherent problems within individual cells that are most likely amplified as time progresses, and which can be extrapolated to predict disease mechanisms in the whole organism. Despite the future work needed, these experiments illustrate the complicated process of excitotoxicity in TSD cells. The major players involved include NPTX1, miR-210, AMPAR and HIF-1 $\alpha$  and aberrant expression of these components contributes to TSD pathology. Furthermore, inhibition of *KCNK2* expression by HIF-1 $\alpha$  has major implications for the study of hypoxia-ischemia, in that it

provides a mechanism for cell death under these conditions. There is no doubt, that this observation could have major implications of cellular viability in TSD and in general.

**REFERENCES**

1. Schnaar RL, Suzuki A, Stanley P. Glycosphingolipids. In: A. Varki, R. D. Cummings, J. D. Esko, et al, editors. *Essentials of glycobiology*. 2nd ed. Cold Spring Harbor (NY): The Consortium of Glycobiology Editors, La Jolla, California; 2009. CI: Copyright (c) 2009.
2. Gravel RA, Clarke JTR, Kaback MM, Proia RL, Sandhoff K, Suzuki K. The GM2 gangliosidosis. In: C. R. Scriver, A. L. Beaudet, W. S. Sly, D. Valle, editors. *The metabolic and molecular bases of inherited disease*. 8th ed. New York, NY: McGraw-Hill; 2001. .
3. Yamashita T, Wada R, Sasaki T, Deng C, Bierfreund U, Sandhoff K, Proia RL. A vital role for glycosphingolipid synthesis during development and differentiation. *Proc Natl Acad Sci U S A* 1999 Aug 3;96(16):9142-7.
4. Takamiya K, Yamamoto A, Furukawa K, Yamashiro S, Shin M, Okada M, Fukumoto S, Haraguchi M, Takeda N, Fujimura K, et al. Mice with disrupted GM2/GD2 synthase gene lack complex gangliosides but exhibit only subtle defects in their nervous system. *Proc Natl Acad Sci U S A* 1996 Oct 1;93(20):10662-7.
5. Susuki K, Baba H, Tohyama K, Kanai K, Kuwabara S, Hirata K, Furukawa K, Furukawa K, Rasband MN, Yuki N. Gangliosides contribute to stability of paranodal junctions and ion channel clusters in myelinated nerve fibers. *Glia* 2007 May;55(7):746-57.
6. Sheikh KA, Sun J, Liu Y, Kawai H, Crawford TO, Proia RL, Griffin JW, Schnaar RL. Mice lacking complex gangliosides develop wallerian degeneration and myelination defects. *Proc Natl Acad Sci U S A* 1999 Jun 22;96(13):7532-7.
7. Pan B, Fromholt SE, Hess EJ, Crawford TO, Griffin JW, Sheikh KA, Schnaar RL. Myelin-associated glycoprotein and complementary axonal ligands, gangliosides, mediate axon stability in the CNS and PNS: Neuropathology and behavioral deficits in single- and double-null mice. *Exp Neurol* 2005 Sep;195(1):208-17.
8. Ohmi Y, Tajima O, Ohkawa Y, Yamauchi Y, Sugiura Y, Furukawa K, Furukawa K. Gangliosides are essential in the protection of inflammation and neurodegeneration via maintenance of lipid rafts: Elucidation by a series of ganglioside-deficient mutant mice. *J Neurochem* 2011 Mar;116(5):926-35.
9. Simons M, Friedrichson T, Schulz JB, Pitto M, Masserini M, Kurzchalia TV. Exogenous administration of gangliosides displaces GPI-anchored proteins from lipid microdomains in living cells. *Mol Biol Cell* 1999 Oct;10(10):3187-96.

10. Kusumi A, Suzuki K. Toward understanding the dynamics of membrane-raft-based molecular interactions. *Biochim Biophys Acta* 2005 Dec 30;1746(3):234-51.
11. Brown DA, London E. Structure and function of sphingolipid- and cholesterol-rich membrane rafts. *J Biol Chem* 2000 Jun 9;275(23):17221-4.
12. Shogomori H, Brown DA. Use of detergents to study membrane rafts: The good, the bad, and the ugly. *Biol Chem* 2003 Sep;384(9):1259-63.
13. Lingwood D, Simons K. Lipid rafts as a membrane-organizing principle. *Science* 2010 Jan 1;327(5961):46-50.
14. Suzuki T. Lipid rafts at postsynaptic sites: Distribution, function and linkage to postsynaptic density. *Neurosci Res* 2002 Sep;44(1):1-9.
15. Allen JA, Halverson-Tamboli RA, Rasenick MM. Lipid raft microdomains and neurotransmitter signalling. *Nat Rev Neurosci* 2007 Feb;8(2):128-40.
16. Suzuki T, Zhang J, Miyazawa S, Liu Q, Farzan MR, Yao WD. Association of membrane rafts and postsynaptic density: Proteomics, biochemical, and ultrastructural analyses. *J Neurochem* 2011 Oct;119(1):64-77.
17. Hering H, Lin CC, Sheng M. Lipid rafts in the maintenance of synapses, dendritic spines, and surface AMPA receptor stability. *J Neurosci* 2003 Apr 15;23(8):3262-71.
18. Pernber Z, Blennow K, Bogdanovic N, Mansson JE, Blomqvist M. Altered distribution of the gangliosides GM1 and GM2 in alzheimer's disease. *Dement Geriatr Cogn Disord* 2012;33(2-3):174-88.
19. Russel PJ. Population genetics. In: *iGenetics A molecular approach*. 2nd ed. Toronto: Pearson Benjamin Cummings; 2006. .
20. Myerowitz R. Tay-sachs disease-causing mutations and neutral polymorphisms in the hex A gene. *Hum Mutat* 1997;9(3):195-208.
21. Myerowitz R, Costigan FC. The major defect in ashkenazi jews with tay-sachs disease is an insertion in the gene for the alpha-chain of beta-hexosaminidase. *J Biol Chem* 1988 Dec 15;263(35):18587-9.
22. Jeyakumar M, Thomas R, Elliot-Smith E, Smith DA, van der Spoel AC, d'Azzo A, Hugh Perry V, Butters TD, Dwek RA, Platt FM. Central nervous system inflammation is a hallmark of pathogenesis in mouse models of GM1 and GM2 gangliosidosis. *Brain* 2003;126:974-987.

23. Tsuji D, Kuroki A, Ishibashi Y, Itakura T, Kuwahara J, Yamanaka S, Itoh K. Specific induction of macrophage inflammatory protein 1-alpha in glial cells of sandhoff disease model mice associated with accumulation of N-acetylhexosaminyl glycoconjugates *J Neurochem* 2005;92(1497-1507).
24. Glass CK, Saijo K, Winner B, Marchetto MC, Gage FH. Mechanisms underlying inflammation in neurodegeneration. *Cell* 2010;140:918-934.
25. Tiribuzi R, D'Angelo F, Berardi AC, Martino S, Orlacchio A. Knock-down of HEXA and HEXB genes correlate with the absence of the immunostimulatory function of HSC-derived dendritic cells. *Cell Biochem Funct* 2011 Oct 13.
26. Wada R, Tiffit CJ, Proia RL. Microglial activation precedes acute neurodegeneration in sandhoff disease and is suppressed by bone marrow transplantation. *Proc Natl Acad Sci USA* 2000;97:10954-10959.
27. Myerowitz R, Lawson D, Mizukami H, Mi Y, Tiffit CJ, Proia RL. Molecular pathophysiology in tay-sachs and sandhoff diseases as revealed by gene expression profiling. *Hum Mol Genet* 2002 May 15;11(11):1343-50.
28. Huang J, Trasler JM, Igdoura S, Michaud J, Hanai N, Gravel RA. Apoptotic cell death in mouse models of GM2 gangliosidosis and observations on human tay-sachs and sandhoff diseases. *Hum Mol Genet* 1997;6(11):1879-1885.
29. Sargeant TJ, Wang S, Bradley J, Smith NJ, Raha AA, McNair R, Ziegler RJ, Cheng SH, Cox TM, Cachon-Gonzalez MB. Adeno-associated virus-mediated expression of beta-hexosaminidase prevents neuronal loss in the sandhoff mouse brain. *Hum Mol Genet* 2011 Nov 15;20(22):4371-80.
30. Vitner EB, Platt FM, Futerman AH. Common and uncommon pathogenic cascades in lysosomal storage diseases. *J Biol Chem* 2010 Jul 2;285(27):20423-7.
31. Phaneuf D, Wakamatsu N, Huang JQ, Borowski A, Peterson AC, Fortunato SR, Ritter G, Igdoura SA, Morales CR, Benoit G, et al. Dramatically different phenotypes in mouse models of human tay-sachs and sandhoff diseases. *Hum Mol Genet* 1996 Jan;5(1):1-14.
32. Product Availability and Regulatory Status [Internet]; c2011 [cited 2011 02/23]. Available from: <http://www1.actelion.com/en/healthcare-professionals/products/zavesca/product-availability-and-regulatory-status.page?>
33. Cox T, Lachmann R, Hollak C, Aerts J, van Weely S, Hrebicek M, Platt F, Butters T, Dwek R, Moyses C, et al. Novel oral treatment of gaucher's disease with N-butyldeoxynojirimycin (OGT 918) to decrease substrate biosynthesis. *Lancet* 2000

- Apr 29;355(9214):1481-5.
34. Jeyakumar M, Norflus F, Tifft CJ, Cortina-Borja M, Butters TD, Proia RL, Perry VH, Dwek RA, Platt FM. Enhanced survival in sandhoff disease mice receiving a combination of substrate deprivation therapy and bone marrow transplantation. *Blood* 2001 Jan 1;97(1):327-9.
  35. Cachon-Gonzalez MB, Wang SZ, Lynch A, Ziegler R, Cheng SH, Cox TM. Effective gene therapy in an authentic model of tay-sachs-related diseases. *Proc Natl Acad Sci U S A* 2006 Jul 5;103(27):10373-8.
  36. Watson AA, Fleet GW, Asano N, Molyneux RJ, Nash RJ. Polyhydroxylated alkaloids -- natural occurrence and therapeutic applications. *Phytochemistry* 2001 Feb;56(3):265-95.
  37. Butters TD, van den Broek LAGM, Fleet GWJ, Krulle TM, Wormald MR, Dwek RA, Platt FM. Molecular requirements of imino sugars for the selective control of N-linked glycosylation and glycosphingolipid biosynthesis. *Tetrahedron-Asymmetry* 2000(11):113-24.
  38. Platt FM, Neises GR, Reinkensmeier G, Townsend MJ, Perry VH, Proia RL, Winchester B, Dwek RA, Butters TD. Prevention of lysosomal storage in tay-sachs mice treated with N-butyldeoxynojirimycin. *Science* 1997 Apr 18;276(5311):428-31.
  39. Gaucher Disease [Internet]; c2010 [cited 2012 06/12]. Available from: <http://dx.doi.org/10.1036/ommbid.176>.
  40. Niemann-Pick Disease Type C: A Lipid Trafficking Disorder [Internet]; c2006 [cited 2012 06/12]. Available from: <http://dx.doi.org/10.1036/ommbid.175>.
  41. Liu Y, Wada R, Kawai H, Sango K, Deng C, Tai T, McDonald MP, Araujo K, Crawley JN, Bierfreund U, et al. A genetic model of substrate deprivation therapy for a glycosphingolipid storage disorder. *J Clin Invest* 1999 Feb;103(4):497-505.
  42. Wu G, Lu ZH, Xie X, Ledeen RW. Susceptibility of cerebellar granule neurons from GM2/GD2 synthase-null mice to apoptosis induced by glutamate excitotoxicity and elevated KCl: Rescue by GM1 and LIGA20. *Glycoconj J* 2004;21(6):305-13.
  43. Platt FM, Neises GR, Dwek RA, Butters TD. N-butyldeoxynojirimycin is a novel inhibitor of glycolipid biosynthesis. *J Biol Chem* 1994 Mar 18;269(11):8362-5.
  44. Platt FM, Reinkensmeier G, Dwek RA, Butters TD. Extensive glycosphingolipid depletion in the liver and lymphoid organs of mice treated with N-

- butyldeoxynojirimycin. *J Biol Chem* 1997 Aug 1;272(31):19365-72.
45. Freeze HH. Genetic disorders of glycan degradation. In: A. Varki, R. D. Cummings, J. D. Esko, editors. *Essentials of glycobiology*. 2nd ed. NY: Cold Spring Harbor Laboratory Press; 2009. .
  46. Nicoll G, Avril T, Lock K, Furukawa K, Bovin N, Crocker PR. Ganglioside GD3 expression on target cells can modulate NK cell cytotoxicity via siglec-7-dependent and -independent mechanisms. *Eur J Immunol* 2003 Jun;33(6):1642-8.
  47. Wu G, Lu ZH, Gabius HJ, Ledeen RW, Bleich D. Ganglioside GM1 deficiency in effector T cells from NOD mice induces resistance to regulatory T-cell suppression. *Diabetes* 2011 Sep;60(9):2341-9.
  48. Nagafuku M, Okuyama K, Onimaru Y, Suzuki A, Odagiri Y, Yamashita T, Iwasaki K, Fujiwara M, Takayanagi M, Ohno I, et al. CD4 and CD8 T cells require different membrane gangliosides for activation. *Proc Natl Acad Sci U S A* 2012 Feb 7;109(6):E336-42.
  49. Bieberich E, Freischutz B, Suzuki M, Yu RK. Differential effects of glycolipid biosynthesis inhibitors on ceramide-induced cell death in neuroblastoma cells. *J Neurochem* 1999 Mar;72(3):1040-9.
  50. Jeyakumar M, Butters TD, Cortina-Borja M, Hunnam V, Proia RL, Perry VH, Dwek RA, Platt FM. Delayed symptom onset and increased life expectancy in sandhoff disease mice treated with N-butyldeoxynojirimycin. *Proc Natl Acad Sci U S A* 1999 May 25;96(11):6388-93.
  51. Heitner R, Elstein D, Aerts J, Weely S, Zimran A. Low-dose N-butyldeoxynojirimycin (OGT 918) for type I gaucher disease. *Blood Cells Mol Dis* 2002 Mar-Apr;28(2):127-33.
  52. Jacobs JF, Willemsen MA, Groot-Loonen JJ, Wevers RA, Hoogerbrugge PM. Allogeneic BMT followed by substrate reduction therapy in a child with subacute tay-sachs disease. *Bone Marrow Transplant* 2005 Nov;36(10):925-6.
  53. Bembi B, Marchetti F, Guerci VI, Ciana G, Addobbati R, Grasso D, Barone R, Cariati R, Fernandez-Guillen L, Butters T, et al. Substrate reduction therapy in the infantile form of tay-sachs disease. *Neurology* 2006 Jan 24;66(2):278-80.
  54. Misago M, Tsukada J, Fukuda MN, Eto S. Suppressive effects of swainsonine and N-butyldeoxynojirimycin on human bone marrow neutrophil maturation. *Biochem Biophys Res Commun* 2000 Mar 5;269(1):219-25.

55. Vitte J, Michel BF, Bongrand P, Gastaut JL. Oxidative stress level in circulating neutrophils is linked to neurodegenerative diseases. *J Clin Immunol* 2004 Nov;24(6):683-92.
56. Puzo J, Alfonso P, Irun P, Gervas J, Pocovi M, Giraldo P. Changes in the atherogenic profile of patients with type 1 gaucher disease after miglustat therapy. *Atherosclerosis* 2010 Apr;209(2):515-9.
57. Wang GL, Jiang BH, Rue EA, Semenza GL. Hypoxia-inducible factor 1 is a basic-helix-loop-helix-PAS heterodimer regulated by cellular O<sub>2</sub> tension. *Proc Natl Acad Sci U S A* 1995 Jun 6;92(12):5510-4.
58. Huang LE, Arany Z, Livingston DM, Bunn HF. Activation of hypoxia-inducible transcription factor depends primarily upon redox-sensitive stabilization of its alpha subunit. *J Biol Chem* 1996 Dec 13;271(50):32253-9.
59. Huang LE, Gu J, Schau M, Bunn HF. Regulation of hypoxia-inducible factor 1alpha is mediated by an O<sub>2</sub>-dependent degradation domain via the ubiquitin-proteasome pathway. *Proc Natl Acad Sci U S A* 1998 Jul 7;95(14):7987-92.
60. Jaakkola P, Mole DR, Tian YM, Wilson MI, Gielbert J, Gaskell SJ, Kriegsheim A, Hebestreit HF, Mukherji M, Schofield CJ, et al. Targeting of HIF-alpha to the von hippel-lindau ubiquitylation complex by O<sub>2</sub>-regulated prolyl hydroxylation. *Science* 2001 Apr 20;292(5516):468-72.
61. Wang GL, Semenza GL. Purification and characterization of hypoxia-inducible factor 1. *J Biol Chem* 1995 Jan 20;270(3):1230-7.
62. Wood SM, Gleadle JM, Pugh CW, Hankinson O, Ratcliffe PJ. The role of the aryl hydrocarbon receptor nuclear translocator (ARNT) in hypoxic induction of gene expression. studies in ARNT-deficient cells. *J Biol Chem* 1996 Jun 21;271(25):15117-23.
63. Lisy K, Peet DJ. Turn me on: Regulating HIF transcriptional activity. *Cell Death Differ* 2008 Apr;15(4):642-9.
64. Forsythe JA, Jiang BH, Iyer NV, Agani F, Leung SW, Koos RD, Semenza GL. Activation of vascular endothelial growth factor gene transcription by hypoxia-inducible factor 1. *Mol Cell Biol* 1996 Sep;16(9):4604-13.
65. Wiesener MS, Jurgensen JS, Rosenberger C, Scholze CK, Horstrup JH, Warnecke C, Mandriota S, Bechmann I, Frei UA, Pugh CW, et al. Widespread hypoxia-inducible expression of HIF-2alpha in distinct cell populations of different organs. *FASEB J*

- 2003 Feb;17(2):271-3.
66. Lin Q, Cong X, Yun Z. Differential hypoxic regulation of hypoxia-inducible factors 1alpha and 2alpha. *Mol Cancer Res* 2011 Jun;9(6):757-65.
  67. Makino Y, Cao R, Svensson K, Bertilsson G, Asman M, Tanaka H, Cao Y, Berkenstam A, Poellinger L. Inhibitory PAS domain protein is a negative regulator of hypoxia-inducible gene expression. *Nature* 2001 Nov 29;414(6863):550-4.
  68. Makino Y, Kanopka A, Wilson WJ, Tanaka H, Poellinger L. Inhibitory PAS domain protein (IPAS) is a hypoxia-inducible splicing variant of the hypoxia-inducible factor-3alpha locus. *J Biol Chem* 2002 Sep 6;277(36):32405-8.
  69. Heidbreder M, Frohlich F, Jöhren O, Dendorfer A, Qadri F, Dominiak P. Hypoxia rapidly activates HIF-3alpha mRNA expression. *FASEB J* 2003 Aug;17(11):1541-3.
  70. Goryo K, Torii S, Yasumoto K, Sogawa K. Tumour necrosis factor-alpha suppresses the hypoxic response by NF-kappaB-dependent induction of inhibitory PAS domain protein in PC12 cells. *J Biochem* 2011 Sep;150(3):311-8.
  71. Maxwell PH, Wiesener MS, Chang GW, Clifford SC, Vaux EC, Cockman ME, Wykoff CC, Pugh CW, Maher ER, Ratcliffe PJ. The tumour suppressor protein VHL targets hypoxia-inducible factors for oxygen-dependent proteolysis. *Nature* 1999 May 20;399(6733):271-5.
  72. Ohh M, Park CW, Ivan M, Hoffman MA, Kim TY, Huang LE, Pavletich N, Chau V, Kaelin WG. Ubiquitination of hypoxia-inducible factor requires direct binding to the beta-domain of the von hippel-lindau protein. *Nat Cell Biol* 2000 Jul;2(7):423-7.
  73. Masson N, Willam C, Maxwell PH, Pugh CW, Ratcliffe PJ. Independent function of two destruction domains in hypoxia-inducible factor-alpha chains activated by prolyl hydroxylation. *EMBO J* 2001 Sep 17;20(18):5197-206.
  74. Mahon PC, Hirota K, Semenza GL. FIH-1: A novel protein that interacts with HIF-1alpha and VHL to mediate repression of HIF-1 transcriptional activity. *Genes Dev* 2001 Oct 15;15(20):2675-86.
  75. Lando D, Peet DJ, Whelan DA, Gorman JJ, Whitelaw ML. Asparagine hydroxylation of the HIF transactivation domain a hypoxic switch. *Science* 2002 Feb 1;295(5556):858-61.
  76. McNeill LA, Hewitson KS, Claridge TD, Seibel JF, Horsfall LE, Schofield CJ. Hypoxia-inducible factor asparaginyl hydroxylase (FIH-1) catalyses hydroxylation at

- the beta-carbon of asparagine-803. *Biochem J* 2002 Nov 1;367(Pt 3):571-5.
77. Richard DE, Berra E, Gothie E, Roux D, Pouyssegur J. p42/p44 mitogen-activated protein kinases phosphorylate hypoxia-inducible factor 1alpha (HIF-1alpha) and enhance the transcriptional activity of HIF-1. *J Biol Chem* 1999 Nov 12;274(46):32631-7.
78. Mylonis I, Chachami G, Samiotaki M, Panayotou G, Paraskeva E, Kalousi A, Georgatsou E, Bonanou S, Simos G. Identification of MAPK phosphorylation sites and their role in the localization and activity of hypoxia-inducible factor-1alpha. *J Biol Chem* 2006 Nov 3;281(44):33095-106.
79. Flugel D, Gorlach A, Michiels C, Kietzmann T. Glycogen synthase kinase 3 phosphorylates hypoxia-inducible factor 1alpha and mediates its destabilization in a VHL-independent manner. *Mol Cell Biol* 2007 May;27(9):3253-65.
80. Gradin K, McGuire J, Wenger RH, Kvietikova I, Fritzel ML, Toftgard R, Tora L, Gassmann M, Poellinger L. Functional interference between hypoxia and dioxin signal transduction pathways: Competition for recruitment of the arnt transcription factor. *Mol Cell Biol* 1996 Oct;16(10):5221-31.
81. Minet E, Mottet D, Michel G, Roland I, Raes M, Remacle J, Michiels C. Hypoxia-induced activation of HIF-1: Role of HIF-1alpha-Hsp90 interaction. *FEBS Lett* 1999 Oct 29;460(2):251-6.
82. Katschinski DM, Le L, Schindler SG, Thomas T, Voss AK, Wenger RH. Interaction of the PAS B domain with HSP90 accelerates hypoxia-inducible factor-1alpha stabilization. *Cell Physiol Biochem* 2004;14(4-6):351-60.
83. Isaacs JS, Jung YJ, Neckers L. Aryl hydrocarbon nuclear translocator (ARNT) promotes oxygen-independent stabilization of hypoxia-inducible factor-1alpha by modulating an Hsp90-dependent regulatory pathway. *J Biol Chem* 2004 Apr 16;279(16):16128-35.
84. Schofield CJ, Ratcliffe PJ. Oxygen sensing by HIF hydroxylases. *Nat Rev Mol Cell Biol* 2004 May;5(5):343-54.
85. Bardos JI, Ashcroft M. Negative and positive regulation of HIF-1: A complex network. *Biochim Biophys Acta* 2005 Jul 25;1755(2):107-20.
86. Camps C, Buffa FM, Colella S, Moore J, Sotiriou C, Sheldon H, Harris AL, Gleadle JM, Ragooussis J. Hsa-miR-210 is induced by hypoxia and is an independent prognostic factor in breast cancer. *Clin Cancer Res* 2008 Mar 1;14(5):1340-8.

87. Pulkkinen K, Malm T, Turunen M, Koistinaho J, Yla-Herttuala S. Hypoxia induces microRNA miR-210 in vitro and in vivo ephrin-A3 and neuronal pentraxin 1 are potentially regulated by miR-210. *FEBS Lett* 2008 Jul 9;582(16):2397-401.
88. Bartel DP. MicroRNAs: Genomics, biogenesis, mechanism, and function. *Cell* 2004 Jan 23;116(2):281-97.
89. Lagos-Quintana M, Rauhut R, Lendeckel W, Tuschl T. Identification of novel genes coding for small expressed RNAs. *Science* 2001 Oct 26;294(5543):853-8.
90. Lau NC, Lim LP, Weinstein EG, Bartel DP. An abundant class of tiny RNAs with probable regulatory roles in *caenorhabditis elegans*. *Science* 2001 Oct 26;294(5543):858-62.
91. Lee Y, Jeon K, Lee JT, Kim S, Kim VN. MicroRNA maturation: Stepwise processing and subcellular localization. *EMBO J* 2002 Sep 2;21(17):4663-70.
92. Cai X, Hagedorn CH, Cullen BR. Human microRNAs are processed from capped, polyadenylated transcripts that can also function as mRNAs. *RNA* 2004 Dec;10(12):1957-66.
93. Lee Y, Kim M, Han J, Yeom KH, Lee S, Baek SH, Kim VN. MicroRNA genes are transcribed by RNA polymerase II. *EMBO J* 2004 Oct 13;23(20):4051-60.
94. Lee Y, Ahn C, Han J, Choi H, Kim J, Yim J, Lee J, Provost P, Radmark O, Kim S, et al. The nuclear RNase III drosha initiates microRNA processing. *Nature* 2003 Sep 25;425(6956):415-9.
95. Bohnsack MT, Czaplinski K, Gorlich D. Exportin 5 is a RanGTP-dependent dsRNA-binding protein that mediates nuclear export of pre-miRNAs. *RNA* 2004 Feb;10(2):185-91.
96. Yi R, Qin Y, Macara IG, Cullen BR. Exportin-5 mediates the nuclear export of pre-microRNAs and short hairpin RNAs. *Genes Dev* 2003 Dec 15;17(24):3011-6.
97. Lund E, Guttinger S, Calado A, Dahlberg JE, Kutay U. Nuclear export of microRNA precursors. *Science* 2004 Jan 2;303(5654):95-8.
98. Knight SW, Bass BL. A role for the RNase III enzyme DCR-1 in RNA interference and germ line development in *caenorhabditis elegans*. *Science* 2001 Sep 21;293(5538):2269-71.
99. Ketting RF, Fischer SE, Bernstein E, Sijen T, Hannon GJ, Plasterk RH. Dicer functions in RNA interference and in synthesis of small RNA involved in

- developmental timing in *C. elegans*. *Genes Dev* 2001 Oct 15;15(20):2654-9.
100. Hutvagner G, McLachlan J, Pasquinelli AE, Balint E, Tuschl T, Zamore PD. A cellular function for the RNA-interference enzyme dicer in the maturation of the let-7 small temporal RNA. *Science* 2001 Aug 3;293(5531):834-8.
101. Bernstein E, Caudy AA, Hammond SM, Hannon GJ. Role for a bidentate ribonuclease in the initiation step of RNA interference. *Nature* 2001 Jan 18;409(6818):363-6.
102. Song JJ, Smith SK, Hannon GJ, Joshua-Tor L. Crystal structure of argonaute and its implications for RISC slicer activity. *Science* 2004 Sep 3;305(5689):1434-7.
103. Lewis BP, Burge CB, Bartel DP. Conserved seed pairing, often flanked by adenosines, indicates that thousands of human genes are microRNA targets. *Cell* 2005 Jan 14;120(1):15-20.
104. Rottiers V, Naar AM. MicroRNAs in metabolism and metabolic disorders. *Nat Rev Mol Cell Biol* 2012 Mar 22;13(4):239-50.
105. Mendell JT, Olson EN. MicroRNAs in stress signaling and human disease. *Cell* 2012 Mar 16;148(6):1172-87.
106. Meza-Sosa KF, Valle-Garcia D, Pedraza-Alva G, Perez-Martinez L. Role of microRNAs in central nervous system development and pathology. *J Neurosci Res* 2012 Jan;90(1):1-12.
107. Schaefer A, O'Carroll D, Tan CL, Hillman D, Sugimori M, Llinas R, Greengard P. Cerebellar neurodegeneration in the absence of microRNAs. *J Exp Med* 2007 Jul 9;204(7):1553-8.
108. Davis TH, Cuellar TL, Koch SM, Barker AJ, Harfe BD, McManus MT, Ullian EM. Conditional loss of dicer disrupts cellular and tissue morphogenesis in the cortex and hippocampus. *J Neurosci* 2008 Apr 23;28(17):4322-30.
109. Tao J, Wu H, Lin Q, Wei W, Lu XH, Cantle JP, Ao Y, Olsen RW, Yang XW, Mody I, et al. Deletion of astroglial dicer causes non-cell-autonomous neuronal dysfunction and degeneration. *J Neurosci* 2011 Jun 1;31(22):8306-19.
110. Sardi F, Fassina L, Venturini L, Inguscio M, Guerriero F, Rolfo E, Ricevuti G. Alzheimer's disease, autoimmunity and inflammation. the good, the bad and the ugly. *Autoimmun Rev* 2011 Dec;11(2):149-53.

111. Lukiw WJ, Zhao Y, Cui JG. An NF-kappaB-sensitive micro RNA-146a-mediated inflammatory circuit in alzheimer disease and in stressed human brain cells. *J Biol Chem* 2008 Nov 14;283(46):31315-22.
112. Lukiw WJ, Alexandrov PN. Regulation of complement factor H (CFH) by multiple miRNAs in alzheimer's disease (AD) brain. *Mol Neurobiol* 2012 Feb 3.
113. Lehmann SM, Kruger C, Park B, Derkow K, Rosenberger K, Baumgart J, Trimbuch T, Eom G, Hinz M, Kaul D, et al. An unconventional role for miRNA: Let-7 activates toll-like receptor 7 and causes neurodegeneration. *Nat Neurosci* 2012 May 20.
114. Liu Y, Liu F, Iqbal K, Grundke-Iqbal I, Gong CX. Decreased glucose transporters correlate to abnormal hyperphosphorylation of tau in alzheimer disease. *FEBS Lett* 2008 Jan 23;582(2):359-64.
115. Schubert D, Soucek T, Blouw B. The induction of HIF-1 reduces astrocyte activation by amyloid beta peptide. *Eur J Neurosci* 2009 Apr;29(7):1323-34.
116. German DC, Liang CL, Song T, Yazdani U, Xie C, Dietschy JM. Neurodegeneration in the niemann-pick C mouse: Glial involvement. *Neuroscience* 2002;109(3):437-50.
117. Oosthuysen B, Moons L, Storkebaum E, Beck H, Nuyens D, Brusselmans K, Van Dorpe J, Hellings P, Gorselink M, Heymans S, et al. Deletion of the hypoxia-response element in the vascular endothelial growth factor promoter causes motor neuron degeneration. *Nat Genet* 2001 Jun;28(2):131-8.
118. Wang Y, Mao XO, Xie L, Banwait S, Marti HH, Greenberg DA, Jin K. Vascular endothelial growth factor overexpression delays neurodegeneration and prolongs survival in amyotrophic lateral sclerosis mice. *J Neurosci* 2007 Jan 10;27(2):304-7.
119. Storkebaum E, Lambrechts D, Dewerchin M, Moreno-Murciano MP, Appelmans S, Oh H, Van Damme P, Rutten B, Man WY, De Mol M, et al. Treatment of motoneuron degeneration by intracerebroventricular delivery of VEGF in a rat model of ALS. *Nat Neurosci* 2005 Jan;8(1):85-92.
120. Iyer NV, Kotch LE, Agani F, Leung SW, Laughner E, Wenger RH, Gassmann M, Gearhart JD, Lawler AM, Yu AY, et al. Cellular and developmental control of O2 homeostasis by hypoxia-inducible factor 1 alpha. *Genes Dev* 1998 Jan 15;12(2):149-62.
121. Tomita S, Ueno M, Sakamoto M, Kitahama Y, Ueki M, Maekawa N, Sakamoto H, Gassmann M, Kageyama R, Ueda N, et al. Defective brain development in mice

- lacking the hif-1alpha gene in neural cells. *Mol Cell Biol* 2003 Oct;23(19):6739-49.
122. Olney JW. Brain lesions, obesity and other disturbances in mice treated with monosodium glutamate. *Science* 1969;164:719-721.
123. Arundine M, Tymianski M. Molecular mechanisms of calcium-dependent neurodegeneration in excitotoxicity. *Cell Calcium* 2003;34:325-337.
124. Hollmann M, Heinemann S. Cloned glutamate receptors. *Annu Rev Neurosci* 1994;17:31-108.
125. Stanfield CL, Germann WJ. Nerve cells and electrical signaling. In: *Principles of human physiology*. Third ed. Toronto: Pearson Benjamin Cummings; 2008. .
126. Belachew S, Gallo V. Synaptic and extrasynaptic neurotransmitter receptors in glial precursors' quest for identity. *Glia* 2004 Nov 15;48(3):185-96.
127. Isaac JT, Ashby M, McBain CJ. The role of the GluR2 subunit in AMPA receptor function and synaptic plasticity. *Neuron* 2007 Jun 21;54(6):859-71.
128. Newpher TM, Ehlers MD. Glutamate receptor dynamics in dendritic microdomains. *Neuron* 2008 May 22;58(4):472-97.
129. Ashby MC, Maier SR, Nishimune A, Henley JM. Lateral diffusion drives constitutive exchange of AMPA receptors at dendritic spines and is regulated by spine morphology. *J Neurosci* 2006 Jun 28;26(26):7046-55.
130. Sharma K, Fong DK, Craig AM. Postsynaptic protein mobility in dendritic spines: Long-term regulation by synaptic NMDA receptor activation. *Mol Cell Neurosci* 2006 Apr;31(4):702-12.
131. Heine M, Groc L, Frischknecht R, Beique JC, Lounis B, Rumbaugh G, Huganir RL, Cognet L, Choquet D. Surface mobility of postsynaptic AMPARs tunes synaptic transmission. *Science* 2008 Apr 11;320(5873):201-5.
132. Carroll RC, Lissin DV, von Zastrow M, Nicoll RA, Malenka RC. Rapid redistribution of glutamate receptors contributes to long-term depression in hippocampal cultures. *Nat Neurosci* 1999 May;2(5):454-60.
133. Heynen AJ, Quinlan EM, Bae DC, Bear MF. Bidirectional, activity-dependent regulation of glutamate receptors in the adult hippocampus in vivo. *Neuron* 2000 Nov;28(2):527-36.

134. Xie X, Liaw JS, Baudry M, Berger TW. Novel expression mechanism for synaptic potentiation: Alignment of presynaptic release site and postsynaptic receptor. *Proc Natl Acad Sci U S A* 1997 Jun 24;94(13):6983-8.
135. Raghavachari S, Lisman JE. Properties of quantal transmission at CA1 synapses. *J Neurophysiol* 2004 Oct;92(4):2456-67.
136. Franks KM, Stevens CF, Sejnowski TJ. Independent sources of quantal variability at single glutamatergic synapses. *J Neurosci* 2003 Apr 15;23(8):3186-95.
137. Nakagawa T, Cheng Y, Ramm E, Sheng M, Walz T. Structure and different conformational states of native AMPA receptor complexes. *Nature* 2005 Feb 3;433(7025):545-9.
138. Mayer ML. Glutamate receptors at atomic resolution. *Nature* 2006 Mar 23;440(7083):456-62.
139. Biou V, Bhattacharyya S, Malenka RC. Endocytosis and recycling of AMPA receptors lacking GluR2/3. *Proc Natl Acad Sci U S A* 2008 Jan 22;105(3):1038-43.
140. Song I, Huganir RL. Regulation of AMPA receptors during synaptic plasticity. *Trends Neurosci* 2002 Nov;25(11):578-88.
141. Xia J, Zhang X, Staudinger J, Huganir RL. Clustering of AMPA receptors by the synaptic PDZ domain-containing protein PICK1. *Neuron* 1999 Jan;22(1):179-87.
142. Dong H, O'Brien RJ, Fung ET, Lanahan AA, Worley PF, Huganir RL. GRIP: A synaptic PDZ domain-containing protein that interacts with AMPA receptors. *Nature* 1997 Mar 20;386(6622):279-84.
143. Chung HJ, Steinberg JP, Huganir RL, Linden DJ. Requirement of AMPA receptor GluR2 phosphorylation for cerebellar long-term depression. *Science* 2003 Jun 13;300(5626):1751-5.
144. Mao L, Takamiya K, Thomas G, Lin DT, Huganir RL. GRIP1 and 2 regulate activity-dependent AMPA receptor recycling via exocyst complex interactions. *Proc Natl Acad Sci U S A* 2010 Nov 2;107(44):19038-43.
145. Volk L, Kim CH, Takamiya K, Yu Y, Huganir RL. Developmental regulation of protein interacting with C kinase 1 (PICK1) function in hippocampal synaptic plasticity and learning. *Proc Natl Acad Sci U S A* 2010 Dec 14;107(50):21784-9.
146. Xia J, Chung HJ, Wihler C, Huganir RL, Linden DJ. Cerebellar long-term depression requires PKC-regulated interactions between GluR2/3 and PDZ domain-

- containing proteins. *Neuron* 2000 Nov;28(2):499-510.
147. Matsuda S, Launey T, Mikawa S, Hirai H. Disruption of AMPA receptor GluR2 clusters following long-term depression induction in cerebellar purkinje neurons. *EMBO J* 2000 Jun 15;19(12):2765-74.
148. Leonard AS, Davare MA, Horne MC, Garner CC, Hell JW. SAP97 is associated with the alpha-amino-3-hydroxy-5-methylisoxazole-4-propionic acid receptor GluR1 subunit. *J Biol Chem* 1998 Jul 31;273(31):19518-24.
149. Tomita S, Chen L, Kawasaki Y, Petralia RS, Wenthold RJ, Nicoll RA, Brecht DS. Functional studies and distribution define a family of transmembrane AMPA receptor regulatory proteins. *J Cell Biol* 2003 May 26;161(4):805-16.
150. Tomita S, Fukata M, Nicoll RA, Brecht DS. Dynamic interaction of stargazin-like TARPs with cycling AMPA receptors at synapses. *Science* 2004 Mar 5;303(5663):1508-11.
151. Vandenberghe W, Nicoll RA, Brecht DS. Stargazin is an AMPA receptor auxiliary subunit. *Proc Natl Acad Sci U S A* 2005 Jan 11;102(2):485-90.
152. Kato AS, Zhou W, Milstein AD, Knierman MD, Siuda ER, Dotzlaef JE, Yu H, Hale JE, Nisenbaum ES, Nicoll RA, et al. New transmembrane AMPA receptor regulatory protein isoform, gamma-7, differentially regulates AMPA receptors. *J Neurosci* 2007 May 2;27(18):4969-77.
153. Fukata Y, Tzingounis AV, Trinidad JC, Fukata M, Burlingame AL, Nicoll RA, Brecht DS. Molecular constituents of neuronal AMPA receptors. *J Cell Biol* 2005 May 9;169(3):399-404.
154. Yamazaki M, Ohno-Shosaku T, Fukaya M, Kano M, Watanabe M, Sakimura K. A novel action of stargazin as an enhancer of AMPA receptor activity. *Neurosci Res* 2004 Dec;50(4):369-74.
155. Tomita S, Adesnik H, Sekiguchi M, Zhang W, Wada K, Howe JR, Nicoll RA, Brecht DS. Stargazin modulates AMPA receptor gating and trafficking by distinct domains. *Nature* 2005 Jun 23;435(7045):1052-8.
156. Jackson AC, Nicoll RA. Stargazin (TARP gamma-2) is required for compartment-specific AMPA receptor trafficking and synaptic plasticity in cerebellar stellate cells. *J Neurosci* 2011 Mar 16;31(11):3939-52.
157. Chen L, El-Husseini A, Tomita S, Brecht DS, Nicoll RA. Stargazin differentially controls the trafficking of alpha-amino-3-hydroxyl-5-methyl-4-isoxazolepropionate

- and kainate receptors. *Mol Pharmacol* 2003 Sep;64(3):703-6.
158. Bedoukian MA, Weeks AM, Partin KM. Different domains of the AMPA receptor direct stargazin-mediated trafficking and stargazin-mediated modulation of kinetics. *J Biol Chem* 2006 Aug 18;281(33):23908-21.
159. Priel A, Kolleker A, Ayalon G, Gillor M, Osten P, Stern-Bach Y. Stargazin reduces desensitization and slows deactivation of the AMPA-type glutamate receptors. *J Neurosci* 2005 Mar 9;25(10):2682-6.
160. Shi Y, Suh YH, Milstein AD, Isozaki K, Schmid SM, Roche KW, Nicoll RA. Functional comparison of the effects of TARPs and cornichons on AMPA receptor trafficking and gating. *Proc Natl Acad Sci U S A* 2010 Sep 14;107(37):16315-9.
161. Wang R, Walker CS, Brockie PJ, Francis MM, Mellem JE, Madsen DM, Maricq AV. Evolutionary conserved role for TARPs in the gating of glutamate receptors and tuning of synaptic function. *Neuron* 2008 Sep 25;59(6):997-1008.
162. Suzuki E, Kessler M, Arai AC. The fast kinetics of AMPA GluR3 receptors is selectively modulated by the TARPs gamma 4 and gamma 8. *Mol Cell Neurosci* 2008 May;38(1):117-23.
163. Turetsky D, Garringer E, Patneau DK. Stargazin modulates native AMPA receptor functional properties by two distinct mechanisms. *J Neurosci* 2005 Aug 10;25(32):7438-48.
164. Choi J, Ko J, Park E, Lee JR, Yoon J, Lim S, Kim E. Phosphorylation of stargazin by protein kinase A regulates its interaction with PSD-95. *J Biol Chem* 2002 Apr 5;277(14):12359-63.
165. Stein EL, Chetkovich DM. Regulation of stargazin synaptic trafficking by C-terminal PDZ ligand phosphorylation in bidirectional synaptic plasticity. *J Neurochem* 2010 Apr;113(1):42-53.
166. Opazo P, Labrecque S, Tigaret CM, Frouin A, Wiseman PW, De Koninck P, Choquet D. CaMKII triggers the diffusional trapping of surface AMPARs through phosphorylation of stargazin. *Neuron* 2010 Jul 29;67(2):239-52.
167. Nomura T, Kakegawa W, Matsuda S, Kohda K, Nishiyama J, Takahashi T, Yuzaki M. Cerebellar long-term depression requires dephosphorylation of TARP in purkinje cells. *Eur J Neurosci* 2012 Feb;35(3):402-10.
168. Malenka RC, Nicoll RA. Silent synapses speak up. *Neuron* 1997 Sep;19(3):473-6.

169. Liao D, Zhang X, O'Brien R, Ehlers MD, Huganir RL. Regulation of morphological postsynaptic silent synapses in developing hippocampal neurons. *Nat Neurosci* 1999 Jan;2(1):37-43.
170. Nusser Z, Lujan R, Laube G, Roberts JD, Molnar E, Somogyi P. Cell type and pathway dependence of synaptic AMPA receptor number and variability in the hippocampus. *Neuron* 1998 Sep;21(3):545-59.
171. Takumi Y, Ramirez-Leon V, Laake P, Rinvik E, Ottersen OP. Different modes of expression of AMPA and NMDA receptors in hippocampal synapses. *Nat Neurosci* 1999 Jul;2(7):618-24.
172. Racca C, Stephenson FA, Streit P, Roberts JD, Somogyi P. NMDA receptor content of synapses in stratum radiatum of the hippocampal CA1 area. *J Neurosci* 2000 Apr 1;20(7):2512-22.
173. Gomperts SN, Rao A, Craig AM, Malenka RC, Nicoll RA. Postsynaptically silent synapses in single neuron cultures. *Neuron* 1998 Dec;21(6):1443-51.
174. Isaac JT, Nicoll RA, Malenka RC. Evidence for silent synapses: Implications for the expression of LTP. *Neuron* 1995 Aug;15(2):427-34.
175. Liao D, Hessler NA, Malinow R. Activation of postsynaptically silent synapses during pairing-induced LTP in CA1 region of hippocampal slice. *Nature* 1995 Jun 1;375(6530):400-4.
176. Durand GM, Kovalchuk Y, Konnerth A. Long-term potentiation and functional synapse induction in developing hippocampus. *Nature* 1996 May 2;381(6577):71-5.
177. Ehlers MD. Reinsertion or degradation of AMPA receptors determined by activity-dependent endocytic sorting. *Neuron* 2000 Nov;28(2):511-25.
178. Zhou Q, Xiao M, Nicoll RA. Contribution of cytoskeleton to the internalization of AMPA receptors. *Proc Natl Acad Sci U S A* 2001 Jan 30;98(3):1261-6.
179. Luscher C, Xia H, Beattie EC, Carroll RC, von Zastrow M, Malenka RC, Nicoll RA. Role of AMPA receptor cycling in synaptic transmission and plasticity. *Neuron* 1999 Nov;24(3):649-58.
180. Lin JW, Ju W, Foster K, Lee SH, Ahmadian G, Wyszynski M, Wang YT, Sheng M. Distinct molecular mechanisms and divergent endocytotic pathways of AMPA receptor internalization. *Nat Neurosci* 2000 Dec;3(12):1282-90.

181. Johnson GL, Lapadat R. Mitogen-activated protein kinase pathways mediated by ERK, JNK, and p38 protein kinases. *Science* 2002 Dec 6;298(5600):1911-2.
182. O'Dell TJ, Kandel ER. Low-frequency stimulation erases LTP through an NMDA receptor-mediated activation of protein phosphatases. *Learn Mem* 1994 Jul-Aug;1(2):129-39.
183. Mulkey RM, Endo S, Shenolikar S, Malenka RC. Involvement of a calcineurin/inhibitor-1 phosphatase cascade in hippocampal long-term depression. *Nature* 1994 Jun 9;369(6480):486-8.
184. Lisman J. A mechanism for the hebb and the anti-hebb processes underlying learning and memory. *Proc Natl Acad Sci U S A* 1989 Dec;86(23):9574-8.
185. Beattie EC, Carroll RC, Yu X, Morishita W, Yasuda H, von Zastrow M, Malenka RC. Regulation of AMPA receptor endocytosis by a signaling mechanism shared with LTD. *Nat Neurosci* 2000 Dec;3(12):1291-300.
186. Hartell NA. cGMP acts within cerebellar purkinje cells to produce long term depression via mechanisms involving PKC and PKG. *Neuroreport* 1994 Mar 21;5(7):833-6.
187. Crepel F, Jaillard D. Protein kinases, nitric oxide and long-term depression of synapses in the cerebellum. *Neuroreport* 1990 Oct;1(2):133-6.
188. Linden DJ, Connor JA. Participation of postsynaptic PKC in cerebellar long-term depression in culture. *Science* 1991 Dec 13;254(5038):1656-9.
189. Sattler R, Tymianski M. Molecular mechanisms of calcium-dependent excitotoxicity. *J Mol Med* 2000;78(1):3-13.
190. Szydlowska K, Tymianski M. Calcium, ischemia and excitotoxicity. *Cell Calcium* 2010 Feb;47(2):122-9.
191. Frandsen A, Schousboe A. Dantrolene prevents glutamate cytotoxicity and Ca<sup>2+</sup> release from intracellular stores in cultured cerebral cortical neurons. *J Neurochem* 1991 Mar;56(3):1075-8.
192. Sommer B, Kohler M, Sprengel R, Seeburg PH. RNA editing in brain controls a determinant of ion flow in glutamate-gated channels *Cell* 1991;67(11-19).
193. Verdoorn TA, Burnashev N, Monyer H, Seeburg PH, Sakmann B. Structural determinants of ion flow through recombinant glutamate receptor channels. *Science*

- 1991 Jun 21;252(5013):1715-8.
194. Swanson GT, Kamboj SK, Cull-Candy SG. Single-channel properties of recombinant AMPA receptors depend on RNA editing, splice variation, and subunit composition. *J Neurosci* 1997 Jan 1;17(1):58-69.
195. Wenthold RJ, Petralia RS, Blahos J,II, Niedzielski AS. Evidence for multiple AMPA receptor complexes in hippocampal CA1/CA2 neurons. *J Neurosci* 1996 Mar 15;16(6):1982-9.
196. Monyer H, Seeburg PH, Wisden W. Glutamate-operated channels: Developmentally early and mature forms arise by alternative splicing. *Neuron* 1991 May;6(5):799-810.
197. Pelled D, Lloyd-Evans E, Riebeling C, Jeyakumar M, Platt FM, Futerman AH. Inhibition of calcium uptake via the sarco/endoplasmic reticulum  $Ca^{2+}$ -ATPase in a mouse model of sandhoff disease and prevention by treatment with N-butyldeoxynojirimycin. *J Biol Chem* 2003 Aug 8;278(32):29496-501.
198. Wu G, Xie X, Lu ZH, Ledeen RW. Cerebellar neurons lacking complex gangliosides degenerate in the presence of depolarizing levels of potassium. *Proc Natl Acad Sci U S A* 2001 Jan 2;98(1):307-12.
199. Ogoshi F, Yin HZ, Kuppumbatti Y, Song B, Amindari S, Weiss JH. Tumor necrosis-factor-alpha (TNF-alpha) induces rapid insertion of  $Ca^{2+}$ -permeable alpha-amino-3-hydroxyl-5-methyl-4-isoxazole-propionate (AMPA)/kainate (ca-A/K) channels in a subset of hippocampal pyramidal neurons. *Exp Neurol* 2005 Jun;193(2):384-93.
200. Bliss RM, Finckbone VL, Trice J, Strahlendorf H, Strahlendorf J. Tumor necrosis factor-alpha (TNF-alpha) augments AMPA-induced purkinje neuron toxicity. *Brain Res* 2011 Apr 22;1386:1-14.
201. Kopach O, Kao SC, Petralia RS, Belan P, Tao YX, Voitenko N. Inflammation alters trafficking of extrasynaptic AMPA receptors in tonically firing lamina II neurons of the rat spinal dorsal horn. *Pain* 2011 Apr;152(4):912-23.
202. Danbolt NC. Glutamate uptake. *Prog Neurobiol* 2001 Sep;65(1):1-105.
203. Kanner BI, Marva E. Efflux of L-glutamate by synaptic plasma membrane vesicles isolated from rat brain. *Biochemistry* 1982 Jun 22;21(13):3143-7.
204. Jarzylo LA, Man HY. Parasynaptic NMDA receptor signaling couples neuronal glutamate transporter function to AMPA receptor synaptic distribution and stability. *J Neurosci* 2012 Feb 15;32(7):2552-63.

205. Schlimgen AK, Helms JA, Vogel H, Perin MS. Neuronal pentraxin, a secreted protein with homology to acute phase proteins of the immune system. *Neuron* 1995 Mar;14(3):519-26.
206. Xu D, Hopf C, Reddy R, Cho RW, Guo L, Lanahan A, Petralia RS, Wenthold RJ, O'Brien RJ, Worley P. Narp and NP1 form hetero-complexes that function in developmental and activity-dependent synaptic plasticity. *Neuron* 2003;39(5):513-528.
207. Emsley J, White HE, O'Hara BP, Oliva G, Srinivasan N, Tickle IJ, Blundell TL, Pepys MB, Wood SP. Structure of pentameric human serum amyloid P component. *Nature* 1994 Jan 27;367(6461):338-45.
208. Srinivasan N, White HE, Emsley J, Wood SP, Pepys MB, Blundell TL. Comparative analyses of pentraxins: Implications for protomer assembly and ligand binding. *Structure* 1994 Nov 15;2(11):1017-27.
209. O'Brien RJ, Xu D. Synaptic clustering of AMPA receptors by the extracellular immediate-early gene product narp. *Neuron* 1999;23:309-323.
210. Sia G, Beique J, Rumbaugh G, Cho R, Worley PF, Huganir RL. Interaction of the N-terminal domain of the AMPA receptor GluR4 subunit with the neuronal pentraxin NP1 mediates GluR4 synaptic recruitment. *Neuron* 2007;55:87-102.
211. Cho RW, Park JM, Wolff BE, Xu D, Hopf C, Kim J, Reddy RC, Petralia RS, Perin MS, Linden DJ, et al. mGluR1/5-dependent long term depression requires the regulated ectodomain cleavage of neuronal pentraxin NPR by TACE. *Neuron* 2008;57:858-871.
212. Kirkpatrick LL, Matzuk MM, Dodds DC, Perin MS. Biochemical interactions of the neuronal pentraxins. neuronal pentraxin (NP) receptor binds to taipoxin and taipoxin-associated calcium-binding protein 49 via NP1 and NP2. *J Biol Chem* 2000 Jun 9;275(23):17786-92.
213. DeGregorio-Rocasolano N, Gasull T, Trullas R. Overexpression of neuronal pentraxin 1 is involved in neuronal death evoked by low K<sup>+</sup> in cerebellar granule cells. *J Biol Chem* 2001;276(1):796-803.
214. Hossain MA, Russell JC, O'Brien R, Laterra J. Neuronal pentraxin 1: A novel mediator of hypoxic-ischemic injury in neonatal brain. *J Neurosci* 2004;24(17):4187-4196.
215. Clayton KB, Podlesniy P, Figueiro-Silva J, Lopez-Domenech G, Benitez L, Enguita M, Abad MA, Soriano E, Trullas R. NP1 regulates neuronal activity-dependent accumulation of BAX in mitochondria and mitochondrial dynamics. *J Neurosci* 2012

Jan 25;32(4):1453-66.

216. Russell JC, Kishimoto K, O'Driscoll C, Hossain MA. Neuronal pentraxin 1 induction in hypoxic-ischemic neuronal death is regulated via a glycogen synthase kinase-3 $\alpha$ /beta dependent mechanism. *Cell Signal* 2011 Apr;23(4):673-82.
217. Abad MA, Enguita M, DeGregorio-Rocasolano N, Ferrer I, Trullas R. Neuronal pentraxin 1 contributes to the neuronal damage evoked by amyloid-beta and is overexpressed in dystrophic neurites in alzheimer's brain. *J Neurosci* 2006 Dec 6;26(49):12735-47.
218. Bjartmar L, Huberman AD, Ullian EM, Renteria RC, Liu X, Xu W, Prezioso J, Susman MW, Stellwagen D, Stokes CC, et al. Neuronal pentraxins mediate synaptic refinement in the developing visual system. *J Neurosci* 2006;26(23):6269-6281.
219. Jiang HX, Siegel JN, Gewurz H. Binding and complement activation by C-reactive protein via the collagen-like region of C1q and inhibition of these reactions by monoclonal antibodies to C-reactive protein and C1q. *J Immunol* 1991 Apr 1;146(7):2324-30.
220. Ying SC, Gewurz AT, Jiang H, Gewurz H. Human serum amyloid P component oligomers bind and activate the classical complement pathway via residues 14-26 and 76-92 of the A chain collagen-like region of C1q. *J Immunol* 1993 Jan 1;150(1):169-76.
221. Nauta AJ, Bottazzi B, Mantovani A, Salvatori G, Kishore U, Schwaeble WJ, Gingras AR, Tzima S, Vivanco F, Egido J, et al. Biochemical and functional characterization of the interaction between pentraxin 3 and C1q. *Eur J Immunol* 2003 Feb;33(2):465-73.
222. Medhurst AD, Rennie G, Chapman CG, Meadows H, Duckworth MD, Kelsell RE, Gloger II, Pangalos MN. Distribution analysis of human two pore domain potassium channels in tissues of the central nervous system and periphery. *Brain Res Mol Brain Res* 2001 Jan 31;86(1-2):101-14.
223. Hervieu GJ, Cluderay JE, Gray CW, Green PJ, Ranson JL, Randall AD, Meadows HJ. Distribution and expression of TREK-1, a two-pore-domain potassium channel, in the adult rat CNS. *Neuroscience* 2001;103(4):899-919.
224. Thierry-Mieg D, Thierry-Mieg J. AceView: A comprehensive cDNA-supported gene and transcripts annotation. *Genome Biol* 2006;7 Suppl 1:S12.1-14.
225. Buckler KJ, Honore E. The lipid-activated two-pore domain K<sup>+</sup> channel TREK-1 is resistant to hypoxia: Implication for ischaemic neuroprotection. *J Physiol* 2005 Jan

- 1;562(Pt 1):213-22.
226. Segal-Hayoun Y, Cohen A, Zilberberg N. Molecular mechanisms underlying membrane-potential-mediated regulation of neuronal K2P2.1 channels. *Mol Cell Neurosci* 2010 Jan;43(1):117-26.
227. Nayak TK, Harinath S, Nama S, Somasundaram K, Sikdar SK. Inhibition of human two-pore domain K<sup>+</sup> channel TREK1 by local anesthetic lidocaine: Negative cooperativity and half-of-sites saturation kinetics. *Mol Pharmacol* 2009 Oct;76(4):903-17.
228. Thomas D, Plant LD, Wilkens CM, McCrossan ZA, Goldstein SA. Alternative translation initiation in rat brain yields K2P2.1 potassium channels permeable to sodium. *Neuron* 2008 Jun 26;58(6):859-70.
229. Veale EL, Rees KA, Mathie A, Trapp S. Dominant negative effects of a non-conducting TREK1 splice variant expressed in brain. *J Biol Chem* 2010 Sep 17;285(38):29295-304.
230. Fink M, Duprat F, Lesage F, Reyes R, Romey G, Heurteaux C, Lazdunski M. Cloning, functional expression and brain localization of a novel unconventional outward rectifier K<sup>+</sup> channel. *EMBO J* 1996 Dec 16;15(24):6854-62.
231. Honore E. The neuronal background K2P channels: Focus on TREK1. *Nat Rev Neurosci* 2007 Apr;8(4):251-61.
232. Charpak S, Gahwiler BH, Do KQ, Knopfel T. Potassium conductances in hippocampal neurons blocked by excitatory amino-acid transmitters. *Nature* 1990 Oct 25;347(6295):765-7.
233. Guerineau NC, Gahwiler BH, Gerber U. Reduction of resting K<sup>+</sup> current by metabotropic glutamate and muscarinic receptors in rat CA3 cells: Mediation by G-proteins. *J Physiol* 1994 Jan 1;474(1):27-33.
234. Talley EM, Lei Q, Sirois JE, Bayliss DA. TASK-1, a two-pore domain K<sup>+</sup> channel, is modulated by multiple neurotransmitters in motoneurons. *Neuron* 2000 Feb;25(2):399-410.
235. Chemin J, Girard C, Duprat F, Lesage F, Romey G, Lazdunski M. Mechanisms underlying excitatory effects of group I metabotropic glutamate receptors via inhibition of 2P domain K<sup>+</sup> channels. *EMBO J* 2003 Oct 15;22(20):5403-11.

236. Sladeczek F, Pin JP, Recasens M, Bockaert J, Weiss S. Glutamate stimulates inositol phosphate formation in striatal neurones. *Nature* 1985 Oct 24-30;317(6039):717-9.
237. Sugiyama H, Ito I, Hirono C. A new type of glutamate receptor linked to inositol phospholipid metabolism. *Nature* 1987 Feb 5-11;325(6104):531-3.
238. Murbartian J, Lei Q, Sando JJ, Bayliss DA. Sequential phosphorylation mediates receptor- and kinase-induced inhibition of TREK-1 background potassium channels. *J Biol Chem* 2005 Aug 26;280(34):30175-84.
239. Lopes CM, Rohacs T, Czirjak G, Balla T, Enyedi P, Logothetis DE. PIP2 hydrolysis underlies agonist-induced inhibition and regulates voltage gating of two-pore domain K<sup>+</sup> channels. *J Physiol* 2005 Apr 1;564(Pt 1):117-29.
240. Czirjak G, Petheo GL, Spat A, Enyedi P. Inhibition of TASK-1 potassium channel by phospholipase C. *Am J Physiol Cell Physiol* 2001 Aug;281(2):C700-8.
241. Kettunen P, Hess D, El Manira A. mGluR1, but not mGluR5, mediates depolarization of spinal cord neurons by blocking a leak current. *J Neurophysiol* 2003 Oct;90(4):2341-8.
242. Chemin J, Patel AJ, Duprat F, Lauritzen I, Lazdunski M, Honore E. A phospholipid sensor controls mechanogating of the K<sup>+</sup> channel TREK-1. *EMBO J* 2005 Jan 12;24(1):44-53.
243. Mathie A. Neuronal two-pore-domain potassium channels and their regulation by G protein-coupled receptors. *J Physiol* 2007 Jan 15;578(Pt 2):377-85.
244. Maingret F, Honore E, Lazdunski M, Patel AJ. Molecular basis of the voltage-dependent gating of TREK-1, a mechano-sensitive K(+) channel. *Biochem Biophys Res Commun* 2002 Mar 29;292(2):339-46.
245. Bockenhauer D, Zilberberg N, Goldstein SA. KCNK2: Reversible conversion of a hippocampal potassium leak into a voltage-dependent channel. *Nat Neurosci* 2001 May;4(5):486-91.
246. Patel AJ, Honore E, Maingret F, Lesage F, Fink M, Duprat F, Lazdunski M. A mammalian two pore domain mechano-gated S-like K<sup>+</sup> channel. *EMBO J* 1998 Aug 3;17(15):4283-90.
247. Meadows HJ, Benham CD, Cairns W, Gloer I, Jennings C, Medhurst AD, Murdock P, Chapman CG. Cloning, localisation and functional expression of the human orthologue of the TREK-1 potassium channel. *Pflugers Arch* 2000 Apr;439(6):714-

22.

248. Maingret F, Patel AJ, Lesage F, Lazdunski M, Honore E. Mechano- or acid stimulation, two interactive modes of activation of the TREK-1 potassium channel. *J Biol Chem* 1999 Sep 17;274(38):26691-6.
249. Maingret F, Lauritzen I, Patel AJ, Heurteaux C, Reyes R, Lesage F, Lazdunski M, Honore E. TREK-1 is a heat-activated background K(+) channel. *EMBO J* 2000 Jun 1;19(11):2483-91.
250. Kang D, Choe C, Kim D. Thermosensitivity of the two-pore domain K<sup>+</sup> channels TREK-2 and TRAAK. *J Physiol* 2005 Apr 1;564(Pt 1):103-16.
251. Patel AJ, Honore E, Lesage F, Fink M, Romey G, Lazdunski M. Inhalational anesthetics activate two-pore-domain background K<sup>+</sup> channels. *Nat Neurosci* 1999 May;2(5):422-6.
252. Patel AJ, Honore E. Anesthetic-sensitive 2P domain K<sup>+</sup> channels. *Anesthesiology* 2001 Oct;95(4):1013-21.
253. Honore E, Maingret F, Lazdunski M, Patel AJ. An intracellular proton sensor commands lipid- and mechano-gating of the K(+) channel TREK-1. *EMBO J* 2002 Jun 17;21(12):2968-76.
254. Lesage F, Terrenoire C, Romey G, Lazdunski M. Human TREK2, a 2P domain mechano-sensitive K<sup>+</sup> channel with multiple regulations by polyunsaturated fatty acids, lysophospholipids, and gs, gi, and gq protein-coupled receptors. *J Biol Chem* 2000 Sep 15;275(37):28398-405.
255. Aimond F, Rauzier JM, Bony C, Vassort G. Simultaneous activation of p38 MAPK and p42/44 MAPK by ATP stimulates the K<sup>+</sup> current ITREK in cardiomyocytes. *J Biol Chem* 2000 Dec 15;275(50):39110-6.
256. Patel AJ, Lazdunski M, Honore E. Lipid and mechano-gated 2P domain K(+) channels. *Curr Opin Cell Biol* 2001 Aug;13(4):422-8.
257. Heurteaux C, Guy N, Laigle C, Blondeau N, Duprat F, Mazzuca M, Lang-Lazdunski L, Widmann C, Zanzouri M, Romey G, et al. TREK-1, a K<sup>+</sup> channel involved in neuroprotection and general anesthesia. *EMBO J* 2004 Jul 7;23(13):2684-95.
258. Alloui A, Zimmermann K, Mamet J, Duprat F, Noel J, Chemin J, Guy N, Blondeau N, Voilley N, Rubat-Coudert C, et al. TREK-1, a K<sup>+</sup> channel involved in polymodal pain perception. *EMBO J* 2006 Jun 7;25(11):2368-76.

259. Heurteaux C, Lucas G, Guy N, El Yacoubi M, Thummler S, Peng XD, Noble F, Blondeau N, Widmann C, Borsotto M, et al. Deletion of the background potassium channel TREK-1 results in a depression-resistant phenotype. *Nat Neurosci* 2006 Sep;9(9):1134-41.
260. Lauritzen I, Blondeau N, Heurteaux C, Widmann C, Romey G, Lazdunski M. Polyunsaturated fatty acids are potent neuroprotectors. *EMBO J* 2000 Apr 17;19(8):1784-93.
261. Champigny MJ, Johnson M, Igdoura SA. Characterization of the mouse lysosomal sialidase promoter. *Gene* 2003 Nov 13;319:177-87.
262. Arpaia E, Dumbrille-Ross A, Maler T, Neote K, Tropak M, Troxel C, Stirling JL, Pitts JS, Bapat B, Lamhonwah AM. Identification of an altered splice site in ashkenazi tay-sachs disease. *Nature* 1988 May 5;333(6168):85-6.
263. Myerowitz R. Splice junction mutation in some ashkenazi jews with tay-sachs disease: Evidence against a single defect within this ethnic group. *Proc Natl Acad Sci U S A* 1988 Jun;85(11):3955-9.
264. Ohno K, Suzuki K. A splicing defect due to an exon-intron junctional mutation results in abnormal beta-hexosaminidase alpha chain mRNAs in ashkenazi jewish patients with tay-sachs disease. *Biochem Biophys Res Commun* 1988 May 31;153(1):463-9.
265. Semenza GL, Neufelt MK, Chi SM, Antonarakis SE. Hypoxia-inducible nuclear factors bind to an enhancer element located 3' to the human erythropoietin gene. *Proc Natl Acad Sci U S A* 1991 Jul 1;88(13):5680-4.
266. Molecular mechanisms of tay sachs disease: Calcium, excitotoxicity, and apoptosis .
267. Liu Y, Cox SR, Morita T, Kourembanas S. Hypoxia regulates vascular endothelial growth factor gene expression in endothelial cells. identification of a 5' enhancer. *Circ Res* 1995 Sep;77(3):638-43.
268. Storkebaum E, Lambrechts D, Carmeliet P. VEGF: Once regarded as a specific angiogenic factor, now implicated in neuroprotection. *Bioessays* 2004 Sep;26(9):943-54.
269. Huang X, Ding L, Bennewith KL, Tong RT, Welford SM, Ang KK, Story M, Le QT, Giaccia AJ. Hypoxia-inducible mir-210 regulates normoxic gene expression involved in tumor initiation. *Mol Cell* 2009 Sep 24;35(6):856-67.

270. Lall S, Grun D, Krek A, Chen K, Wang YL, Dewey CN, Sood P, Colombo T, Bray N, Macmenamin P, et al. A genome-wide map of conserved microRNA targets in *C. elegans*. *Curr Biol* 2006 Mar 7;16(5):460-71.
271. Bogaert E, Van Damme P, Poesen K, Dhondt J, Hersmus N, Kiraly D, Scheveneels W, Robberecht W, Van Den Bosch L. VEGF protects motor neurons against excitotoxicity by upregulation of GluR2. *Neurobiol Aging* 2010 Dec;31(12):2185-91.
272. Lee DW, Rajagopalan S, Siddiq A, Gwiazda R, Yang L, Beal MF, Ratan RR, Andersen JK. Inhibition of prolyl hydroxylase protects against 1-methyl-4-phenyl-1,2,3,6-tetrahydropyridine-induced neurotoxicity: Model for the potential involvement of the hypoxia-inducible factor pathway in parkinson disease. *J Biol Chem* 2009 Oct 16;284(42):29065-76.
273. O'Brien RJ, Kamboj S, Ehlers MD, Rosen KR, Fischbach GD, Huganir RL. Activity-dependent modulation of synaptic AMPA receptor accumulation. *Neuron* 1998 Nov;21(5):1067-78.
274. Turrigiano GG, Leslie KR, Desai NS, Rutherford LC, Nelson SB. Activity-dependent scaling of quantal amplitude in neocortical neurons. *Nature* 1998 Feb 26;391(6670):892-6.
275. Lissin DV, Gomperts SN, Carroll RC, Christine CW, Kalman D, Kitamura M, Hardy S, Nicoll RA, Malenka RC, von Zastrow M. Activity differentially regulates the surface expression of synaptic AMPA and NMDA glutamate receptors. *Proc Natl Acad Sci U S A* 1998 Jun 9;95(12):7097-102.
276. Turovskaya MV, Turovsky EA, Zinchenko VP, Levin SG, Shamsutdinova AA, Godukhin OV. Repeated brief episodes of hypoxia modulate the calcium responses of ionotropic glutamate receptors in hippocampal neurons. *Neurosci Lett* 2011 May 27;496(1):11-4.
277. Mutharasan RK, Nagpal V, Ichikawa Y, Ardehali H. microRNA-210 is upregulated in hypoxic cardiomyocytes through akt- and p53-dependent pathways and exerts cytoprotective effects. *Am J Physiol Heart Circ Physiol* 2011 Oct;301(4):H1519-30.
278. Enguita M, DeGregorio-Rocasolano N, Abad A, Trullas R. Glycogen synthase kinase 3 activity mediates neuronal pentraxin 1 expression and cell death induced by potassium deprivation in cerebellar granule cells. *Mol Pharmacol* 2005 Apr;67(4):1237-46.
279. Lee DW, Futami M, Carroll M, Feng Y, Wang Z, Fernandez M, Whichard Z, Chen Y, Kornblau S, Shpall EJ, et al. Loss of SHIP-1 protein expression in high-risk myelodysplastic syndromes is associated with miR-210 and miR-155. *Oncogene*

2012 Jan 16.

280. Fasanaro P, D'Alessandra Y, Di Stefano V, Melchionna R, Romani S, Pompilio G, Capogrossi MC, Martelli F. MicroRNA-210 modulates endothelial cell response to hypoxia and inhibits the receptor tyrosine kinase ligand ephrin-A3. *J Biol Chem* 2008 Jun 6;283(23):15878-83.
281. Chan SY, Zhang YY, Hemann C, Mahoney CE, Zweier JL, Loscalzo J. MicroRNA-210 controls mitochondrial metabolism during hypoxia by repressing the iron-sulfur cluster assembly proteins ISCU1/2. *Cell Metab* 2009 Oct;10(4):273-84.
282. Qi J, Qiao Y, Wang P, Li S, Zhao W, Gao C. microRNA-210 negatively regulates LPS-induced production of proinflammatory cytokines by targeting NF-kappaB1 in murine macrophages. *FEBS Lett* 2012 Apr 24;586(8):1201-7.
283. Vallabhapurapu S, Karin M. Regulation and function of NF-kappaB transcription factors in the immune system. *Annu Rev Immunol* 2009;27:693-733.
284. Hayden MS, Ghosh S. Shared principles in NF-kappaB signaling. *Cell* 2008 Feb 8;132(3):344-62.
285. Beinke S, Ley SC. Functions of NF-kappaB1 and NF-kappaB2 in immune cell biology. *Biochem J* 2004 Sep 1;382(Pt 2):393-409.
286. Palombella VJ, Rando OJ, Goldberg AL, Maniatis T. The ubiquitin-proteasome pathway is required for processing the NF-kappa B1 precursor protein and the activation of NF-kappa B. *Cell* 1994 Sep 9;78(5):773-85.
287. Lang V, Janzen J, Fischer GZ, Soneji Y, Beinke S, Salmeron A, Allen H, Hay RT, Ben-Neriah Y, Ley SC. betaTrCP-mediated proteolysis of NF-kappaB1 p105 requires phosphorylation of p105 serines 927 and 932. *Mol Cell Biol* 2003 Jan;23(1):402-13.
288. Heissmeyer V, Krappmann D, Hatada EN, Scheidereit C. Shared pathways of IkappaB kinase-induced SCF(betaTrCP)-mediated ubiquitination and degradation for the NF-kappaB precursor p105 and IkappaBalpha. *Mol Cell Biol* 2001 Feb;21(4):1024-35.
289. Liou HC, Nolan GP, Ghosh S, Fujita T, Baltimore D. The NF-kappa B p50 precursor, p105, contains an internal I kappa B-like inhibitor that preferentially inhibits p50. *EMBO J* 1992 Aug;11(8):3003-9.
290. Chow JC, Young DW, Golenbock DT, Christ WJ, Gusovsky F. Toll-like receptor-4 mediates lipopolysaccharide-induced signal transduction. *J Biol Chem* 1999 Apr

- 16;274(16):10689-92.
291. Madigan MT, Martinko JM. Cell membranes and cell walls. In: Brock biology of microorganisms. 11th ed. New Jersey: Pearson Prentice Hall; 2006. .
292. Rius J, Guma M, Schachtrup C, Akassoglou K, Zinkernagel AS, Nizet V, Johnson RS, Haddad GG, Karin M. NF-kappaB links innate immunity to the hypoxic response through transcriptional regulation of HIF-1alpha. *Nature* 2008 Jun 5;453(7196):807-11.
293. Jou I, Lee JH, Park SY, Yoon HJ, Joe EH, Park EJ. Gangliosides trigger inflammatory responses via TLR4 in brain glia. *Am J Pathol* 2006 May;168(5):1619-30.
294. Huynh C, Roth D, Ward DM, Kaplan J, Andrews NW. Defective lysosomal exocytosis and plasma membrane repair in chediak-Higashi/beige cells. *Proc Natl Acad Sci U S A* 2004 Nov 30;101(48):16795-800.
295. Jaiswal JK, Andrews NW, Simon SM. Membrane proximal lysosomes are the major vesicles responsible for calcium-dependent exocytosis in nonsecretory cells. *J Cell Biol* 2002 Nov 25;159(4):625-35.
296. McNeil PL, Steinhardt RA. Plasma membrane disruption: Repair, prevention, adaptation. *Annu Rev Cell Dev Biol* 2003;19:697-731.
297. Reddy A, Caler EV, Andrews NW. Plasma membrane repair is mediated by ca(2+)-regulated exocytosis of lysosomes. *Cell* 2001 Jul 27;106(2):157-69.
298. Roy D, Liston DR, Idone VJ, Di A, Nelson DJ, Pujol C, Bliska JB, Chakrabarti S, Andrews NW. A process for controlling intracellular bacterial infections induced by membrane injury. *Science* 2004 Jun 4;304(5676):1515-8.
299. Munnell JF, Cork LC. Exocytosis of residual bodies in a lysosomal storage disease. *Am J Pathol* 1980 Feb;98(2):385-94.
300. Yogalingam G, Bonten EJ, van de Vlekkert D, Hu H, Moshiach S, Connell SA, d'Azzo A. Neuraminidase 1 is a negative regulator of lysosomal exocytosis. *Dev Cell* 2008 Jul;15(1):74-86.
301. Krek A, Grun D, Poy MN, Wolf R, Rosenberg L, Epstein EJ, MacMenamin P, da Piedade I, Gunsalus KC, Stoffel M, et al. Combinatorial microRNA target predictions. *Nat Genet* 2005 May;37(5):495-500.

302. Tanguay RL, Gallie DR. Translational efficiency is regulated by the length of the 3' untranslated region. *Mol Cell Biol* 1996 Jan;16(1):146-56.
303. Miller P, Kemp PJ, Lewis A, Chapman CG, Meadows HJ, Peers C. Acute hypoxia occludes hTREK-1 modulation: Re-evaluation of the potential role of tandem P domain K<sup>+</sup> channels in central neuroprotection. *J Physiol* 2003 Apr 1;548(Pt 1):31-7.
304. Narravula S, Colgan SP. Hypoxia-inducible factor 1-mediated inhibition of peroxisome proliferator-activated receptor alpha expression during hypoxia. *J Immunol* 2001 Jun 15;166(12):7543-8.
305. Jeong CH, Lee HJ, Cha JH, Kim JH, Kim KR, Kim JH, Yoon DK, Kim KW. Hypoxia-inducible factor-1 alpha inhibits self-renewal of mouse embryonic stem cells in vitro via negative regulation of the leukemia inhibitory factor-STAT3 pathway. *J Biol Chem* 2007 May 4;282(18):13672-9.
306. Lee KJ, Lee KY, Lee YM. Downregulation of a tumor suppressor RECK by hypoxia through recruitment of HDAC1 and HIF-1alpha to reverse HRE site in the promoter. *Biochim Biophys Acta* 2010 May;1803(5):608-16.